Generation and Application of Squeezed Light

A thesis
submitted in partial fulfilment
of the requirements for the Degree
of
Doctor of Philosophy in Theoretical Physics
at the
University of Waikato

by

MONIKA ALICE MARIA MARTE

University of Waikato
1988

To Helmut

who understands

ABSTRACT

This thesis investigates some aspects of future applications of squeezed states. Subsequent to an introductory part summarizing a few basic notions and facts related to squeezing, a detailed study of the generation of squeezed light and its effects in two different quantum optical systems is presented.

Firstly a more technology-oriented application of squeezed states is discussed, namely a four-wave mixing optical rotation sensor. In an optical rotation sensor or "laser gyroscope" an external rotation is measured by means of the so-called Sagnac effect; that is one detects the relative phase shift which is induced between a co-rotating and a counter-rotating beam, when the cavity or fiber is in a state of rotation. It is demonstrated that the non-linearity in the fiber medium of a laser gyroscope can be used to produce squeezed light, which leads to a better signal to noise ratio in the subsequent heterodyne detection of the Sagnac phase shift.

The major part of this thesis is dedicated to the analysis of the "squeezed reservoir laser", which is of a more theoretical nature. The laser is treated as an open quantum system which is coupled to a squeezed environment. Both possibilities have been investigated: squeezing the reservoir which models the incoherent pumping process and the spontaneous emission or, alternatively, squeezing the other heatbath, modelling the vacuum modes entering the laser cavity.

The analysis includes a detailed discussion of the semiclassical theory, the rotating wave van der Pol oscillator model for the squeezed reservoir laser, the derivation of the laser linewidth and the calculation of the spectrum of fluctuations from a linearized theory. Two main results are the locking of the laser phase due to the anisotropy of the fluctuations in the squeezed reservoirs and the possibility of generating squeezed laser light .

Acknowledgements

First of all I wish to thank my supervisors for making it possible for me to come to New Zealand. To Prof. Dan Walls I owe many thanks for suggesting interesting research projects which I very much enjoyed working on and for the ideas he provided guiding me along the way and to Prof. Crispin Gardiner for his patience in answering countless questions on various general topics in physics or whenever I was "stuck" somewhere.

I am also very grateful to Margaret Reid, Craig Savage, Scott Parkins, Andrew Smith, Alistair Lane and Matthew Collett for their readiness to help me and for many encouraging discussions. Special thanks to Craig and Margaret for their support during my first weeks at Waikato University when everything was so new.

Furthermore I am indebted to David Murray, Peter Hoban and many others for their help whenever the computer would not do what I actually wanted it to do! Many thanks to David Murray and Matthew Collett for carefully reading the manuscript and eliminating my "English" mistakes. I also wish to thank Heidi Eschmann for her assistance and support throughout my stay.

Last but not least I would like to thank Dr. Peter Zoller for suggesting that I should go to Waikato University to do my D. Phil. in Quantum Optics.

Zuallerletzt möchte ich meiner Familie und Helmut danken, ohne deren ständiger Unterstützung und Aufmunterung dies alles nicht möglich gewesen wäre.

Contents

List of Figures

Scio me nihil scire

Introduction

At present, squeezing is a well established field of research in quantum optics. In the wake of recent reports on successful generation of squeezing in the laboratory (see Section 1.1 for a list of the schemes that have so far been successful in producing squeezed light), the physics of squeezed states is no longer restricted to theoretical predictions on the properties of some "utopian" quantum states of the electromagnetic field and to attempts to generate them. Instead squeezed light has become an experimental reality. This renders the prospects of applications of squeezing less academic, although one should not underestimate the experimental difficulties involved in producing squeezed light.

In quantum optics light is treated as a quantized field (for a detailed discussion of the quantization of the electromagnetic field see for example the textbooks by Louisell (1973) or Loudon (1973)). This entails "intrinsic quantum noise" as a consequence of an appropriate Heisenberg's uncertainty principle. Thus any light source displays some residual noise, no matter how carefully one tries to eliminate environmental influences causing stochastic fluctuations. When concerned with this "quantum barrier" preventing knowledge with infinite precision of all system observables of a given quantum system, it has proven useful to define the so-called standard quantum limit as the noise level of the vacuum state of the electromagnetic field. In quantum optics in particular, it imposes a seemingly insurmountable limit on the accuracy of any measurement involving light.

The essential feature of squeezed light is the anisotropic distribution of these inevitable quantum fluctuations: the noise in one quadrature phase is quenched or "squeezed" as the name suggests, while the fluctuations in the other are enhanced accordingly. Thus compared to a coherent state with an equal amount of "total noise" (cf. Section 1.2.3), the noise is redistributed. Phase-dependent fluctuations of this kind afford the possibility of somehow "by-passing" the Heisenberg uncertainty principle by decreasing the noise in some observable of interest. This done by cleverly designing the experimental set-up so that the increased fluctuations in the canonical conjugate variable do not influence the performance, such as in the so-called back action evading and "quantum non demolition" measurements,.which have been studied extensively over the past few years (Caves et al., 1980). This idea lies at the root of all future applications. For example, it will be demonstrated that by means of squeezed light one can enhance the signal to noise ratio in homodyne or heterodyne detection phase-measurements performed by optical devices such as laser gyroscopes.

The present thesis deals with applications of squeezing in a rather wide sense. This is reflected in the polarity between the perspectives in the two main parts of this thesis that contain original work: the more technology-oriented scheme of a laser gyroscope using squeezed light to achieve improved sensitivity on one hand, and on the other hand the more general investigation of the quantum theory of the "squeezed reservoir laser", a laser system which is coupled to a squeezed quantum environment.

Before setting out to discuss applications of squeezed states, one has to explain in some detail what exactly the advantages of squeezed techniques are, compared to conventional devices using coherent light. Therefore Chapter 1 and parts of Chapter 2 are of an introductory

nature, briefly revising some basic facts on the definition and properties of squeezed states as well as the methods used to detect squeezing. No attempt is made to present a complete review, giving due credit to all contributions on squeezing over the past few years; considering the amount of material, this seems too enormous a task. The special issues on squeezing in the Journal of the Optical Society of America B (J. Opt. Soc. Am. B **4**(10), 1987) and the Journal of Modern Optics (J. Mod. Opt. **34**(6,7), 1987) are recommended if one wishes to obtain a general view on the present level of knowledge or on the existing variety of aspects of squeezing.

Chapter 1 defines squeezing and emphasizes the mathematical properties of squeezed states for later reference.

In Section 1.1 the history of squeezed states in quantum optics is briefly outlined. Then in Section 1.2 coherent, single- mode and two-mode squeezed states are systematically classified, stressing their common aspect as pure quantum states with Gaussian wave-functions, following Schumaker (1986). The class of interaction Hamiltonians which are quadratic in the photon creation and annihilation operators is shown to formally generate Gaussian states. These Hamiltonians are then associated with physical interactions in non-linear sytems of quantum optics, most of which have been studied in the quest to generate squeezing experimentally. Subsequently the important special case of general single-mode coherent and squeezed states is treated at some length, establishing a notation which will be used repeatedly throughout the thesis. Finally, towards the end of Section 1.2 the concept of minimum uncertainty states is introduced and discussed with respect to squeezed states.

The contents of section 1.3 comprise a side issue, viewing some aspects of squeezed states already encountered in the previous sections, but from a different angle: it is explained that squeezed states are related to SU(1,1) transformations.

Because of applications in Chapter 2, which discusses the broadband detection of squeezing, and Chapter 3, which deals with a broadband input in the squeezed reservoir laser, a brief introduction on broadband squeezed light is given in Section 1.4. This follows the theory by Yurke (1985a).

As the necessary basic ideas and mathematical tools have been reviewed in Chapter 1, Chapter 2 investigates the effects brought about by squeezed light, that is discusses possible methods of detecting squeezing as well as some applications in optical devices.

Section 2.1 provides a list of applications of squeezed states in quantum optics under recent or current consideration. As many optical devices, such as interferometers, measure essentially a phase or frequency, in Section 2.2 special care is given to the photon-number and phase "uncertainty relation". As a simple example, the minimum error is calculated that results from a balanced homodyne measurement of the relative phase between two squeezed inputs which are recombined on a 50% beamsplitter.

In Section 2.2, after outlining the conventional squeezing detection schemes such as direct photodetection, homodyning and heterodyning, the photon counting statistics of a squeezed state are calculated explicitly. This generalizes a previous result by Walls and Milburn (1983), with the difference that the depletion of the squeezed field coupled to the photo-detector is taken into account.

The remainder of Chapter 2 is dedicated to a demonstration that squeezed states can be successfully applied to improve the performance of optical rotation sensors. After explaining the principle underlying all modern laser gyroscopes, that is the Sagnac effect, a novel type of fiber-optic rotation sensor is studied. In this device the fiber does not merely act as a (passive) Sagnac interferometer, giving rise to a rotation-dependent relative phase shift between two counterpropagating light waves, but at the same time its non-linearity is utilized to produce squeezed light via a four-wave mixing interaction. Similar to the simple example considered in Section 2.2, this allows a better signal to noise ratio in the subsequent heterodyne detection of the induced relative phase shift.

Chapter 3 deals with a spectroscopic application of the squeezed states. Recently Gardiner (1986) and Carmichael et al.(1987), have predicted the appearance of a narrow peak in the resonance fluorescence spectrum of a single atom which is irradiated with broadband squeezed light coming from all directions. Ritsch and Zoller (1987) have calculated the weak-field absorption spectrum of a coherently driven two-level atom embedded in a squeezed vacuum. Scanning the absorption as a function of the probe detuning, they found a subnatural linewidth in the absorption spectrum, when the squeezed light as well as the coherent pump field were tuned to the atomic resonance. Motivated by these results we calculate the spectroscopic linewidth of a laser system coupled to a squeezed environment.

Another motivation for studying such a system was provided by the interest has recently arisen in lasers displaying sub-Poissonian statistics in the output. Thus Yamamoto and co-workers have predicted and measured sub-Poissonian statistics in a semiconductor laser system,

where the pump noise is suppressed below the "shot noise" (or vacuum) level by means of a feed-back loop (Yamamoto et al., 1986, Machida et al., 1987, Machida and Yamamoto, 1988).

Similarly, in "micro-maser" systems (Filipowicz et al., 1986, Krause et al., 1986), truly microscopic masers, which possess the characteristic quantum behaviour of few-atom-systems, sub-Poissonian statistics have been predicted among other quantum effects.

Two cases of a "squeezed reservoir laser" are studied. Firstly the reservoir coupled to the atoms (which models the incoherent pumping process and the spontaneous emission in Haken's approach of treating the laser as an open quantum system) is assumed to be in a squeezed state. The term "squeezed-pump laser" has been chosen to refer to such a system. Secondly, a situation is studied, where the vacuum modes entering the laser cavity are squeezed. This relates to some results recently derived by Gea-Banacloche (1987). Such a system will be referred to as a "squeezed-cavity laser".

Section 3.1 explains the model Hamiltonian of the squeezed reservoir laser in great detail. Then in Section 3.2, following Haken (1970), the corresponding master equation for the proper laser system is derived by tracing over the reservoir's degrees of freedom and converted into a generalized Fokker-Planck equation.

Section 3.3 presents some initial qualitative conclusions drawn from the semiclassical theory. As a main outcome it is shown that the anisotropy of noise in the reservoirs gives rise to a locking of the laser phase. However, there is an important difference between the squeezed-pump laser and the squeezed-cavity laser. Squeezing in the bath coupled to the laser atoms leads to a change in the deterministic first order derivative terms (or drift terms, as they are often called) in the Fokker-Planck equation for the generalized P–representation. Squeezing

the cavity modes influences only the second order derivatives (or diffusion terms), introducing new phase-dependent noise correlations. Hence the squeezed-cavity laser requires different techniques; transformation to phase and intensity variables has proven useful.

The three cases of firstly a squeezed-pump laser with the bath being in a squeezed vacuum state; secondly with the bath in a squeezed state with non-zero coherent component; and finally the squeezed-cavity laser are treated in separate sub-sections. In each case the semiclassical steady states are calculated and their stability is examined.

For the squeezed-pump laser a semiclassical potential function is shown to exist and used for illustration. However, for the squeezed-cavity laser the semiclassical potential condition is not satisfied. Another important feature of the squeezed-pump laser alone (which is absent in the squeezed-cavity laser) is the lowering of the laser threshold due to the squeezing: hence one can operate such a laser above threshold in a regime of parameter-space where an ordinary laser would not work as an amplifier.

In Section 3.4 a rotating wave van der Pol oscillator model for the squeezed-pump laser is derived by adiabatically eliminating the atoms and expanding around threshold. The adiabatic elimination procedure is valid if the cavity decay rate is the smallest damping rate of the system, that is, it is small compared to the longitudinal relaxation rate and to the decay rates of the real and imaginary parts of the atomic polarization, which differ from each other in the squeezed-pump laser (similar to the situation of atomic phase-decay inhibition discussed by Gardiner). In principle one of the two transverse relaxation rates can be made as small as one pleases, but in this section it is assumed that the cavity damping rate is still smaller.

The rotating wave van der Pol equation, which is derived along these lines, is seen to possess a phase-dependent gain. This explains how a stable field amplitude with a well-defined phase dynamically builds up above threshold in the squeezed-pump laser. The spectroscopic linewidth of the squeezed-pump laser is then calculated in an approach which resembles the treatment of the laser with injected signal (Chow et al., 1975). This is necessary because there is no phase diffusion as in an ordinary laser. The laser phase is locked and the formal expression for the phase diffusion, which is also calculated, corresponds here to phase fluctuations about a stabilized phase. In this sense the squeezing in the bath has led to a narrow linewidth, since it destroys the random walk of the laser phase. The linewidth resulting from fluctuations around a locked phase can be decreased by increasing the squeezing parameter in the bath. This, however, is shown to be caused mainly by the change of the steady state values and the effect of lowering the laser threshold which arises due to the squeezing.

Finally, for the squeezed-cavity laser an analogous procedure is performed (with the difference that one uses phase and intensity variables to start with). In this case one still gets localization of the phase, but it is found that the phase noise is actually increased for operation about a stable steady state. Comparing this to the squeezed-pump laser, we see that this is a consequence of the fact that squeezing the cavity modes is a lower order effect which does not influence the steady state intensity or the laser threshold.

In Section 3.6 fluctuation spectra of the output of the squeezed-pump laser are calculated from a linearized theory, using a generalized P-representation. This represents a general analysis which does not require a high-Q cavity (allowing adiabatic elemination) or operation very far from saturation. It is demonstrated that sub-Poissonian

statistics is in fact possible in the output of a squeezed-pump laser. The squeezing can be improved by adding an appropriate coherent part to the squeezed state in the bath, which corresponds to sub-Poissonian statistics in the bath itself.

Finally, Section 3.6 summarizes the conclusions drawn from the preceeding analysis of the squeezed reservoir laser.

CHAPTER1 INTRODUCTION: WHAT ARE SQUEEZED STATES ?

1.1 Coherent and Squeezed States in Quantum Optics

Anybody involved in quantum optics today will know how important *coherent states* are. They truly constitute the "heart of quantum optics", as B. L. Schumaker put it (Schumaker, 1986). Their importance arises from the fundamental role that the harmonic oscillator plays in the theoretical foundations of quantum optics. Since the early 1960s Glauber (1963a) and others have applied the coherent states of the quantum mechanical harmonic oscillator to build a powerful and concise description of the quantized electromagnetic field.

One feature of these coherent (or "classical") states is that they constitute the closest counterpart to a classical field. More precisely, they can be defined as the set of wavefunctions of a quantum mechanical harmonic oscillator which yield the well-known classical expressions for the expectation values of the vector potential and the Hamiltonian. Hence they have proven to be particularly useful in studying quantum systems in a nearly classical state of large excitation with intrinsic quantum noise.

It was not until the late1970s that some researchers began to study in detail the class of states which are now known as *squeezed states* , a name coined by Hollenhorst (1979). They had been introduced previously by independent workers under the names "minimum uncertainty packets" (Stoler, 1970, 1971), "new coherent states" (Lu, 1971, 1972), and "two-photon coherent states" (Yuen, 1976).

As these names suggest, the squeezed states represent some kind of generalization of the coherent states. They are minimum uncertainty states just as coherent states are; however, they differ in one important

respect: the noise of a squeezed state is not equally distributed in phase. As an illustration, in a nearly monochromatic plane wave one could "squeeze" the noise in one quadrature component, say the one proportional to $\sin\omega t$, as much as one pleases- at the expense of increasing the fluctuations in the $\cos\omega t$ component. It seems that this offers the intriguing possibility of somehow "getting around" the limit on the accuracy of a measurement imposed by the zero-point or vacuum fluctuations, the so-called *standard quantum limit* in quantum optics.

It has long been known that such states would be of great advantage in optical communication systems (Yuen and Shapiro, 1978,1980). They would also prove useful in other fields involving high-precision measurements ranging from gravitational wave detection (Braginsky et al., 1980, Caves et al., 1981) to modern laser gyroscopes, where performance has almost reached the standard quantum limit.

This accounts for the current interest in generating squeezed states in the laboratory. So far there have been reports on successful generation of squeezing in several systems, employing four-wave mixing in atomic vapours (Slusher et al., 1985, Maeda et al., 1987), optical fibers (Shelby et al., 1986) and optical parametric oscillation (Wu et al., 1986). In the parametric oscillator a 50% reduction of the vacuum noise has already been achieved. More recently, parametric down-conversion has been applied to produce a squeezed output (Slusher et al.,1987, Heidmann et al., 1987) and squeezing has also been observed in optical bistability situations (Raizen et al., 1987).

1.2 Coherent and Squeezed States as Gaussian Pure States

Gaussian pure states (GPS) are quantum mechanical pure states with wavefunctions that are exponentials of complex-valued linear and quadratic forms in the canonical "position" or "momentum" variables (Schumaker, 1986).

Let us consider the system of N quantum oscillators. The free Hamiltonian reads

$$H_0^{(N)} = \sum_{j=1}^{N} \hbar\, \omega_j\, a_j^\dagger a_j \tag{1.1}$$

with ω_j being the (real, positive, constant) frequency of the j^{th} mode. The annihilation and creation operators a_j and $a^\dagger_j$ satisfy the commutation relation

$$[a_j\,,\, a_k^\dagger\,] = \delta_{jk}\ . \tag{1.2}$$

The eigenstates of this Hamiltonian are tensor products of the numberstates

$$|n_j\rangle = \frac{1}{\sqrt{n_j!}}\,(a^\dagger)^{n_j}\ |0\rangle_j \tag{1.3}$$

of each mode.

1.2.1 Quadratic Interaction Hamiltonians

All interaction Hamiltonians producing or preserving GPS are polynomials that are linear or quadratic in creation and annihilation operators (Schumaker, 1986). These interactions can be divided into two distinct types: those that *conserve the total photon number,* that is contain equal numbers of creation and annihilation operators, and those that do not.

Consequently, if an interaction is to preserve the photon number of a GPS, its Hamiltonian must be made up of terms of the form

$$H_R(t) = \Omega_i(t)\, a_i^\dagger a_i\,, \qquad \Omega_i(t) = \Omega_i(t)^* \tag{1.4}$$

or

$$H_{R_{ij}}(t) = \Omega_{ij}(t)\, a_i^\dagger a_j + \Omega_{ij}^*(t)\, a_j^\dagger a_i \qquad i \neq j\ . \tag{1.5}$$

An interaction of the type in Eq.(1.4) conserves the photon number in each mode separately, whereas Eq.(1.5) only conserves the *total* photon number of the pair of modes. As interactions like Eq.(1.4) conserve the total energy and the total photon number they are called rotation Hamiltonians. Eq.(1.5) can be interpreted as a frequency converting interaction, where a photon of frequency $\Omega_i < \Omega_j$ is annihilated together with a pump photon to produce a photon of frequency Ω_j or vice versa.

More interesting than the above interactions, whose only effect is to redistribute the photons among the different modes, are the remaining terms of the quadratic polynomial with unequal numbers of a_j and $a\dagger_j$:

$$H_1(t) = \sum_{j=1}^{N} \lambda_j^*(t)\, a_j + \lambda_j(t)\, a_j^\dagger \qquad (1.6)$$

$$H_2(t) = \frac{1}{2} \sum_{i,j=1}^{N} \xi_{ij}^*(t)\; a_j\, a_i + \xi_{ij}(t)\;\; a_j^\dagger\, a_i^\dagger\,, \qquad \xi_{ij}(t) = \xi_{ji}(t) \qquad (1.7)$$

Eq.(1.6) may be interpreted as the interaction of the oscillator with classical fields characterized by the numbers λ_j (j=1,2,....N). The terms with $i \neq j$ in Eq.(1.7) describe interactions which conserve the difference - but not the sum - of the photon number of any pair of modes, e.g. ideal non-degenerate two-photon processes such as in a non-degenerate parametric amplifier. The degenerate case is included in the terms i=j.

1.2.2 Displacement Operator and Single-Mode Squeeze Operator

The unitary evolution operators which map one GPS onto another with different photon number are again of two types: those acting on one mode only, and those coupling pairs of modes. For each mode we define the following unitary operators:

$$D(a;\alpha) = \exp\left(\alpha\, a^\dagger - \alpha^*\, a\right) = e^{-\frac{|\alpha|^2}{2}}\, e^{\alpha a^\dagger}\, e^{-\alpha^* a} \qquad \alpha \in \mathbb{C} \qquad (1.8a)$$

$$S(a;\zeta) = \exp\left[\frac{1}{2}\, r\left(e^{-i\vartheta}\, a^2 - e^{i\vartheta}\, a^{\dagger 2}\right)\right] \qquad \zeta = r\, e^{i\vartheta} \qquad (1.8b)$$

$$0 \le r < \infty, \quad 0 \le \vartheta < 2\pi\,.$$

Note that the inverse operations are easily found by taking negative parameters, that is

$$D^{\dagger}(\alpha) = D^{-1}(\alpha) = D(-\alpha)$$
$$S^{\dagger}(\zeta) = S^{-1}(\zeta) = S(-\zeta) \ . \qquad (1.9)$$

When operating on a, the effect of the so-called *displacement operator* $D(a;\alpha)$ is to add a constant α, thus "displacing" the mean value of a:

$$D^{\dagger}(a,\alpha)\, a\, D(a,\alpha) = a + \alpha$$
$$D^{\dagger}(a,\alpha)\, a^{\dagger} D(a,\alpha) = a^{\dagger} + \alpha^{*} \ . \qquad (1.10)$$

The set of states one can generate by displacing the vacuum state (which is a GPS) by an arbitrary complex number α

$$|\alpha\rangle = D(a,\alpha)\,|0\rangle \qquad (1.11)$$

comprises the (single mode) *coherent states.*

The single-mode *squeeze operator* $S(a;\alpha)$ correlates or "mixes" a with $a\dagger$ in the following way:

$$S^{\dagger}(a;r,\vartheta)\, a\, S(a;r,\vartheta) = a \cosh r - a^{\dagger} e^{i\vartheta} \sinh r$$
$$S^{\dagger}(a;r,\vartheta)\, a^{\dagger} S(a;r,\vartheta) = a^{\dagger} \cosh r - a\, e^{-i\vartheta} \sinh r \ . \qquad (1.12)$$

By first squeezing the vacuum state and then displacing it, one obtains the set of (single mode) *squeezed states* :

$$|\alpha,\zeta\rangle = D(a;\alpha)\, S(a;\zeta)\,|0\rangle \ . \qquad (1.13)$$

1.2.3 Minimal Total Noise and Minimum Uncertainty States

It is useful to introduce the concept of the *total noise* of a GPS. We define the total noise of a multi-mode light-field as the sum over all modes of the squared uncertainties ΔX_1 and ΔX_2 of the real and imaginary part, defined as

$$a = X_1 + i X_2 \tag{1.14}$$

for all modes a. As usual the uncertainty ΔA of an observable A in a particular state is defined as the square root of the variance V(A):

$$\Delta A = \sqrt{V(A)} = \sqrt{\langle A^2 \rangle - \langle A \rangle^2} \ . \tag{1.15}$$

Thus the total noise is given by

$$\text{Total noise} = \sum_{\text{all modes}} (\Delta X_1)^2 + (\Delta X_2)^2 \ .$$

The minimum total noise allowed by quantum mechanics (that is consistent with the commutation relation Eq.(1.2)) is the "zero-point noise" of one half in each mode. This minimum is realized only in tensor products of eigenstates of the annihilation operator of each mode, such as the vacuum state in particular. It can be proved (Schumaker, 1986) that all linear interaction Hamiltonians of type Eq.(1.6) as well as all photon number conserving interaction Hamiltonians (Eq.(1.4) and Eq.(1.5)) conserve the total noise of a multimode GPS. Consequently, all GPS that are unitarily related to the vacuum by (products of) rotation,

mixing, or displacement operators - such as the coherent states in particular - carry the minimal total noise of the vacuum state.

Most textbooks on quantum mechanics include a derivation of the Heisenberg uncertainty principle from a given commutation relation for two unbounded operators with non-zero overlap of domains (see for example Cohen-Tannoudji (1984) or references in Milburn (1982)). From Eq.(1.2), or equivalently from

$$[X_1, X_2] = \frac{i}{2} \tag{1.16}$$

one derives

$$\Delta X_1 \, \Delta X_2 \geq \frac{1}{4} \ . \tag{1.17}$$

Those states that minimize the product of the uncertainties in X_1 and X_2 (and hence also the product of the uncertainties of the position and momentum operator of the harmonic oscillator), or in other words satisfy Eq.(1.17) with an equals sign, are called *minimum uncertainty states.* With the following useful relations for coherent states $|\alpha\rangle$

$$\langle X_1 + i X_2 \rangle \equiv \langle a \rangle = \alpha \tag{1.18}$$

$$\langle N \rangle \equiv \langle a^\dagger a \rangle = |\alpha|^2 \tag{1.19}$$

$$\Delta X_1 = \Delta X_2 = \frac{1}{2} \tag{1.20}$$

$$\Delta N = |\alpha| \tag{1.21}$$

and for squeezed states $|\alpha, r\, e^{i\vartheta}\rangle$

$$\langle X_1 + i X_2 \rangle \equiv \langle Y_1 + i Y_2 \rangle e^{i\frac{\vartheta}{2}} = \alpha \tag{1.22}$$

$$\langle N \rangle = |\alpha|^2 + \sinh^2 r \tag{1.23}$$

$$\Delta Y_1 = \frac{1}{2} e^{-r} \quad \Delta Y_2 = \frac{1}{2} e^{r} \tag{1.24}$$

$$\Delta N = \sqrt{| \alpha \cosh r - \alpha^* e^{i\vartheta} \sinh r |^2 + 2\cosh^2 r \sinh^2 r} \ , \tag{1.25}$$

one can easily verify that the coherent states as well as the squeezed states constitute minimum uncertainty states in the above sense: the coherent states with respect to X_1 and X_2, the squeezed states with respect to Y_1 and Y_2.

However, from Eq.(1.24) it is clear that the squeezed states - in contrast to the coherent states - do *not* constitute states with minimum total noise, since ΔY_1 and ΔY_2 are unequal and the sum of their squares obviously always exceeds one half.

In Fig.1 we illustrate the above statements in a so-called "error diagram" (see the review article on squeezed states by Walls (1983) and the references therein).It is a polar plot of the uncertainty in the quadrature operator

$$X_\varphi = \cos\varphi \, X_1 + \sin\varphi \, X_2 \, . \tag{1.26}$$

Since in a coherent state the noise is equally distributed in φ, the result is a circle, whereas for a squeezed state we get an ellipse with principal axes Y_1 and Y_2. A non-zero expectation value of the annihilation operator a, usually referred to as a *coherent excitation,* is represented by an arrow displacing the polar plot of the noise from the origin. However, note that the free dynamics of a single mode constitutes a rotation of the real and imaginary part of a, hence in a physical situation

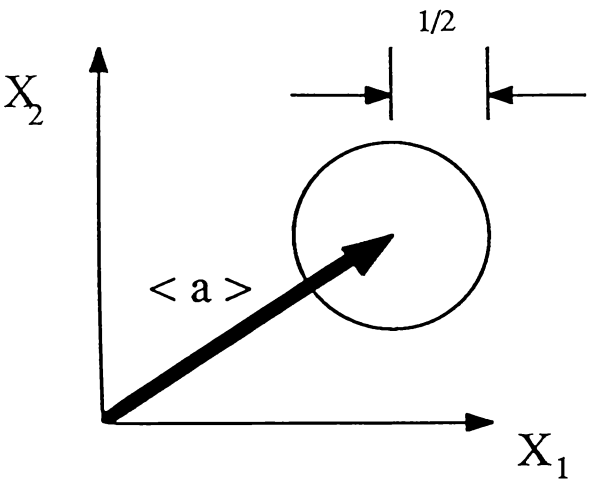

Fig.1a

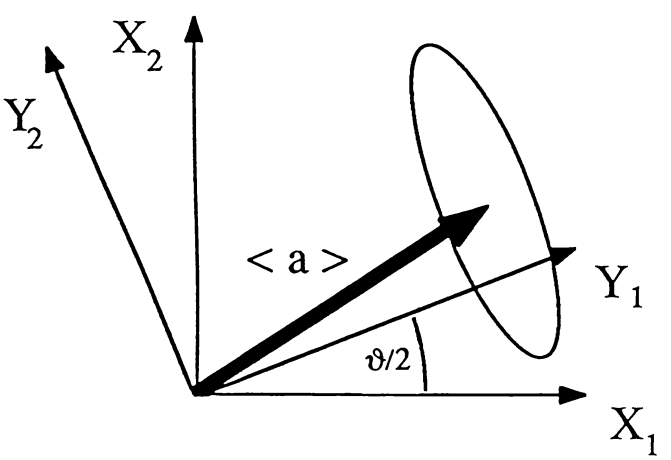

Fig.1b

Fig. 1 Error diagram in the complex-amplitude plane for
(a) coherent state $|\alpha\rangle$ (b) squeezed state $|\alpha, r\, e^{i\vartheta}\rangle$

these diagrams have to be viewed as rotating around the origin at a rate ω_0. Equivalently, they can be interpreted as amplitudes with respect to a rotating frame of reference. Viewing the rotated noise circles and ellipses for coherent or squeezed states, respectively (see Fig.1), it becomes obvious that the coherent states can be characterized as the set of states which remain minimum uncertainty states for X_1 and X_2 *for all times* when evolving freely (Grübl, 1985).

The above concepts can also be applied to atomic (angular-momentum) states (Wódkiewicz and Eberly, 1985). In this case, however, the commutator is not a c-number. This implies that some states may satisfy the Heisenberg uncertainty relation with an equals sign without ever reaching the *global* minimum product of the uncertainties.

1.3 Some Group Theoretical Remarks on Squeezed States

For the sake of compactness in the following we introduce a vector notation:

$$\mathbf{a} = \begin{pmatrix} a \\ a^\dagger \end{pmatrix} \qquad \mathbf{x} = \begin{pmatrix} x \\ p \end{pmatrix} \equiv A\,\mathbf{a} \tag{1.27}$$

with

$$A = \frac{1}{\sqrt{2}} \sqrt{\frac{\hbar}{\omega}} \begin{pmatrix} 1 & 1 \\ -i\omega & i\omega \end{pmatrix} = (A^\dagger)^{-1} \; . \tag{1.28}$$

Here x and p denote the "position" and "momentum" operators of the oscillator. We establish the commutation matrices

$$[\,\mathbf{a}, \mathbf{a}^{\dagger}\,] \equiv \mathbf{a}\,\mathbf{a}^{\dagger} - (\,\mathbf{a}^{*}\,\mathbf{a}^{T}\,)^{T} = \sigma_3 \tag{1.29}$$

$$[\,\mathbf{x}, \mathbf{x}^{T}\,] \equiv \mathbf{x}\,\mathbf{x}^{T} - (\,\mathbf{x}\,\mathbf{x}^{T}\,)^{T} = -\,\sigma_2\ , \tag{1.30}$$

where the matrices on the right hand side stand for two of the Pauli matrices

$$\sigma_1 = \begin{pmatrix} 0 & 1 \\ 1 & 0 \end{pmatrix} \qquad \sigma_2 = \begin{pmatrix} 0 & -i \\ i & 0 \end{pmatrix} \qquad \sigma_3 = \begin{pmatrix} 1 & 0 \\ 0 & -1 \end{pmatrix}\ , \tag{1.31}$$

which satisfy

$$[\,\sigma_i, \sigma_j\,] = 2\,\varepsilon_{ijk}\,\sigma_k \qquad\qquad i,j,k \in \{1,2,3\} \tag{1.32}$$

with ε_{ijk} being the antisymmetric Levi-Civita symbol (summation over the repeated index k is implied in Eq.(1.32)).

Unitary transformations of x and p are often called *canonical transformations* by analogy with classical mechanics, since they preserve the commutation relation Eq.(1.30). If such a canonical transformation is also *linear*, that is a matrix M_x can be found so that

$$U^{\dagger}\,\mathbf{x}\,U = M_x\,\mathbf{x}\ , \tag{1.33}$$

then consequently the following relation must hold:

$$M_x\,\sigma_2\,M_x^{T} = \sigma_2 = M_x^{T}\,\sigma_2\,M_x\ . \tag{1.34}$$

Real matrices M_x solving Eq.(1.34) are representations of the *symplectic group* Sp(2,R), the group of two-dimensional real matrices with unity

determinant that preserve a bilinear antisymmetric metric (which has σ_2 as canonical or standard representation) in the Fock space; for details see the textbooks by Wybourne (1974) or Gilmore (1974).

Alternatively, transforming **a** with the *same* unitary operator one easily derives the following relation:

$$U^\dagger \mathbf{a}\, U = M_{\mathbf{a}}\, \mathbf{a} \quad \text{with} \quad M_{\mathbf{a}} = A^\dagger M_{\mathbf{x}} A \ , \tag{1.35}$$

involving the matrix A of Eq.(1.28). The complex matrices $M_{\mathbf{a}}$ preserve the commutator Eq.(1.29)

$$M_{\mathbf{a}}\, \sigma_3\, M_{\mathbf{a}}^\dagger = \sigma_3 = M_{\mathbf{a}}^\dagger\, \sigma_3\, M_{\mathbf{a}} \ . \tag{1.36}$$

They comprise a representation of a group which is isomorphic to Sp(2,R): the three parameter Lie group SU(1,1). This is the group of two-dimensional complex matrices with determinant plus one which preserve a sesquilinear metric with signature (1,1) (which has the canonical representation σ_3).

Moreover, a unitary transformation of **a** (or **x**) will be linear if and only if U is an exponential of a *Hermitean* linear combination of a^2 , $a^{\dagger 2}$ and $a^\dagger a$. More precisely, such unitary transformations are generated by a Hermitean representation

$$\begin{aligned} G_1 &= \frac{1}{4}\,(a^{\dagger 2} + a^2) \\ G_2 &= -\frac{i}{4}\,(a^{\dagger 2} - a^2) \\ G_3 &= \frac{1}{4}\,(a^\dagger a + a\, a^\dagger) \end{aligned} \tag{1.37}$$

of the algebra of SU(1,1):

$$[G_1, G_2] = -iG_3$$
$$[G_2, G_3] = iG_1 \qquad (1.38)$$
$$[G_3, G_1] = iG_2 .$$

Schumaker (1986) has proved that three real parameters r, ϑ and Θ can always be found *uniquely*, so that such a unitary matrix, corresponding to a linear canonical transformation, is a product of the single-mode squeeze operator $S(r, \vartheta)$ and a rotation $R(\Theta)$. Hence we conclude that the single-mode squeeze operator relates (up to a rotation) to SU(1,1) transformations. The three parameters r, ϑ and Θ correspond to the three free parameters of the above mentioned Hermitean linear combination of the exponent of U, or to the three parameters of SU(1,1).

A similar approach has been used by Yurke (1986) in his group theoretical analysis of several passive and active (four-wave mixing) interferometer schemes. Generalization to more than one mode is possible but rather complicated. For example, Milburn (1984) has shown that N-mode squeezed states are generated by unitary representations of a subset of the symplectic group Sp(2N,R).

1.4 Broadband Squeezing

In the above sections the emphasis was mostly on single-mode squeezed states. However, broadband squeezed light, that is multi-mode light which exhibits squeezing in one quadrature phase operator (defined with respect to the centre frequency Ω) of the electric field, is important from an experimental point of view. A multi-mode or "broadband" situation arises naturally for example in squeezing

detection schemes such as wide-band homodyne detection or heterodyne detection (which will be discussed briefly in Section 2.3.1).

If only a very narrow bandwidth of the photocurrent at zero frequency is analyzed, which is the case in the so-called homodyne detection technique, then one is more or less dealing with single-mode squeezing. If one examines a narrow bandwidth around a non-zero frequency Ω, then correlations between signal modes at frequencies $\Omega \pm \Delta\omega$, which corresponds to two-mode squeezing, are important. A broadband description would cover these two aspects of what is essentially the same phenomenon. Such a description of squeezed states and their role in practical detection schemes has been presented independently by Caves and Schumaker (1985, 1986, Schumaker and Caves, 1985) and Yurke (1985a, 1985b).

Here an outline of Yurke's treatment of broadband squeezing will be given. Restricting oneself to one spatial dimension and one polarization of the electromagnetic field, the quantized electric field operator of an electromagnetic wave travelling in the positive x–direction, which is incident on a detector with bandwidth B may be expanded in plane-wave modes as follows:

$$E(x,t) = \mathcal{E} \int_B d\omega\, \omega^{1/2} \left[a(\omega)\, e^{-i\omega(t - x/c)} + a^{\dagger}(\omega)\, e^{i\omega(t - x/c)} \right]$$

$$\equiv E^{(+)}(x,t) + E^{(-)}(x,t) \qquad (1.39)$$

where the electric field amplitude $\mathcal{E}$ contains the polarization and all constants necessary to make the photon creation and annihilation operators dimensionless. $E^{(+)}$ and $E^{(-)}$ are usually referred to as positive- and negative-frequency part of the electric field. In the following the spatial dependence will be suppressed for simplicity by evaluating the

field operator at the position of the detector, which is chosen as origin $x = 0$.

The creation and annihilation operators satisfy the usual continuum commutation relations:

$$[\, a(\omega), a^{\dagger}(\omega') \,] = \delta(\omega - \omega')$$
$$[\, a(\omega), a(\omega') \,] = [\, a^{\dagger}(\omega), a^{\dagger}(\omega') \,] = 0 \; . \qquad (1.40)$$

Let Ω denote some reference frequency (such as the frequency of the local oscillator in homodyne or heterodyne detection for example). Then the electric field operator may be expressed in the following way:

$$E(x,t) = \sqrt{2\Omega}\; \mathcal{E}\, [\, X_1(t,\Theta) \cos(\Omega t + \Theta) + X_2(t,\Theta) \sin(\Omega t + \Theta) \,] \; , \qquad (1.41)$$

with *quadrature phase operators* which are defined *with respect to the carrier frequency* Ω :

$$X_1(t,\Theta) = \int_B d\omega \left(\frac{\Omega + \omega}{2\Omega} \right)^{\frac{1}{2}} [\, a(\Omega + \omega)\, e^{i\Theta} e^{-i\omega t} + \text{h.c.} \,]$$
$$= \int_0^{\Delta\omega} d\omega \; [\, \chi_1(\omega,\Theta)\, e^{-i\omega t} + \text{h.c.} \,] \qquad (1.42)$$
$$\text{with} \quad \chi_1(\omega,\Theta) = \left(\frac{\Omega + \omega}{2\Omega} \right)^{\frac{1}{2}} a(\Omega + \omega)\, e^{i\Theta} + \left(\frac{\Omega - \omega}{2\Omega} \right)^{\frac{1}{2}} a^{\dagger}(\Omega - \omega)\, e^{-i\Theta}$$

(the second expression holds only in the case of a frequency band that is symmetric about the centre frequency Ω, which will be assumed from now on). The orthogonal quadrature phase operator may be found by means of the following relation:

$$X_2(t,\Theta) = X_1\left(t,\Theta - \frac{\pi}{2}\right) . \qquad (1.43)$$

Squeezing results if a non-linear device such as a four-wave mixer establishes correlations of the type

$$b(\Omega \pm \omega) = C(\pm\omega)\, a(\Omega \pm \omega) + S(\pm\omega)\, a^{\dagger}(\Omega \mp \omega) \qquad (1.44)$$

between pairs of sideband-modes

$$a_{\pm} \equiv a(\Omega \pm \omega) . \qquad (1.45)$$

Since all of the operators $a_{\pm}$ and $b_{\pm}$ must satisfy the commutation relation Eq.(1.40), the functions $C(\omega)$ and $S(\omega)$ must obey

$$\begin{aligned} &|C(\omega)|^2 - |S(\omega)|^2 = 1 \\ &C(\omega)\, S(-\omega) = C(-\omega)\, S(\omega) \end{aligned} \qquad (1.46)$$

and consequently $|C(\omega)|$ and $|S(\omega)|$ must be symmetric functions of ω. It is worth mentioning that the above transformation thus constitutes a linear canonical transformation (cf. the previous section). Note the similarity of Eq.(1.44) with the squeezed *single-mode* annihilation operators given by the Bogoljubov transformation Eq.(1.12).

The vacuum states of the operators $a(\omega)$, uniquely determined by

$$\begin{aligned} &a(\omega)\,|0\rangle_a = 0 \qquad \text{for all } \omega \\ &{}_a\langle 0\,|\,0\rangle_a = 1 , \end{aligned} \qquad (1.47)$$

constitute squeezed states for the modes $b(\omega)$ of Eq.(1.44), as was discovered by Yuen (1976) for the single-mode case $\omega = 0$. Substituting Eq.(1.44) into Eq.(1.42) and making use of Eq.(1.46), it is straightforward to prove

$$
\begin{aligned}
&{}_a\langle 0 \mid X_1(t,\Theta) \mid 0 \rangle_a = 0 \\
&{}_a\langle 0 \mid X_1^2(t,\Theta) \mid 0 \rangle_a = \int_0^{\Delta\omega} d\omega \left\{ \mid C(\omega) \mid^2 + \mid S(\omega) \mid^2 \right. \\
&\qquad \left. + 2\sqrt{1-\left(\frac{\omega}{\Omega}\right)^2}\ \mathrm{Re}\left[C(\omega)\, S(-\omega)\, e^{2i\Theta} \right] \right\}.
\end{aligned}
\tag{1.48}
$$

In order to define broadband squeezing it is useful to introduce the spectral variance

$$
V(\omega,\Theta) = \mid C(\omega) \mid^2 + \mid S(\omega) \mid^2 + 2\sqrt{1-\left(\frac{\omega}{\Omega}\right)^2}\ \mathrm{Re}\left[C(\omega)\, S(-\omega)\, e^{2i\Theta} \right] . \tag{1.49}
$$

For the identity tranformation $C(\omega) = 1$ and $S(\omega) = 0$, and therefore for a coherent input, $V(\omega,\Theta) = 1$ holds. Hence *squeezing* is said to occur in the quadrature phase X_1 (or X_2) of the electric field whenever the spectral noise level in X_1 (or X_2) drops below the coherent level, i.e. $V(\omega,\Theta) < 1$.

In practical situations the carrier frequency $\frac{\Omega}{2\pi}$ is an optical frequency, i.e. of the order of 5×10^{14} Hz, while $\frac{\Delta\omega}{2\pi}$ will extend to roughly 10^4 Hz; under these circumstances the fraction $\frac{\omega}{\Omega}$ may be ignored.

Finally, anticipating some concepts concerning the detection of squeezing, explained in Section 2.3, it should be remarked that Yurke (1985) has shown that the spectral quantity given by Eq.(1.49) can be measured directly by feeding the output of the heterodyne detector into a spectrum analyzer. In other words, by scanning the frequency ω one can monitor $V(\omega)$, and a recorded drop below unity thus indicates the presence of squeezing in the light-field.

Broadband squeezing is an important feature in the applications of squeezing which the present thesis will be dealing with. Thus in the novel type of laser gyroscopes (Marte and Walls, 1987) which employ squeezed light to enhance the sensitivity (cf. Section 2.4.2), the optical fiber produces broadband squeezed light via a non-linear interaction. In the squeezed reservoir lasers introduced in Chapter 3 the broadband character of the squeezed bath modelling the incoherent pumping as well as the spontaneous decay is also essential.

CHAPTER 2 HOW CAN SQUEEZED STATES BE APPLIED ?

2.1 Quantum Noise in Optical High Precision Measurements

The practical importance of squeezed states techniques lies in the fact that in a squeezed state the inevitable quantum noise is redistributed. Thus one may eliminate fluctuations in some observable of interest - at the cost of "aggravated" noise in its canonical counterpart. This opens up the possibility of a better signal to noise ratio by means of measurement schemes where the enhanced noise of the other system observable does *not* feed back into the measurement, as in the so-called *back action evading quantum non-demolition measurements* (for references see Chapter 5 of Milburn (1982)).

Of course considerations of this kind are of practical interest only if the standard quantum limit has been reached, that is if all other, classical, noise sources have been reduced to an extent that the intrinsic quantum noise becomes a noticeable limitation. Although this quantum limit involves Planck's constant h, which is a very small number indeed, it can still represent a serious obstacle when trying to measure as minute an effect as the displacement of a macroscopic (free) mass by a gravitational wave (for a thorough discussion of such measurements see the review article by Caves et al. (1980)).

Optical interferometers in particular are among the devices whose performance has reached a level, where quantum noise becomes apparent. In Fig.2 two common types of interferometer are depicted: the Mach-Zehnder and the Fabry-Perot interferometer. Because of the high precision achievable, interferometry has been employed in an extremely wide spectrum of applications, including astronomy, laser gyroscopes

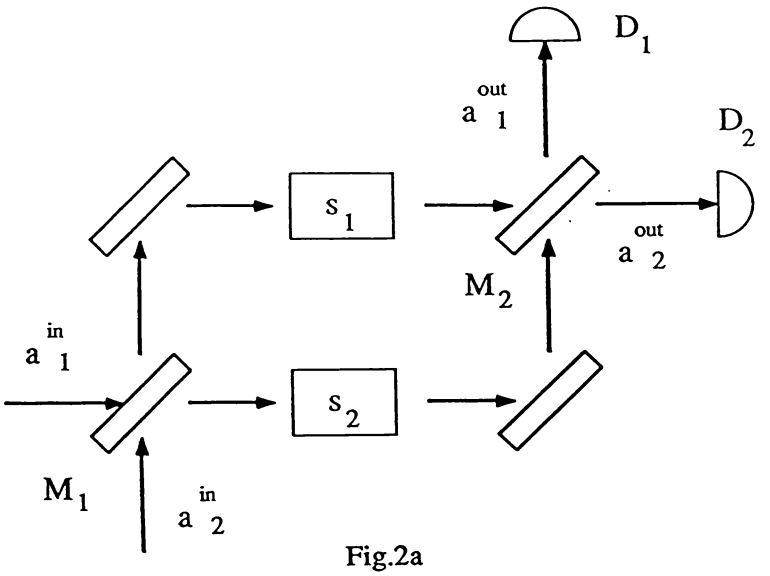

Fig.2a

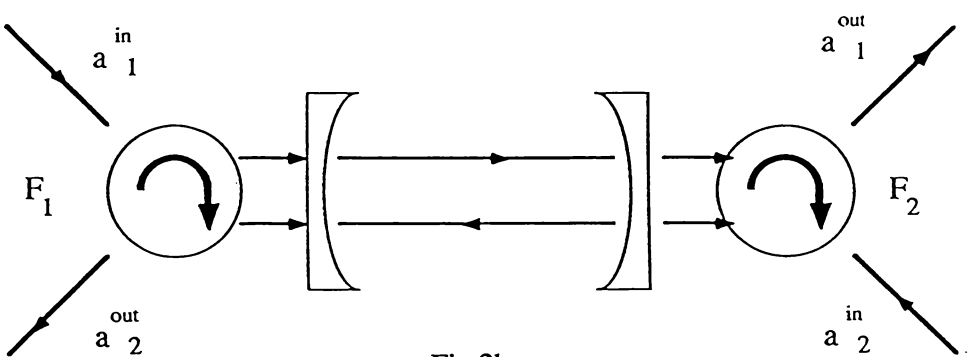

Fig.2b

Fig. 2 Two common types of interferometers:

(a) Mach-Zehnder interferometer (b) Fabry-Perot interferometer

M_i semitransparent mirrors F_i Faraday rotators

S_i phase shifters

D_i photodetectors

used for navigation in modern airplanes and optical tests of general relativity.

Thus it is not surprising that a considerable amount of literature is available on squeezing with respect to the problem of noise in interferometers, such as the analysis of interferometer noise due to photon number fluctuations and radiation pressure (Caves, 1981, Walls and Milburn, 1983). Only recently Grangier et al. (1987) have reported enhanced sensitivity in a polarization interferometer (a kind of Mach-Zehnder interferometer with polarizing beamsplitters) by injecting the squeezed output from a parametric amplifier into the "dark" or unused port of their interferometer.

Noise-reduction in optical devices is only *one* aspect of squeezing and by no means covers the interest physicists take in squeezed states. The broadness of the field is reflected in the variety of contributions to the recent special issues on squeezing of the Journal of the Optical Society of America and of the Journal of Modern Optics (J. Opt. Soc. Am. B **4**(10), 1987, and J. Mod. Opt. **34**(6,7), 1987). Besides the various generation schemes for squeezing, the mathematical properties, coherence, propagation and detection of squeezed states are investigated.

Another effect brought about by squeezing is the *inhibition of the phase decay* of two-level atoms irradiated by squeezed light, predicted by Gardiner (1986, Gardiner, Parkins, and Collett, 1987). This led to the investigation of a new type of lasers, the *squeezed reservoir lasers* (Marte and Walls, 1988, Marte, Ritsch, and Walls, 1988), which will be dealt with in Chapter 3. In such a laser either the resonator cavity or the atoms are coupled to a bath prepared in a broadband squeezed state.

2.2 The Phase/Photon Number Uncertainty Relation

Typically, in an interferometer one infers an unknown quantity from the phase (or frequency) shift it induces. However, there is no proper quantum mechanical operator associated with phase. A considerable number of contributions on how to resolve this problem exist in the relevant literature (see, e.g., the references given by Sanders et al. (1986)). One approach, first introduced by Susskind and Glogower (1964) and later applied by Carruthers and Nieto (1968), Loudon (1973) and others, establishes independent, non-commuting "sine" and "cosine" operators

$$C_\varphi = \frac{1}{2}(e + e^\dagger)$$
$$S_\varphi = \frac{1}{2i}(e - e^\dagger), \qquad (2.1)$$

where e = "$e^{i\varphi}$" stands for a non-Hermitean operator defined by

$$e = (n+1)^{-\frac{1}{2}} a = \sum_{\nu=0}^{\infty} |\nu\rangle\langle\nu+1| \qquad (2.2)$$

with n being the photon number operator $n = a^\dagger a$. (Since the operator (n+1) and its inverse are positive definite, the formal square root is well defined.) Note that $ee^\dagger$ is equal to the identity operator, but $e^\dagger e$ is not, and e and $e^\dagger$ do not commute. The following commutation relations can be derived:

$$[C_\varphi, n] = i S_\varphi$$
$$[S_\varphi, n] = -i C_\varphi , \qquad (2.3)$$

which lead to the uncertainty relations

$$\Delta n\, \Delta C_\varphi \geq \frac{1}{2} \; | \langle S_\varphi \rangle |$$

$$\Delta n\, \Delta S_\varphi \geq \frac{1}{2} \; | \langle C_\varphi \rangle | \,. \qquad (2.4)$$

However, Haken (1970) shows that in the classical limit $1 \ll \langle n \rangle$ a heuristic phase "operator" φ satisfying

$$[\, n, \varphi \,] = i \qquad (2.5)$$

$$\Delta n\, \Delta\varphi \geq \frac{1}{2} \qquad (2.6)$$

may be used.

Strictly speaking the squeezed states introduced in Chapter 1 constitute minimum uncertainty states of the quadrature phase observables X_1 and X_2 and thus do *not* minimize the photon number and phase uncertainty relation. Sanders et al. (1986) discuss in some detail the limit where the squeezed states approach number/phase uncertainty states. They come to the conclusion that the coherent states become approximate photon number and phase uncertainty states in the classical high excitation limit $\langle n \rangle \rightarrow \infty$. They also demonstrate that a strongly squeezed vacuum state cannot constitute a photon number and phase uncertainty state, since in the limit $r \rightarrow \infty$ both products, $\Delta n\, \Delta C_\varphi$ and $\Delta n\, \Delta S_\varphi$, diverge.

On the other hand, squeezed light obviously exhibits phase-sensitive fluctuations (demonstrated, e.g., by Fig.1). Thus by adding a sufficiently large coherent part to the squeezed vacuum it is possible to reduce the variance in the quadrature orthogonal to the coherent excitation, i.e. the "phase noise", compared to a coherent state with the same mean photon number, whilst increasing the quadrature noise along the coherent excitation, the "amplitude noise".

Assuming that the mean photon number is sufficiently large, so that Eq.(2.6) may be used and the equality sign holds approximately, we immediately get the following estimate for the spread in phase of a coherent state :

$$\Delta\varphi = \frac{1}{2\sqrt{< n >}} \quad , \tag{2.7}$$

since $(\Delta n)^2 = < n >$ holds in a coherent state.

Note that from Eq.(2.7) one can infer that the error of a phase measurement in a two-port interferometer with coherent inputs is given by $\Delta\varphi = (2<n>)^{-1/2}$ (Dorschner et al., 1980).

Using Eq.(1.25) for a squeezed state with "reduced phase noise" or "bunching", as it is often called, i.e. with $\vartheta = \pi$ for the choice $\alpha \in R$, we find the following measure for $\Delta\varphi$:

$$\Delta\varphi = \frac{1}{2\sqrt{(<n> - \sinh^2 r)\, e^{2r} + 2 \sinh^2 r \cosh^2 r}} \tag{2.8}$$

or

$$\Delta\varphi \approx \frac{e^{-r}}{2\sqrt{<n>}} \qquad \text{for } <n> \gg \sinh^2 r \ . \tag{2.9}$$

Along these lines Caves (1981) and others (cf. Yurke et al. (1986) and the references therein) have demonstrated that by feeding a squeezed vacuum instead of an ordinary vacuum into the usually unused port of the interferometer, one can improve the sensitivity of the interferometer.

2.3 Detection of Squeezing

Before proceeding to applications of squeezed states methods of detecting squeezed light will be discussed briefly.

2.3.1 Homodyne and Heterodyne Detection

Since one of the main characteristics of squeezed light is the fact that the two quadrature operators X_1 and X_2 have unequal noise, we require some sort of measuring device which allows a selective measurement of one quadrature or the other.

In a *homodyne scheme* (cf. for example the review article by Loudon and Knight (1987)) an input signal characterized by an operator a and a very strong *local oscillator* field with operator a_{LO} are combined on a beamsplitter with amplitude reflection and transmission coefficients r and t. The effect of the lossless symmetric beamsplitter can be described as a unitary transformation:

$$\begin{bmatrix} b_1 \\ b_2 \end{bmatrix} = \begin{pmatrix} r & t \\ t & r \end{pmatrix} \begin{bmatrix} a_{LO} \\ a \end{bmatrix}$$

$$\text{with} \qquad |r|^2 + |t|^2 = 1, \qquad t^* r + r^* t = 0. \tag{2.10}$$

In conventional homodyning one choses $|r|^2 \ll |t|^2$ and the output from only one photodetector is analyzed. Hence one measures the photon number

$$b_1^\dagger b_1 = |r|^2 a_{LO}^\dagger a_{LO} + t^* r a^\dagger a_{LO} + r^* t a_{LO}^\dagger a + |t|^2 a^\dagger a \,, \tag{2.11}$$

which is time-independent, since the signal and the local oscillator have the *same* frequency in homodyne detection. When the local oscillator light is prepared in a coherent state $|\alpha_{LO}\rangle$, the expectation value of the above operator is given by

$$\begin{aligned} &\langle b_1^\dagger b_1 \rangle = |r|^2 |\alpha_{LO}|^2 + 2|t||r||\alpha_{LO}| \langle E(\vartheta) \rangle + |t|^2 \langle a^\dagger a \rangle \ , \\ &\text{where} \qquad E(\vartheta) = \frac{1}{2}\left[e^{i\vartheta} a^\dagger + e^{-i\vartheta} a \right] \\ &\text{with} \qquad \vartheta = \arg(r) - \arg(t) + \phi_{LO} = \frac{\pi}{2} + \phi_{LO} \ . \end{aligned} \tag{2.12}$$

Here ϕ_{LO} denotes the phase of the local oscillator and the relative phase of r and t has been chosen to be $\frac{\pi}{2}$ in order to satisfy the second condition in Eq.(2.10). For a sufficiently large local oscillator amplitude α_{LO}, or more precisely if the *fundamental assumption* of all homodyning schemes

$$|t||\alpha| \ll |r||\alpha_{LO}| \tag{2.13}$$

is satisfied (with α denoting the complex amplitude of the signal), only the dominant terms proportional to α_{LO} have to be kept in the expression Eq.(2.13). Then the expectation value and variance of the photon number operator $N_1 = d_1^\dagger d_1$ are given approximately by

$$\begin{aligned} &\langle N_1 \rangle = |r|^2 |\alpha_{LO}|^2 + 2|t||r||\alpha_{LO}| \langle E(\vartheta) \rangle \\ &V(N_1) = |r|^2 |\alpha_{LO}|^2 \left[|r|^2 + 4|t|^2 V(E(\vartheta)) \right] \ . \end{aligned} \tag{2.14}$$

From this it becomes obvious that the condition $|r|^2 \ll |t|^2$ in conventional homodyning guarantees that the noise in the local oscillator is largely

suppressed and the fluctuations in the input signal determine the resulting noise.

This makes such a device an ideal tool to detect squeezing since the dominant noise term depends on the phase of the local oscillator. By scanning the phase ϕ_{LO} of the local oscillator, one can "project" onto the quadrature phase observable

$$X_{\phi_{LO}} = \frac{1}{2}\left(a\, e^{-i\phi_{LO}} + a^{\dagger} e^{i\phi_{LO}}\right) \qquad (2.15)$$

(cf. Eq.(1.26)) in the signal and detect the characteristic phase-dependence in the departure from Poissonian statistics that is typical for a squeezed input. Sub-Poissonian statistics correspond to $V(E(\vartheta)) < \frac{1}{4}$.

In order to avoid the additional noise from the local oscillator, Yuen and Chan (1983) have suggested a two-port or *balanced homodyne scheme,* depicted in Fig.3a, where a 50% beamsplitter is used ($|r| = |t| = \frac{1}{\sqrt{2}}$) and the *difference* of the photocurrents from two photodetectors is recorded. Schumaker (1984) has presented a comparison of the signal to noise ratios in one-port compared to two-port homodyning or direct detection.

Heterodyning (cf. Yuen and Shapiro (1978, 1980) and Shapiro and Wagner (1984)) represents a *non-degenerate* version of homodyning (see Fig.3b): a broadband signal centered around a frequency Ω and a local oscillator are recombined on a beamsplitter (in practical situations the frequency of the local oscillator and Ω coincide). Feeding the output of the photodetector into a spectrum analyzer allows one to observe the interference or "beating" between the centre frequency mode Ω and a particular sideband at, say, $\Omega + \Delta\omega$, the so-called signal, in contrast to the dc photocurrent observed in the degenerate case of homodyning.

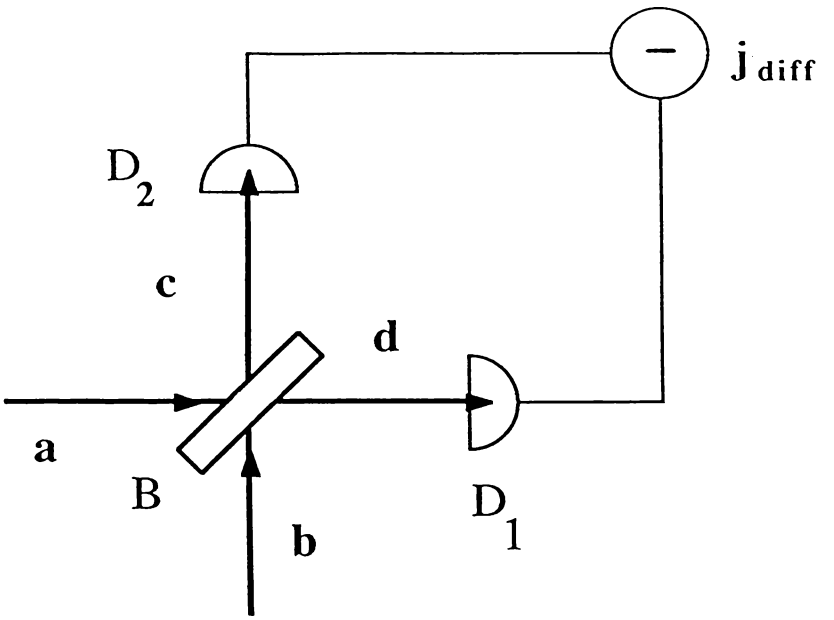

Fig.3a

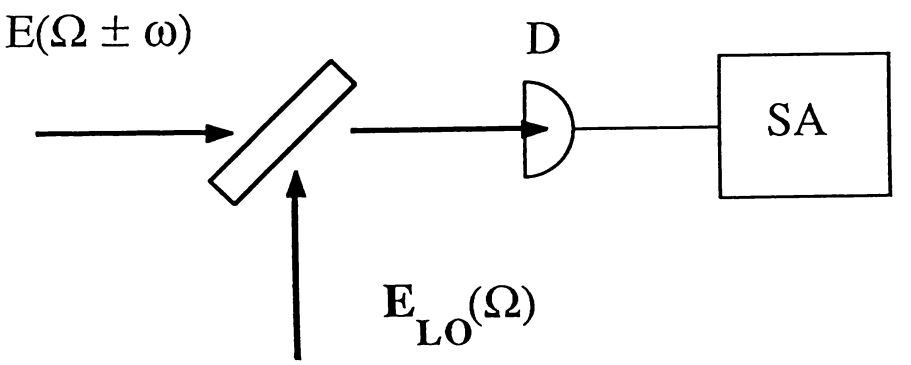

Fig.3b

Fig.3 Two conventional schemes used for detection of squeezing:

(a) balanced homodyning: the signal is combined with a strong local oscillator on a 50% beamsplitter B, behind the beamsplitter the difference of the photocurrents induced in the photodetectors D_1 and D_2 is recorded

(b) heterodyning: a broadband signal centered around a frequency Ω is combined with a strong local oscillator field of frequency Ω, the output from the beamsplitter is detected by a photodetector D and analyzed by a spectrum analyzer SA

Such a device is used to detect broadband squeezing which involves correlated pairs of sideband modes $\Omega \pm \Delta\omega$, as was discussed in Section 1.4.

Here one should point out that although squeezing and sub-Poissonian statistics are two *independent* features which some light source may or may not exhibit, L. Mandel (1982) has proved that whenever a homodyne detection scheme is used to detect squeezing then one will also find sub-Poissonian statistics if the squeezing parameter r is in phase with the coherent amplitude α. This is so because of the fundamental assumption in homodyning that the local oscillator is in a highly excited classical state. This forces Mandel's Q parameter (Mandel, 1979)

$$Q = \frac{[\,<(\Delta n)^2> - <n>\,]}{<n>}\ , \qquad (2.16)$$

a measure of the departure from Poissonian statistics (with Q = 0 corresponding to Poissonian statistics and Q negative/positive corresponding to sub/super-Poissonian statistics), to be always negative for appropriately prepared squeezed light entering such a detection device. Hence in the following amplitude squeezing and sub-Poissonian statistics will be often referred to interchangeably - although this is not strictly rigorous.

Finally, it will be demonstrated by means of a simple calculation that a balanced homodyne scheme such as depicted in Fig.3a, used to determine the relative phase ϕ between two input modes which are *both* prepared in squeezed states, can indeed give rise to a reduced final variance $V(\phi)$ in the detected phase. What is meant is a reduction

compared to conventional phase-measurement devices using coherent light.

Let a and $b\,e^{-i\phi}$ denote the two incident modes which are prepared in squeezed states:

$$|\psi\rangle_{in} = |\alpha, r_a e^{i\vartheta_a}\rangle \; |\beta, r_b e^{i\vartheta_b}\rangle \; . \tag{2.17}$$

For simplicity we take all parameters to be real and assume $\vartheta_a = \vartheta_b = \pi$; as discussed above, the latter assumption means that the two modes have reduced phase fluctuations. Introducing modes c and d behind the 50% beamsplitter:

$$c = \frac{a + be^{-i\phi}}{\sqrt{2}} \qquad\qquad d = \frac{a - be^{-i\phi}}{\sqrt{2}} \; , \tag{2.18}$$

the differenced photocurrent measured by the two photo-diodes D_1 and D_2 can be written as

$$j_{diff}(\phi) = c^{\dagger} c - d^{\dagger} d = 2\,\mathrm{Re}\{\, a\, b^{\dagger} e^{i\phi} \,\} \; . \tag{2.19}$$

The expectation value of j_{diff} in the state Eq.(2.17) is easily found to be

$$\langle j_{diff}(\phi) \rangle = 2\,\alpha\,\beta\cos\phi \tag{2.20}$$

and the variance can be approximated by

$$V(\, j_{diff}(\phi)\,) = \alpha^2 e^{-2r_b} + \beta^2 e^{-2r_a} + 2\,(\,\alpha^2 \sinh 2r_b + \beta^2 \sinh 2r_a\,)\cos^2\phi$$
$$\text{for} \qquad |\alpha|^2 \gg \sinh^2 r_a, \qquad |\beta|^2 \gg \sinh^2 r_b \; . \tag{2.21}$$

From the error Δj_{diff} one can infer the error of the phase measurement with the help of the usual linear regression formula:

$$\Delta\phi = \frac{\Delta j_{diff}}{\left| \frac{\partial \langle j_{diff} \rangle}{\partial \phi} \right|}$$

$$= \frac{\sqrt{\alpha^2 e^{-2r_b} + \beta^2 e^{-2r_a} + 2\,(\alpha^2 \sinh 2r_b + \beta^2 \sinh 2r_a)\cos^2\phi}}{|\,2\,\alpha\,\beta \sin\phi\,|} \,. \qquad (2.22)$$

Clearly, the minimum error occurs at angles $\phi = n\,\pi/2$ (n integer); that is maximal resolution is achieved when one operates at a zero fringe intensity of the photocurrent. In this case we obtain the result

$$(\Delta\phi)_{min} = \frac{\sqrt{\alpha^2 e^{-2r_b} + \beta^2 e^{-2r_a}}}{2\,\alpha\,\beta}$$

$$= \frac{e^{-r}}{\sqrt{2}\alpha} \qquad \text{for} \quad \alpha = \beta,\ r_a = r_b \equiv r \,, \qquad (2.23)$$

in agreement with the estimate given in Section 2.2. This suggests an improvement by a factor e^{-r} over the standard quantum limit, which in this context is defined as the noise-level due to a coherent input of the same intensity that is $|\alpha|^2$ (since we have assumed $|\alpha|^2 + \sinh^2 r_a \approx |\alpha|^2$). However, the restriction $|\alpha|^2 \gg \sinh^2 r_a$, $|\beta|^2 \gg \sinh^2 r_b$ limits the validity of Eq.(2.23), hence it holds for weak squeezing only. If we had chosen an input with reduced amplitude fluctuations, formally achieved by replacing r_a and r_b by $-r_a$ and $-r_b$, we would have found increased noise in $\Delta\phi$. Also, if only one input is prepared in a squeezed state and the other is in a coherent state, then the performance will be improved, but only by a factor of roughly $\frac{1}{\sqrt{2}}$, since $1 \gg e^{-r}$ for strong squeezing.

2.3.2 Photo-Counting Statistics of a Squeezed State

In this Section the case of *direct* detection is studied: the photon counting statistics of a single-mode squeezed state incident on a photodetector is calculated from an explicit quantum model of the photodetector. In the standard theories, developed by Glauber, Mollow and others, the photodetector is modelled as a reservoir of quantum harmonic oscillators. Walls, Milburn and Carmichael (1982) have already derived a photo-counting formula for non-classical fields on very general grounds, using generalized P-representations. However, they assume a constant field, thus ignoring the attenuation of the field coupled to the detector.

The goal of this section is to generalize Mollow's quantum theory of field attenuation (Mollow, 1968) to squeezed states. The model consists of a single-mode field in a squeezed state $| \gamma; r, \vartheta=0 >$, in a cavity coupled for $t > 0$ to a bath of N harmonic oscillators. Assuming dipole coupling and making the rotating wave approximation (RWA), the Hamiltonian of the system is given by:

$$H = \hbar\,\omega\, a^{\dagger}a + \hbar \sum_{j=1}^{N} \omega_j\, b_j^{\dagger} b_j - i\hbar \left(a^{\dagger} \sum_{j=1}^{N} g_j\, b_j - \text{h.c.} \right) . \qquad (2.24)$$

We assume a zero-temperature bath, that is the detector is in its groundstate at $t = 0$. Thus the initial condition for the total density matrix W(t), describing the field and the bath, reads:

$$W(0) = \rho_F(0) \otimes \rho_B(0)$$

with

$$\rho_F(0) = |\gamma; r,\vartheta=0><\gamma; r,\vartheta=0|$$

$$\rho_B(0) = |0>_B\,{}_B<0| \qquad |0>_B = \prod_{j=0}^{N} |0>_j \ . \tag{2.25}$$

Following standard methods for Markovian systems (Gardiner, 1983) one may eliminate the information in the bath, which is not of immediate interest, and establish a *master equation* for the reduced density matrix ρ_F describing the field alone:

$$\frac{\partial \rho_F}{\partial t} = \frac{\kappa}{2}\left(2\, a\, \rho_F\, a^\dagger - a^\dagger a\, \rho_F - \rho_F\, a^\dagger a\right) . \tag{2.26}$$

(Eq.(2.26) is expressed in the interaction picture, i.e. the free evolution of the field has been transformed away so that only terms proportional to the cavity damping rate κ occur.) This master equation is easily converted to a corresponding Fokker-Planck equation:

$$\frac{\partial P}{\partial t} = \frac{\kappa}{2}\left(\frac{\partial}{\partial \alpha}\alpha + \frac{\partial}{\partial \beta}\beta\right) P(\alpha, \beta; t) \tag{2.27}$$

for a *complex P-represenation* $P(\alpha, \beta; t)$. The complex P-representation, a function of two independent complex variables α and β and one of the generalized P-representations introduced by Drummond and Gardiner (1980), is used here since the single-mode field is prepared in a squeezed that is non-classical state, where one would not expect a positive definite Glauber P-representation to exist. Eq.(2.26) has to be solved subject to the initial condition Eq.(2.25), which now takes on the form

$$P_0(\alpha,\beta) \equiv P(\alpha,\beta;t=0) \qquad (2.28)$$
$$= -\frac{1}{2\pi \sinh r}\exp\left\{(\alpha-\gamma)(\beta-\gamma^*)+\frac{1}{2}\coth r\left[(\alpha-\gamma)^2+(\beta-\gamma^*)^2\right]\right\},$$

that is the complex P-represenation of a pure squeezed state $|\gamma; r, \vartheta=0>$ (Walls and Milburn, 1983). The solution is easily found to be

$$P(\alpha,\beta;t) = e^{\kappa t}\, P_0\left(\alpha e^{\frac{\kappa t}{2}}, \beta e^{\frac{\kappa t}{2}}\right) . \qquad (2.29)$$

Given this result one is able to calculate the photo-counting probability. The general expression for the probability for m photo-counts in a time interval T has been derived by Kelly and Kleiner (1964) (see also Lax and Zwanziger (1973) and the brief review in Risken (1984)) :

$$P(m,T) = \mathrm{Tr}_F\left\{\rho_F : \frac{\Omega^m}{m!}\exp(-\Omega) :\right\} , \qquad (2.30)$$

where

$$\Omega = \eta\int_0^T I(t)\,dt \qquad (2.31)$$

with I (t) being the intensity operator and η a parameter representing the fraction of the intensity taken out from the cavity, multiplied by the quantum efficiency of the photo-electron counter. For the simple present case of a single-mode situation and *short* time intervals T, Eq.(2.30) reduces to the more tractable form

$$P(m,T) = \sum_{n=0}^{\infty} <n|\left\{\rho_F : \frac{(\mu\, a^\dagger a)^m}{m!}\exp(-\mu\, a^\dagger a) :\right\}|n> , \qquad (2.32)$$

where $\mu = \eta T$ and the trace over the field variables has been conveniently expressed in number states. Using a correspondence between c–numbers and normally ordered operators given by Gardiner (1983), one can re-express this in terms of the complex P-representation:

$$P(m, T) = \frac{\mu^m}{m!} \int_{C_1} d\alpha \int_{C_2} d\beta \; P(\alpha, \beta; t) \; e^{-\mu \alpha\beta} \; (\alpha\beta)^m . \tag{2.33}$$

Here the contours C_1 and C_2 denote the respective imaginary axes from $-\infty$ to ∞. Taking Eq.(2.29) into account and introducing new variables z and z' according to

$$z = \alpha \; e^{\frac{\kappa t}{2}}, \qquad z' = \beta \; e^{\frac{\kappa t}{2}} \tag{2.34}$$

yields

$$P(m, T) = \frac{\mu(t)^m}{m!} \int_{C_1} dz \int_{C_2} dz' \; P_0(z, z') \; e^{-\mu(t)\, zz'} \; (z\, z')^m \tag{2.35}$$

with the re-parametrization

$$\mu(t) \equiv \mu \, e^{-\kappa t} . \tag{2.36}$$

This integral has been calculated by Walls et al. (1982), except that now μ has to be replaced by the explicitly time-dependent parameter $\mu(t)$ in order to take the field attenuation into account. Hence one can adopt their solution with this slight modification:

$$P(m;\mu(t)) = \sum_{n=m}^{\infty} \binom{n}{m} [\mu e^{-\kappa t}]^{n-m} (1 - \mu e^{-\kappa t})^{m} P_n , \qquad (2.37a)$$

where P_n denotes the *photon number distribution* of a squeezed state $|\alpha; r e^{i\vartheta}\rangle$ which explicitly reads

$$P_n = |\langle n | \alpha; r e^{i\vartheta}\rangle|^2 = \frac{1}{n!\,\mu} e^{-|\beta|^2 + \frac{\nu^* \beta^2}{2\mu} + \frac{\nu \beta^{*2}}{2\mu}}$$

$$\times \left|\frac{\nu}{2\mu}\right|^n \left|H_n\left(\frac{\beta}{\sqrt{2\mu\nu}}\right)\right|^2$$

$$\text{with} \quad \mu = \cosh r, \; \nu = e^{i\vartheta} \sinh r, \; \beta = \mu\alpha + \nu\alpha^* . \qquad (2.37b)$$

The photon number distribution P_n and the photo-absorption probability $P(m; \mu(t))$ given by Eqs.(2.37a,b) are plotted in Fig.4. The solid reference curve corresponds to the Poissonian distribution of a coherent state with the same value of α . Fig.4a demonstrates that the distribution of a squeezed state with $\vartheta = 0$ is significantly narrower, that is displays sub-Poissonian statistics; on the other hand $\vartheta = \pi$ yields a super-Poissonian photon number distribution. For $t \to \infty$ the entire incident field is absorbed by the detector, thus the photo-absorption probability approaches the photon number distribution for $\mu(t) \to 0$. For shorter times the peak of the distribution is shifted towards smaller photon numbers, as can be seen in Fig.4b.

Letting the squeezing parameter approach zero, one recovers the result derived by Mollow (1968) for coherent states and, by using a similar model, also by Scully and Lamb (1969) if one realizes that the latter authors were treating intracavity absorption and ideal photodetection, i.e. $\eta = 1$.

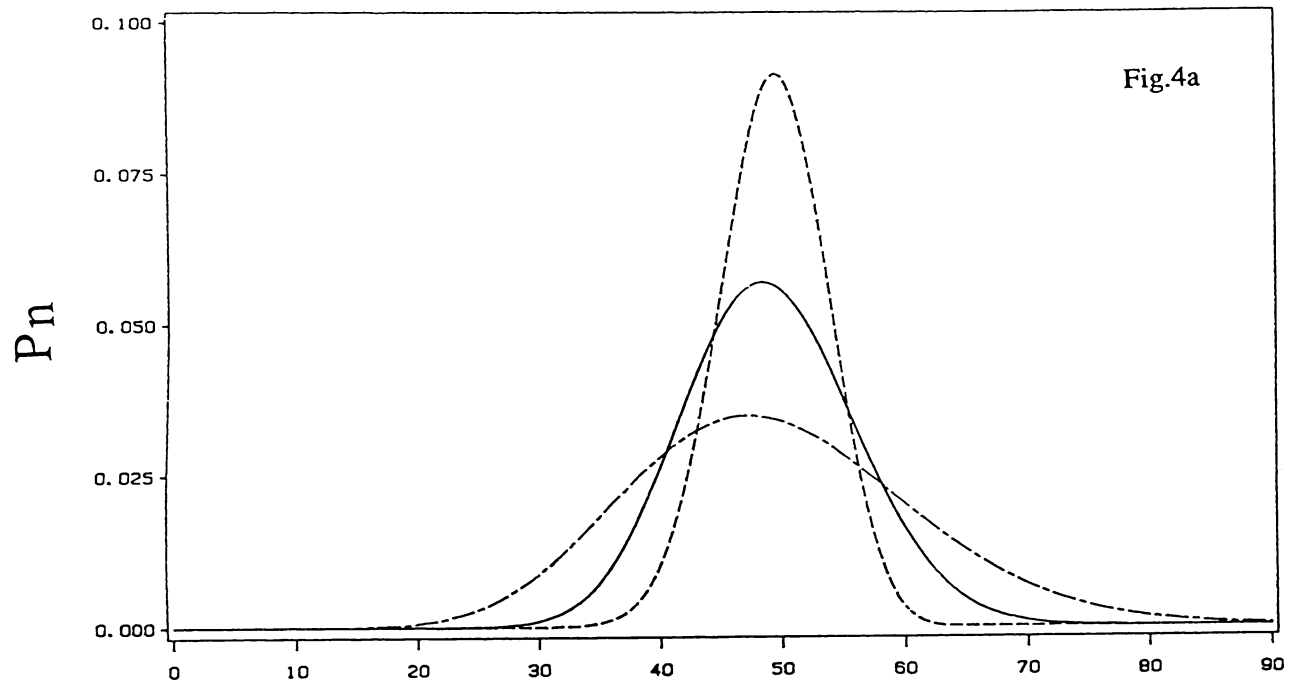

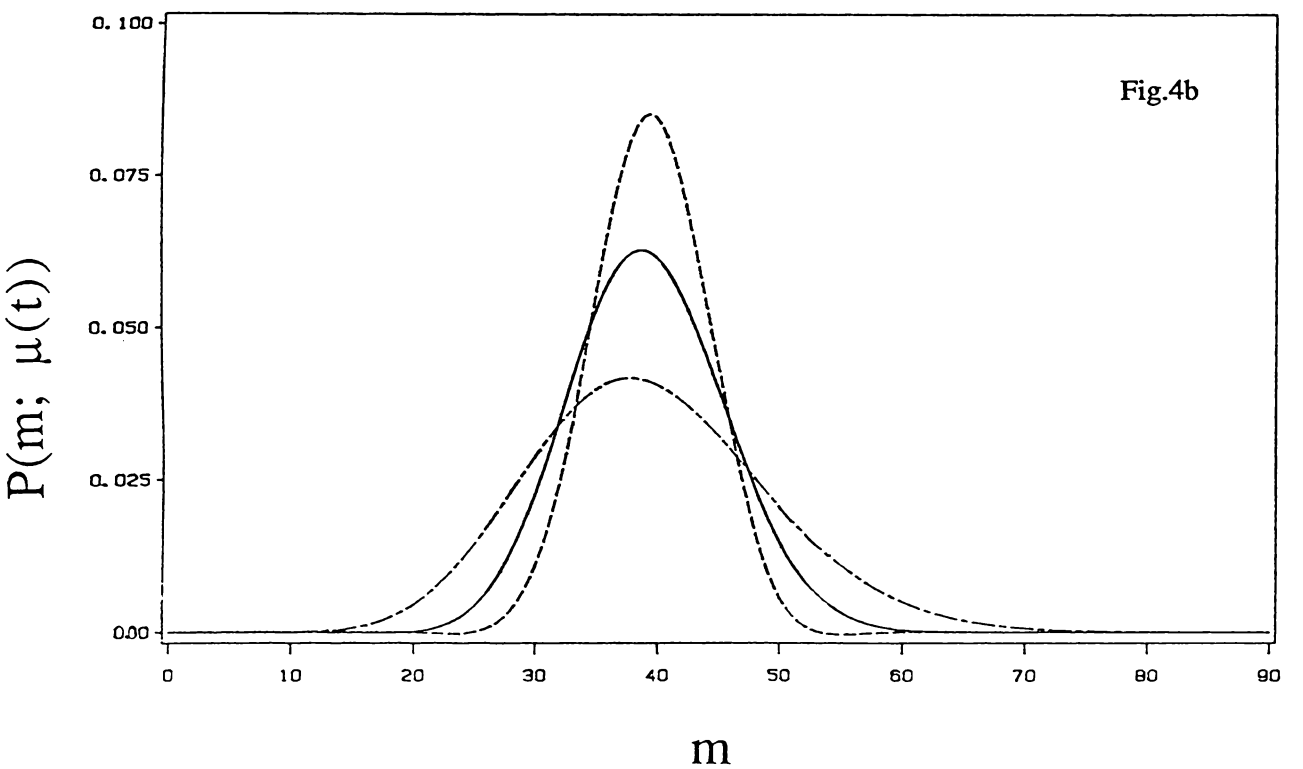

Fig. 4 Photon number distribution and photo-counting statistics of a squeezed state $|\alpha, r e^{i\vartheta}\rangle$ with $\alpha = 7$

(a) the photon number distribution P_n

(b) the photo-absorption probability $P(m; \mu(t))$ for $\mu(t) = 0.2$

_____ $r = 0$

_ · _ · _ · _ · _ $r = 0.5, \vartheta = 0$

_ _ _ _ _ _ $r = 0.5, \vartheta = \pi$

In Appendix A a quantum mechanical model is presented for the photodetection of light consisting of two (or possibly more) monochromatic modes with distinctive frequencies.

2.4 Enhanced Sensitivity of a Laser gyroscope by Means of Squeezed Light

2.4.1 The Sagnac Effect

Long before the invention of laser gyroscopes, mechanical gyroscopes were used to detect rotations (especially in ships and airplanes). Such a mechanical gyroscope basically consists of a spinning mass which is suspended in a frame and retains its axis of rotation when tilted or subjected to an external rotation, due to conservation of angular momentum. In 1913 Sagnac described an effect which - along with the development of lasers - was to revolutionize the technology of gyroscopes: he had discovered that *light* may be used to detect external rotations. All modern laser gyroscopes are based on this effect. There are two classes of modern laser gyroscopes, the *passive* ones, also referred to as Sagnac interferometers, which consist of an empty ring cavity with injected signals from an external source, and the *active* gyroscopes, where the ring cavity is filled with a lasing medium.

For the sake of simplicity the Sagnac effect will be explained first for the simpler case of a passive device. A Sagnac interferometer comprises a ring cavity with one port, consisting of a beamsplitter coupling two counterpropagating light beams of the same frequency from an external source into the cavity. The two independent counterpropagating waves interfere to form a standing wave inside the cavity; this interference pattern may be observed through the

beamsplitter. For the sake of transparency in the following intuitive argument, we visualise the Sagnac interferometer as possessing the simple geometry of a circular optical ring, as shown in Fig.5. The arrow X indicates the location of the beamsplitter, where light is coupled into or taken out of the cavity and where the interference pattern is observed.

What will happen if this entire set-up is set rotating at a rate Ω about an axis specified by the unit vector $\mathbf{n}_\Omega$ (which is assumed to have a non-zero component normal to the plane area A spanned by the interferometer ring)? Viewing Fig.5 it becomes evident that the effective optical cavity lengths for the clockwise and the counterclockwise wave drift apart due to the external rotation, because the location of the beamsplitter, as seen from an outside stationary inertial frame, changes from X to a new position X' during a finite time interval Δt. Thus the time required for a "full round trip" (the time elapsed, since the beam left X at $t = t_0$ until it reaches the beamsplitter at X' again) is unequal for the co- and counter-rotating waves. This difference in optical path length Δs due to the external rotation induces a phase shift $\Delta\varphi$ in the interference pattern behind the beamsplitter at X', where the two beams are recombined.

Of course, such a simple qualitative argument cannot replace a proof. A rigorous yet rather lengthy, derivation of the classical Sagnac effect from first principles, i.e. Maxwell's equations, can be found in a review article by Post (1967). There the induced phase shift is calculated assuming non-relativistic velocities and linear dispersion, yielding

$$\Delta\varphi = \frac{8\pi}{\lambda_0 c_0}\,\Omega\;\mathbf{A}\cdot\mathbf{n}_\Omega \quad . \tag{2.38}$$

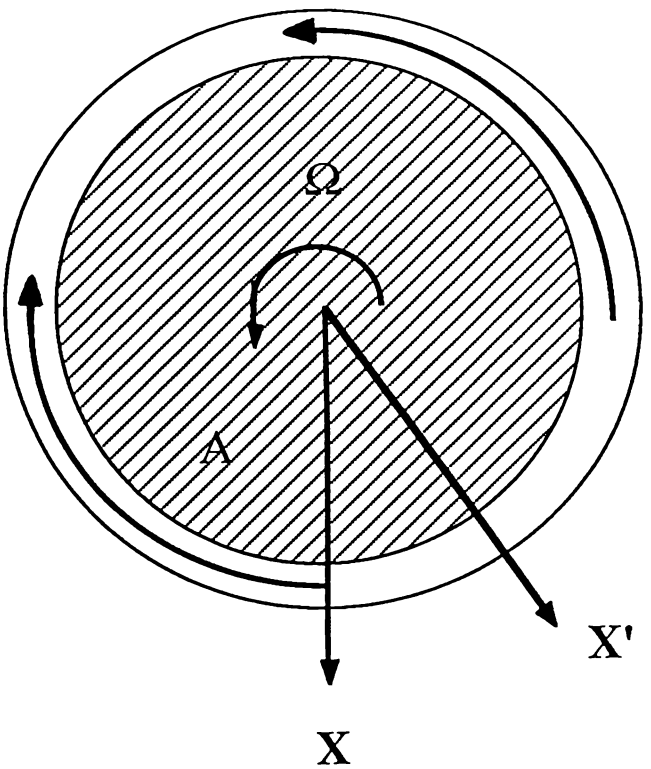

Fig.5 Simplified Sagnac interferometer: two counterpropagating waves in a ring cavity which is rotating at a rate Ω ,

A area confined by the cavity ring

X location of the cavity output mirror at an initial time

X' location of the cavity output mirror at a later time

Here, λ_o and c_o denote the wave length and the speed of light in vacuum, respectively, and **A** stands for a vector of magnitude A normal to the area A enclosed by the ring cavity of the interferometer. The linear relation between $\Delta\varphi$ and the rotation rate Ω enables one to monitor external rotations by measuring this phase shift. Note that the effect is also proportional to the area confined by the interferometer ring. It has been demonstrated that the expression Eq.(2.38) is widely insensitive to the shape and geometry of the plane loop (even generalizations to curved surfaces are possible), and that Eq.(2.38) also applies if the ring cavity is filled with a dispersive medium.

Finally it should be remarked that there is an *additional* phase shift due to the Doppler-effect; however the Doppler-shift is smaller by a factor of v/c, so it can be ignored in the non-relativistic regime we are concerned with.

In an *active* rotation sensor, that is a rotating ring laser (see the textbook by Sargent, Scully, and Lamb (1974) for a detailed discussion of the ring laser), a similar effect occurs: in the presence of an external rotation the cavity resonance frequencies of the clockwise and counterclockwise running mode in the laser become two distinct frequencies, separated by a frequency-shift $\Delta\omega$, which, again, is proportional to $\Omega\ \mathbf{n}_\Omega \cdot \mathbf{A}$.

2.4.2 A Four-Wave mixing Fiber-Optic Rotation Sensor

In this Section a new fiber-optic rotation sensor technique is presented (Marte and Walls, 1987). The novelty lies in the fact that the fiber acts not only as a passive Sagnac rotation sensor, but at the same time its non-linearity *produces* squeezed light via a four-wave mixing interaction, thus giving rise to improved resolution. This enhanced

sensitivity corresponds to a noise reduction below the standard quantum limit of a passive Sagnac interferometer; for a thorough discussion of the quantum noise in an *active* ring-laser gyroscope see the treatment by Cresser et al. (1982a,b).

The theory of four-wave mixing in optical fibers has been investigated by Reid (1987) and Shelby et al. (1986). Dealing with an experimental situation where one injects light consisting of a strong pump beam at frequency ω and weaker sidebands with frequencies $\omega \pm \Delta\omega$ into both ends of a fiber, as shown in Fig.6, we study the following model Hamiltonian:

$$H = H_a + H_b \tag{2.39}$$

with

$$H_a = \hbar(\omega + \Delta\omega)\, a_+^\dagger a_+ + \hbar(\omega - \Delta\omega)\, a_-^\dagger a_- + 4\hbar\chi |\varepsilon_a|^2 a_+^\dagger a_+ + 4\hbar\chi |\varepsilon_a|^2 a_-^\dagger a_-$$
$$+ \{ [\, 2\hbar\chi \varepsilon_a^2 e^{-2i\omega t} a_+^\dagger a_-^\dagger + a_+ \Gamma_{a_+}^\dagger + a_- \Gamma_{a_-}^\dagger + (a_+^\dagger \varepsilon_a + a_- \varepsilon_a^*)\, B_a] + \text{h.c.} \}$$

(with H_b obtained by replacing $a \leftrightarrow b$ in the expression for H_a). This describes the interaction of the two classical pump fields with amplitudes ε_a and ε_b with two pairs of quantized sideband modes $a_\pm$ and $b_\pm$ in the fiber medium, which is characterized by the non-linear susceptibility χ. Absorption losses are modelled by coupling the quantized sidebands to independent reservoirs $\Gamma_{a\pm}$ and $\Gamma_{b\pm}$. Following the theory of Shelby et al. (1986), guided acoustic wave Brioullin scattering is taken into account by coupling the modes to the phonon baths B_a and B_b.

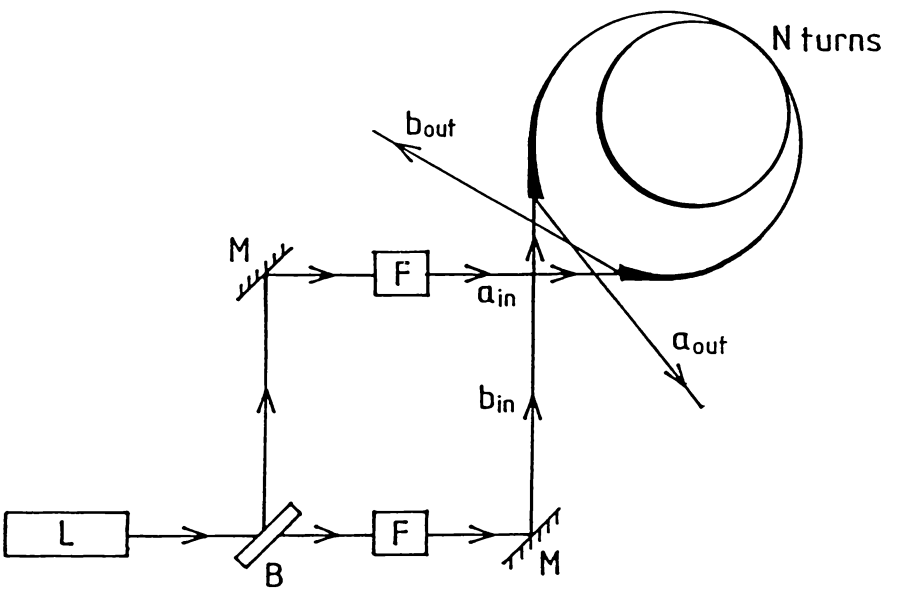

Fig.6 A four-wave-mixing fiber-optic Sagnac interferometer: light coming from a laser L is split by a 50% beamsplitter B (M denoting mirrors and F Faraday rotators) into two modes a_{in} and b_{in} propagating through the non-linear fiber medium in opposite directions; the output modes a_{out} and b_{out} are subsequently recombined in a heterodyne detection scheme

This model Hamiltonian involving pairs of quantized sidebands is used, because the output from the fiber will be fed into a balanced heterodyning scheme and finally analyzed with a spectrum analyzer, tuned to a frequency $\Delta\omega$. It has already been discussed in Section 1.4 (which dealt with broadband squeezing) and in Section 2.3.1 (which briefly discussed heterodyning) that such a procedure brings about contributions from sidebands at $\omega\pm\Delta\omega$. Since the total result is found by simply adding up all these contributions, it is sufficient to study a model Hamiltonian describing only a particular - but arbitrary - pair of sideband modes of each broadband light-field in the input, instead of taking the *whole* continuum.

Note that there is *no* direct coupling between the a and b modes; this is so because, for two beams travelling in opposite directions through the fiber, the terms coupling $a_\pm$ and $b_\pm$ together fail to satisfy the phase-matching condition and are thus suppressed.

The solutions to the Heisenberg equation of motion following from Eq.(2.39) have been calculated by Milburn et al.(1987). Evaluated at the end of a fiber of length l, these solutions read

$$\begin{aligned} \varepsilon_a(l) &= \exp\left(2i\chi\, |\varepsilon_a(0)|^2\, l \right) \varepsilon_a(0) \\ a_\pm(l) &= \exp\left(2i\chi\, |\varepsilon_a(0)|^2\, l \right) \tilde{a}_\pm(l) \ , \end{aligned} \tag{2.40}$$

where $\tilde{a}_\pm(l)$ may be obtained from the result

$$\tilde{X}_a(l) = e^{-\gamma l}\,\tilde{X}_a(0) + e^{-\gamma l}\int_0^l dz\, e^{\gamma z}\,[\,\Gamma_{a_+}(z) + \Gamma_{a_-}^{\dagger}(z)\,]\ ,$$

$$\tilde{Y}_a(l) = e^{-\gamma l}\,\tilde{Y}_a(0) + 4\chi l\,|\varepsilon_a(0)|^2\, e^{-\gamma l}\,\tilde{X}_a(0)$$

$$- 2\,\varepsilon_a(0)\, e^{-\gamma l}\int_0^l dz\, e^{\gamma z} B_a + e^{-\gamma l}\int_0^l dz\, e^{\gamma z}\frac{[\,\Gamma_{a_+}(z) - \Gamma_{a_-}^{\dagger}(z)\,]}{i}$$

$$+ 4\chi\,|\varepsilon_a(0)|^2\, e^{-\gamma l}\int_0^l dz \int_0^z dz'\, e^{\gamma z'}\,[\,\Gamma_{a_+}(z') + \Gamma_{a_-}^{\dagger}(z')\,]\ , \qquad (2.41)$$

with the definitions

$$\tilde{X}_a(z) = \tilde{a}_+(z) + \tilde{a}_-^{\dagger}(z)$$

$$\tilde{Y}_a(z) = \frac{1}{i}\,[\,\tilde{a}_+(z) - \tilde{a}_-^{\dagger}(z)\,]\ . \qquad (2.42)$$

Corresponding equations hold for b.

After the beams have left the fiber they evolve freely. Here, a preferential phase shift Ψ is introduced into the pump ε_b with respect to the sidebands. The output of the fiber is then fed into a balanced heterodyne detection scheme (cf. Fig.3b), discussed in Section 2.3.1. The two beams incident on the beamsplitter now read

$$a(t) = \varepsilon_a(l)\, e^{-i\omega t} + a_+(l)\exp[\,-i\,(\omega+\Delta\omega)\,t\,] + a_-(l)\exp[\,-i\,(\omega-\Delta\omega)\,t\,]$$

$$b(t) = e^{i\phi}\,(\,\varepsilon_b(l)\, e^{-i\omega t} e^{i\Psi} + b_+(l)\exp[\,-i\,(\omega+\Delta\omega)\,t\,] + b_-(l)\exp[\,-i\,(\omega-\Delta\omega)\,t\,]\,), \qquad (2.43)$$

with $a_\pm(l)$ and $b_\pm(l)$ given by Eq.(2.40) to Eq.(2.41). If the fiber undergoes rotations the Sagnac effect will give rise to a relative phase shift between the modes $a_\pm$ travelling in, say, the clockwise direction and the modes $b_\pm$ travelling in the opposite direction within the fiber. This

(classical) effect has been incorporated in Eq.(2.43) by simply introducing an overall relative phase factor $e^{i\phi}$ into the mode b with respect to a. For a fiber of length l wound in a coil of diameter D the Sagnac shift is found to be (Ezekiel and Arditty, 1982)

$$\phi = \frac{l D \omega}{c^2} \Omega \; \mathbf{n}_A \cdot \mathbf{n}_\Omega \quad , \tag{2.44}$$

where c is the speed of light in vacuum and $\mathbf{n}_A$ a unit vector normal to the area confined by the fiber coil. However, if the fiber medium possess a non-linear refractive index, then the "signal", that is the Sagnac phase shift, can be greatly enhanced compared to the linear result Eq.(2.44), as has been demonstrated by Kaplan and Meystre (1981). This non-linear effect by itself represents a way of improving the signal to noise ratio in a conventional laser gyroscope using coherent light (Kaplan et al., 1985). In the currently considered Sagnac interferometer using squeezed light such an amplification of the classical Sagnac phase shift (in an appropriately chosen non-linear four-wave mixing fiber medium) could also contribute to an enhancement of the signal to noise ratio.

Note that ϕ depends upon the frequency ω of the travelling beam. Thus, for the sake of simplicity, we assume that the sideband frequencies are close enough to the pump frequency to ignore the difference in the Sagnac shift for pump and sidebands, i.e. $\phi(\omega) \approx \phi(\omega \pm \Delta\omega)$.

Using Eq.(2.19), we get

$$j_{diff}(\phi) = 2\,\mathrm{Re}\{\, a\, b^\dagger \,\} = [\, A\, e^{-i\Delta\omega t} + B\, e^{-2i\Delta\omega t} + C\,] + \text{h.c.} \quad , \tag{2.45}$$

where the operators A,B and C are functions of the operators given in Eq.(2.43). If one uses a spectrum analyzer operating at frequency $\Delta\omega$ to analyze the photocurrent, one essentially measures the component

$$j_\Delta(\phi) = \mathrm{Re}\,(A)$$

$$= \varepsilon\,\mathrm{Re}\,\{\,\tilde{b}_+ e^{i\phi} + \tilde{b}_-^\dagger e^{-i\phi} + \tilde{a}_+ e^{-i(\phi+\Psi)} + \tilde{a}_- e^{i(\phi+\Psi)}\} \qquad (2.46)$$

with $\varepsilon = |\varepsilon_a(1)| = |\varepsilon_b(1)|$.

By means of Eq.(2.42) one may re-write this equation as

$$j_\Delta(\phi) = \varepsilon\,\mathrm{Re}\,\{\,X_b(\phi) + X_a(-\phi-\Psi)\,\}\ . \qquad (2.47)$$

The expectation values and variances of the photocurrent have been calculated by Shelby et al. (1986). Assuming a coherent input

$$\langle \tilde{a}_+(0) + \tilde{a}_-^\dagger(0)\rangle = \langle \tilde{b}_+(0) + \tilde{b}_-^\dagger(0)\rangle = \alpha\ , \quad \alpha \text{ real}$$

$$\frac{1}{i}\langle \tilde{a}_+(0) - \tilde{a}_-^\dagger(0)\rangle = \frac{1}{i}\langle \tilde{b}_+(0) - \tilde{b}_-^\dagger(0)\rangle = 0\ , \qquad (2.48)$$

we find

$$\langle j_\Delta(\phi)\rangle = \varepsilon\,\alpha\, e^{-\frac{L}{2}}\{\,[\cos\phi + \cos(-\Psi-\phi)] + 2r\,[\sin\phi + \sin(-\Psi-\phi)]\,\}\ . \qquad (2.49)$$

L represents the absorption loss $L = l\gamma$. The "squeezing parameter" r is given by

$$r = 2\chi\varepsilon^2 t_1\ , \qquad (2.50)$$

with t_1 being the propagation time of the beams through the fiber.

The variance of the real part of the quadrature operator $X(\phi)$ is found to be

$$V(\phi) \equiv V(\mathrm{Re}\{\tilde{X}(\phi)\}) \tag{2.51}$$
$$= \frac{1}{4}\left[1 + 2r\left(\frac{1-e^{-L}}{L}\right)\sin 2\phi + \left\{ \frac{\beta}{2\chi}\left(\frac{1-e^{-L}}{L}\right) + 2r\left(\frac{1-(1+L)e^{-L}}{L^2}\right)\right\} 2r\,(1-\cos 2\phi)\right],$$

where β is a measure of the strength of the guided-acoustic-wave Brioullin scattering.

Since the modes a and b are statistically independent, their variances simply add. Thus we infer

$$V(j_\Delta(\phi)) = \varepsilon^2[\, V_a(-\Psi-\phi) + V_b(\phi)\,] \,. \tag{2.52}$$

The aim is to minimize the error in ϕ. Again, since the modes a and b are independent, the respective terms can be optimized independently. Let these minima be reached at, say, $\phi = \phi_a{}^{min}$ and $-\Psi-\phi = \phi_b{}^{min}$, respectively. The symmetrical appearance of terms corresponding to a and b in Eq.(2.49) and Eq.(2.51) then imposes $\phi_a{}^{min} = \phi_b{}^{min}$; hence we adjust the phases so that $\Psi = -2\phi$.

First, we wish to treat the simple case with *no* losses (L = 0) and *no* Brioullin scattering ($\beta = 0$). In this case Eq.(2.52) reduces to

$$V(j_\Delta(\phi)) = \frac{\varepsilon^2}{2}\left[\, 1 + 2r\sin 2\phi + \frac{(2r)^2}{2}\,(1-\cos 2\phi)\,\right] \,. \tag{2.53}$$

From Eq.(2.49) we derive

$$S = \left| \frac{\partial \langle j_\Delta(\phi) \rangle}{\partial \phi} \right| = 2\alpha\varepsilon \left| -\sin\phi + 2r\cos\phi \right| \tag{2.54}$$

for the slope. Strictly speaking there is a difference in the procedure of minimizing $\Delta\phi$ compared to the simple example in Section 2.2, since the angle minimizing the variance,

$$\phi_V = \frac{1}{2} \arctan\left(-\frac{1}{r}\right) , \tag{2.55}$$

and the angle maximizing the slope,

$$\phi_S = \arctan\left(-\frac{1}{2r}\right) , \tag{2.56}$$

do not coincide. But considering that the difference between ϕ_V and ϕ_S is of order $1/r^2$ for the case of interest $1 \ll r$ we may neglect this difference. Evaluating Eq.(2.54) at ϕ_S and Eq.(2.53) at ϕ_V and expanding in powers of $1/r$ we find

$$V_{min} = \frac{\varepsilon^2}{2} \left(\frac{1}{2r}\right)^2 \left[1 + O\left(\frac{1}{r^2}\right) \right] \tag{2.57}$$

$$S_{max} = 2\alpha\, \varepsilon\, 2r \left[1 + O\left(\frac{1}{r^2}\right) \right] \tag{2.58}$$

and therefore

$$(\Delta\phi)_{min} = \frac{1}{\sqrt{2}\alpha_0} \frac{1}{(2r)^2} \tag{2.59}$$

with

$$\alpha_0 \equiv 2\alpha = \langle \tilde{X}_a(0) + \tilde{X}_b(0) \rangle \ . \tag{2.60}$$

Here, the final error in ϕ has been expressed in terms of α_o, the total input amplitude. The result Eq.(2.59) displays an improvement over standard measurements by a factor $1/(2r)^2$. Compared to the ideal case discussed in Section 2.2 the exponential behaviour is replaced by a power law $\propto 1/r^2$.

We emphasize that a factor 1/(2r) in Eq.(2.59) is due to *amplification* of the coherent input by the non-linearity in the fiber, whereas the remaining factor 1/(2r) is the actual squeezing effect, that is it stems from the reduced phase noise. The *practically achievable* gain in sensitivity of the proposed squeezing techique opposed to the standard technique is given by the ratio

$$\frac{[(\Delta\phi_{min})]_{SQ}}{[(\Delta\phi)_{min}]_{ST}} = \frac{\alpha_{ST}}{2\alpha_{SB}(2r)^2} \quad . \tag{2.61}$$

Here, α_{SB} denotes the amplitude input of one sideband and α_{ST} the coherent input entering a standard Sagnac interferometer. The most interesting case is the one in which the total input into both schemes is the same, that is α_{ST} equals the input of both sidebands α_{SB} plus the pump ε in each beam. In this case the ratio Eq.(2.61) will be less than unity, provided the squeezing parameter is at least

$$r = \frac{1}{2}\sqrt{\frac{2\alpha_{SB}+\varepsilon}{\alpha_{SB}}} \quad . \tag{2.62}$$

In other words, for values r exceeding this limit the squeezing technique outperforms conventional gyroscopes.

Finally, we may include small losses that are due to absorption and Brioullin scattering. Linearization with respect to L and β ($1 \ll L,\beta$) yields the following approximate expression:

$$(\Delta\phi)_{min} \approx \frac{1}{2r} \frac{\sqrt{\left(\frac{1}{2r}\right)^2 + \left(\frac{L}{3} + \frac{\beta}{2\chi r}\right)}}{\sqrt{2}\, 2\alpha\left(1 - \frac{L}{2}\right)} \quad . \tag{2.63}$$

Provided that $L \ll 1/r^2$ and $\beta/\chi \ll 1/r$, the corrections will be insignificant.

Summarizing it has been shown in this Section that the sensitivity of a passive Sagnac rotation sensor consisting of a fiber loop can be improved beyond the standard quantum limit. A new technique has been proposed in which the fiber generates the Sagnac phase shift to be measured *and* at the same time generates squeezed light with a better defined phase. This leads to an increase in sensitivity in the detection of the phase shift which is proportional to $1/r^2$. The squeezing parameter r is proportional to the non-linear susceptibility of the fiber medium, the intensity of the pump light and the length of the fiber.

Chapter 3 Quantum Theory of the Squeezed Reservoir Laser: Can Squeezed States be Used to Stabilize a Laser ?

Recently Gardiner has studied the effects of irradiating a two-level atom with squeezed light (Gardiner, 1986, Gardiner et al., 1987). As a result inhibition of atomic phase decay was predicted, provided the light consists of electric dipole radiation in a broadband squeezed state incident from a 4π solid angle. For the inversion decay the usual decay rate is found, but the polarization decay in such a situation involves *two* different transverse relaxation times for the real and imaginary parts of the atomic dipole moment. These relaxation times are inversely proportional to the variances of the two corresponding quadrature phases of the incident light. In the limit that the state of the electromagnetic field approaches a quadrature operator eigenstate, one transverse relaxation time becomes arbitrarily long, whereas the other transverse and longitudinal relaxation times tend towards zero accordingly. As a consequence of this an arbitrarily narrow peak appears in the spectrum of the fluorescent light emitted from the atom. A similar result was found investigating the fluorescence from a coherently driven two-level atom that is damped by a squeezed vacuum bath (Carmichael et al., 1987).

This raises the question of whether a similar effect would occur for N atoms inside an optical cavity such as a *laser system.* Will squeezing in the bath of electromagnetic modes which damps the laser atoms (or alternatively squeezing in the vacuum modes coupled to the laser cavity) alter the operating characteristics of the laser? How will the laser fluctuations and the laser linewidth be influenced? Since the phase fluctuations usually determine the linewidth of a laser, this might lead to the possibility of reducing the laser linewidth by squeezing the bath

quadrature phase operator which couples to the laser phase. This chapter will deal with questions of this kind, investigating the properties of the so-called *squeezed reservoir lasers* (Marte and Walls, 1988, Marte et al., 1988).

Another interesting question is whether the output from such a laser system coupled to a squeezed bath will display *sub-Poissonian photon statistics* . Recently laser schemes with sub-Poissonian statistics have been proposed by various research groups: Yamamoto and others have predicted (Yamamoto et al.,1986) and observed (Machida et al., 1987) sub-Poissonian statistics in a semiconductor laser which is incoherently pumped by a beam of electrons with pump-fluctuations suppressed below the shot noise. In a recent publication (Machida and Yamamoto, 1988) a 32% reduction below the standard quantum limit of the amplitude noise in such a laser system was reported to exist over a large bandwidth. Another way to achieve stabilization of the laser intensity below the shot noise level has been suggested by Caves (1987). He demonstrates that a negative feedback loop with one beamsplitter illuminated by low-power squeezed light can transform an ordinary laser output into a high-power squeezed state.

Sub-Poissonian statistics has (among other quantum effects) also been predicted for the so-called *micro-maser* (Filipowicz et al., 1986, Krause et al., 1986). A micro-maser consists of a single-mode microwave cavity with extremely high quality factor into which a monoenergetic beam of excited two-level atoms is injected at such a low rate that at most a single atom is present inside the resonator at a time. The microscopic nature of such a device prevents the loss of some quantum effects which are usually unobservable because they are averaged out.

This Chapter is organized as follows. Section 3.1 explains the quantum mechanical model of the laser and introduces the concept of

the squeezed reservoir laser. The corresponding master equation and Fokker-Planck equation are established in Section 3.2. Then the semiclassical theory will be investigated in Section 3.3 for the three cases of a so-called squeezed vacuum pump, a squeezed-pump laser in a general squeezed state and a laser model with a squeezed cavity. Section 3.4 deals with an appropriate van der Pol oscillator model and discusses the phase diffusion rate and the linewidth of both the squeezed-pump and the squeezed-cavity laser. In Section 3.5 the spectrum of the laser output fluctuations will be calculated from a linearized theory for the squeezed-pump laser. Finally, in Section 3.6 the conclusions of this investigation are summarized.

3.1 Quantum Mechanical Model of a Squeezed Reservoir Laser

In the early 1970s Haken and others (see Haken(1970) and references therein) developed a theory which treats the laser as an open quantum system, which is influenced by its surroundings (or "heatbath") that cause both damping and fluctuations. In the following we will study the modifications to the steady state characteristics and fluctuations of the laser that are brought about if one *squeezes* the reservoirs which comprise the environment of the laser system.

Two cases have to be considered. Firstly, we will analyze the influence of squeezing the reservoir interacting with the laser which is usually used to describe the spontaneous emission noise in the laser. This reservoir is assumed to consist of *inverted* (or negative frequency) harmonic oscillators. That is to say Glauber's quantum amplifier theory (Glauber, 1986) is applied to model the incoherent pumping of the two-

level atoms in the cavity. Preparing this reservoir in a squeezed state involves the above mentioned inhibition of atomic phase decay.

Note that such a model does not necessarily describe the pumping of real atoms with squeezed light from a third level which is later eliminated. It rather describes a situation where the lasing transition itself interacts with the squeezed electric dipole radiation. We call this system a *squeezed-pump laser* because such a scheme permits a reduction of the fluctuations in the atomic inversion.

Alternatively, one might squeeze the vacuum modes entering the laser cavity. Some aspects of such a system have recently been studied by Gea-Banacloche (1987). The conclusions drawn from the present theory include and confirm these predictions.

Along the lines of Haken's fully quantum mechanical treatment of a homogeneously broadened laser (Haken, 1970, 1981), we model the laser system by the simplest conceivable system consisting of N two-level atoms with transition frequency ω_0, coupled to a resonant single-mode running wave field in the laser cavity. Such a model has proven successful in describing a typical solid state laser. Assuming dipole coupling, the Hamiltonian governing the evolution of the atoms and the laser field alone is given by

$$H_{AF} = \hbar\omega_0 a^\dagger a + \frac{1}{2}\hbar\omega_0 S_z + ig\hbar (a^\dagger S_- - a S_+) \qquad (3.1)$$

within the rotating wave approximation (RWA). Here a and $a^\dagger$ are the boson annihilation and creation operators, g denotes the dipole coupling constant and $S_\pm$ and S_z denote the *collective* atomic operators

$$S_z = \sum_{\mu=1}^{N} \sigma_\mu^3$$

$$S_\pm = \sum_{\mu=1}^{N} \sigma_\mu^\pm \, e^{\pm i \mathbf{k} \cdot \mathbf{x}_\mu} \ , \tag{3.2}$$

where $\sigma_\mu{}^3$, $\sigma_\mu{}^\pm = \frac{1}{2}(\sigma_\mu{}^1 \pm i\, \sigma_\mu{}^2)$ (with the Pauli matrices $\sigma_\mu{}^j$ given by Eq.(1.31)).

In such a model the two-level "atoms" describe the lasing transition only; all other transitions of the real laser atoms that contribute quantum noise are formally absorbed in a quantum reservoir coupled to the two-level atoms. As stated above, in the present model the *incoherent pumping mechanism* and the *spontaneous decay* are taken into account by means of a reservoir of inverted harmonic oscillators (often referred to as a "negative temperature bath") coupled linearly to the lasing transition; thus we consider

$$H_{AB} = i\hbar\gamma (S_- \Gamma_p - \text{h.c.}) \tag{3.3}$$

within the RWA. The coupling constant γ is assumed real and frequency-independent (like all the other coupling constants of the problem). Note that in a bath of negative frequency oscillators the bath ladder operators $b\dagger(\omega)$ and $b(\omega)$ exchange roles. Hence we have the formal replacement

$$\begin{aligned} \hbar\omega &\longrightarrow -\hbar\omega \\ b(\omega) &\longrightarrow b^\dagger(\omega) \end{aligned} \tag{3.4}$$

compared to a bath of ordinary harmonic oscillators. Here is a possible way to model the population inversion in the laser due to optical

pumping directly from a model Hamiltonian. However, there are other means to achieve this and we emphasize that the choice of a bath of inverted harmonic oscillators is *not essential* for the results for the squeezed reservoir lasers derived below.

We assume that the fluctuations in the reservoir coupled to the atoms can be described by *squeezed white noise* (Gardiner and Collett, 1985). By definition this means that the bath is prepared in a broadband squeezed state (cf. Section 1.4), centered around a frequency Ω, where the number of quanta per unit bandwidth is constant. The bandwidth related to this broadband squeezed state is assumed broad compared to any other bandwidth in the problem (such as the atomic decay rates), but considerably less than Ω. For the sake of simplicity we assume resonance with the atomic transition, i.e. $\Omega = \omega_o$. Under these assumptions the correlations of the bath operator

$$\Gamma_p(t) = \int_{-\infty}^{0} d\omega\, e^{-i\omega t}\, b(\omega) \tag{3.5}$$

(which is a field operator evaluated at the position where all atoms are assumed to be located) can be approximated by Dirac delta functions in time:

$$\begin{aligned}
&< \Gamma_p^{\dagger}(t)\, \Gamma_p(t') > \;=\; (n_p + 1)\, \delta(t-t') \\
&< \Gamma_p(t)\, \Gamma_p^{\dagger}(t') > \;=\; n_p\, \delta(t-t') \\
&< \Gamma_p(t)\, \Gamma_p(t') > \;=\; m_p^{*}\, e^{i\omega_o(t+t')}\, \delta(t-t') \\
&< \Gamma_p^{\dagger}(t)\, \Gamma_p^{\dagger}(t') > \;=\; m_p\, e^{-i\omega_o(t+t')}\, \delta(t-t') \;.
\end{aligned} \tag{3.6}$$

This approximation by Dirac delta-functions is a valid description, provided the "memory" of the macroscopic reservoir is much shorter than any other time constant of interest in the system; in other words, if the environment is *Markovian* .

In Eq.(3.6) n_p is the number of photons in the bath and m_p stands for a complex squeezing parameter. (Note that as a consequence of Eq.(3.4) the roles of $\Gamma_p(t)$ and $\Gamma_p^\dagger(t)$ are exchanged in Eq.(3.6) when compared to the usual set of equations.) Note that the modulus of m_p is limited by

$$|m_p|^2 \leq n_p (n_p + 1) , \tag{3.7}$$

as follows from the requirement that $< [\Gamma_p(t) + \lambda \Gamma_p^\dagger(t)] [\Gamma_p^\dagger(t) + \lambda^* \Gamma_p(t)] >$ has to be positive for all complex numbers λ.

We also wish to investigate the effects of an additional classical (c–number) field driving the atoms. Hence we include the interaction Hamiltonian:

$$H_{cl} = i\hbar (S_- \varepsilon_p e^{i\omega_o t} - \text{h.c.}) . \tag{3.8}$$

A somewhat unusual notation ε_p for the amplitude of the *negative* frequency part of the classical field has been chosen. This is done in order to stress the fact that adding such a coherent classical part to the interaction between the (inverted!) bath and the atoms amounts to modelling the inverted bath prepared in a squeezed state with a *non-zero coherent mean* , as is well known. The relative phase between the large classical amplitude ε_p and the squeezing parameter m_p determines whether the photon-statistics in the bath are sub- or super-Poissonian,

that is whether the input displays reduced phase or amplitude fluctuations (cf. Section 2.2).

Finally, the cavity mode is also coupled to a reservoir characterized by the operator Γ_c modelling the vacuum modes of the electromagnetic field external to the cavity:

$$H_{FB} = i\hbar\kappa (a\Gamma_c^\dagger - \text{h.c.}) . \qquad (3.9)$$

Gea-Banacloche (1987) has recently studied some aspects of squeezing the modes of the vacuum field entering the cavity. Again assuming a Markovian system, that is a flat spectrum in the reservoir with correlations

$$\begin{aligned}
&< \Gamma_c^\dagger(t)\,\Gamma_c(t') > = n_c\,\delta(t-t') \\
&< \Gamma_c(t)\,\Gamma_c^\dagger(t') > = (n_c+1)\,\delta(t-t') \\
&< \Gamma_c(t)\,\Gamma_c(t') > = m_c\,e^{-i\omega_o(t+t')}\,\delta(t-t') \\
&< \Gamma_c^\dagger(t)\,\Gamma_c^\dagger(t') > = m_c^*\,e^{i\omega_o(t+t')}\,\delta(t-t') \qquad |m_c|^2 \le n_c\,(n_c+1) \qquad (3.10)
\end{aligned}$$

enables us to include his results. In sum we are thus dealing with the Hamiltonian

$$H = H_{AF} + H_{AB} + H_{cl} + H_{FB} + H_B , \qquad (3.11)$$

given by Eqs.(3.1), (3.3), (3.8) and (3.9). H_B stands for the (infinite energy) Hamiltonian of the reservoirs alone. It should be remarked that the theory characterized by a Hamiltonian of the general form Eq.(3.11) which couples the atoms and the cavity mode to *independent* reservoirs

is inappropriate if one is dealing with extremely strong fields (Haken, 1970).

3.2 The Master Equation and the Fokker-Planck Equation for the Squeezed Reservoir Laser

Given the above Hamiltonian for the proper laser system and its quantum environment, the standard procedure is to eliminate the reservoir degrees of freedom and derive equations which contain only the variables of the proper laser system explicitly, but implicitly incorporate the stochastic effects of the reservoirs which manifest themselves as damping and fluctuations.

There are at least three possible ways to deal with this problem: one can use quantum mechanical Langevin equations, a quantum master equation for the density matrix or a generalized Fokker-Planck equation. In the following we will choose whatever is most convenient. To start with, in this section a master equation will be derived and converted into a generalized Fokker-Planck equation. Later on, when calculating the linewidth and the noise in the laser, a method combining a Fokker-Planck and a Langevin equation will prove useful.

Here the approach of eliminating the information in the reservoir which was taken by Gardiner and Collett (1985) will be adopted. They have derived a *quantum master equation* for a system driven by squeezed white noise. Later Gardiner (1986) applied this general result to the case of a single two-level atom. Since we assume that there is no *direct* interaction (such as collisions) between the atoms in the laser cavity, a condition which typically holds in solid state lasers, it is straightforward to generalize the latter result to N two-level atoms simply by using collective operators. Thus the density matrix describing

N independent two-level atoms embedded in a (broadband) squeezed vacuum is found to obey the following master equation:

$$\frac{\partial \rho_A}{\partial t} = \frac{\gamma n_p}{2} [\, 2S_- \rho_A S_+ - \rho_A S_+ S_- - S_+ S_- \rho_A \,] + \frac{\gamma(n_p+1)}{2} [\, 2S_+ \rho_A S_- - \rho_A S_- S_+ - S_- S_+ \rho_A \,] - \gamma m_p [\, S_- \rho_A S_- \,] - \gamma m_p^* [\, S_+ \rho_A S_+ \,] \,. \tag{3.12}$$

In Eq.(3.12) the fast rotation at the optical frequency ω_o has been transformed away, thus the density matrix ρ_A describes the atomic degrees of freedom in a frame rotating at a rate ω_o. Note also that due to the fact that we are dealing with a bath of *inverted* harmonic oscillators the prefactors n_p and (n_p+1) are interchanged compared to the usual equation.

Following the standard derivation of the master equation of the laser (cf. Haken (1970) or Haake (1973) and the references found therein) and making use of the above master equation Eq.(3.12) in order to incorporate the new terms arising from the squeezing in the bath, we end up with a master equation for the density matrix ρ_{AF} which describes the N atoms and the cavity mode and explicitly reads:

$$\frac{\partial \rho_{AF}}{\partial t} = \left(\frac{\partial \rho_{AF}}{\partial t}\right)_A + \left(\frac{\partial \rho_{AF}}{\partial t}\right)_F + \left(\frac{\partial \rho_{AF}}{\partial t}\right)_{AF} + [\, \varepsilon_p S_- - \varepsilon_p^* S_+, \rho_{AF} \,] \tag{3.13}$$

where

$$\left(\frac{\partial \rho_{AF}}{\partial t}\right)_A = \frac{\gamma n_p}{2} [\, 2S_- \rho_{AF} S_+ - \rho_{AF} S_+ S_- - S_+ S_- \rho_{AF} \,] + \frac{\gamma(n_p+1)}{2} [\, 2S_+ \rho_{AF} S_- - \rho_{AF} S_- S_+ - S_- S_+ \rho_{AF} \,] - \gamma m_p [\, S_- \rho_{AF} S_- \,] - \gamma m_p^* [\, S_+ \rho_{AF} S_+ \,] \tag{3.13a}$$

$$\left(\frac{\partial \rho_{AF}}{\partial t}\right)_F = \frac{\kappa}{2} n_c \left[2\, a^\dagger \rho_{AF}\, a - a\, a^\dagger \rho_{AF} - \rho_{AF}\, a\, a^\dagger \right]$$

$$+ \frac{\kappa}{2} (n_c + 1) \left[2\, a\, \rho_{AF}\, a^\dagger - a^\dagger a\, \rho_{AF} - \rho_{AF}\, a^\dagger a \right]$$

$$- \frac{\kappa}{2} \left\{ m_c^* \left[2\, a\, \rho_{AF}\, a - a\, a\, \rho_{AF} - \rho_{AF}\, a\, a \right] + \text{h.c.} \right\} \qquad (3.13b)$$

$$\left(\frac{\partial \rho_{AF}}{\partial t}\right)_{AF} = \frac{1}{i\hbar} \left[H_{AF}, \rho_{AF} \right] . \qquad (3.13c)$$

Still following the standard procedure we make use of a characteristic function χ, defined as

$$\chi(\xi,\xi^*,\zeta,\beta,\beta^*) = \mathrm{Tr}_{AF} \left\{ e^{i\xi^* S_+}\, e^{i\zeta S_z}\, e^{i\xi S_-}\, e^{i\beta^* a^\dagger}\, e^{i\beta a} \right\} \qquad (3.14)$$

in order to establish the following correspondence between normally ordered operators and c-numbers:

$$\begin{array}{ccccc} v & \Leftrightarrow & S_- & \qquad \alpha & \Leftrightarrow & a \\ v^* & \Leftrightarrow & S_+ & \qquad \alpha^* & \Leftrightarrow & a^\dagger \\ \frac{D}{2} & \Leftrightarrow & S_z & & & \end{array} \qquad (3.15)$$

in the laser "Fokker-Planck Equation" (FPE) for the function P defined by

$$P(\alpha,\alpha^*,v,v^*,D) = \int d^2\xi\, d\zeta\, d^2\beta\; e^{-i\left(v\xi + v^*\xi^* + \frac{D}{2}\zeta + \alpha\beta + \alpha^*\beta^* \right)} \times \chi(\xi,\xi^*,\zeta,\beta,\beta^*) \qquad (3.16)$$

(with $d^2\beta \equiv d(\mathrm{Re}\beta)d(\mathrm{Im}\beta)$ etc.). The differential equation that follows for P is actually not a proper FPE since it involves derivatives up to fourth order in the atomic polarization variables v and v^* and even *infinite order derivatives*. in the atomic inversion D.

However, on grounds that N (the number of atoms in the cavity) is very large and assuming that the atomic polarization and inversion are proportional to N, one may truncate the equation and keep only derivatives up to second order. This yields an equation similar to a FPE (it is well-known that the diffusion matrix need not be positive definite in the presence of squeezing and therefore strictly speaking this still is not a proper FPE):

$$\frac{\partial P}{\partial t} = [\, L_A + L_F + L_{AF} + L_{cl} + L_{sq} \,]\, P \tag{3.17}$$

$$L_A = \gamma_\perp\left(\frac{\partial}{\partial v}\, v + \frac{\partial}{\partial v^*}\, v^*\right) + \frac{\partial}{\partial D}\,(\gamma_{||}\, D - \gamma N) + w_{12}\,\frac{\partial^2}{\partial v \partial v^*}\, N$$

$$- 2w_{12}\left(\frac{\partial^2}{\partial v \partial D}\, v + \frac{\partial^2}{\partial D \partial v^*}\, v^*\right) + \frac{\partial^2}{\partial D^2}\,(\gamma_{||}\, N - \gamma D) \tag{3.17a}$$

$$L_F = \kappa\left(\frac{\partial}{\partial \alpha}\,\alpha + \frac{\partial}{\partial \alpha^*}\,\alpha^*\right) + 2\,\kappa\, n_c\,\frac{\partial^2}{\partial \alpha \partial \alpha^*} \tag{3.17b}$$

$$L_{AF} = g\left(-\frac{\partial}{\partial \alpha}\, v - \frac{\partial}{\partial \alpha^*}\, v^* - \frac{\partial}{\partial v}\, D\,\alpha - \frac{\partial}{\partial v^*}\, D\,\alpha^* + 2\,\frac{\partial}{\partial D}\,(v^*\alpha + \alpha^* v)\right)$$

$$+ g\left(\frac{\partial^2}{\partial v^2}\, v\,\alpha + \frac{\partial^2}{\partial v^{*2}}\, v^*\alpha^* - 2\,\frac{\partial^2}{\partial D^2}\,(v^*\alpha + \alpha^* v)\right) \tag{3.17c}$$

$$L_{cl} = \varepsilon_p^*\left[\, 2\,\frac{\partial}{\partial D}\, v^* - \frac{\partial}{\partial v}\, D - 2\,\frac{\partial^2}{\partial D^2}\, v^* + \frac{\partial^2}{\partial v^2}\, v\,\right] + \text{h.c.} \tag{3.17d}$$

$$L_{sq} = \left\{ \gamma m_p\left[\,\frac{\partial}{\partial v}\, v^* + \frac{1}{2}\,\frac{\partial^2}{\partial v^2}\,(N + D)\,\right] + 2\,\kappa\, m_c\,\frac{\partial^2}{\partial \alpha^2}\right\} + \text{h.c.} \tag{3.17e}$$

Here the following new parameters have been introduced:

$$\gamma_{\parallel} = w_{12} + w_{21} , \qquad \gamma_{\perp} = \frac{1}{2}\gamma_{\parallel} \tag{3.18a}$$

and

$$w_{12} = \gamma(n_p + 1) , \qquad w_{21} = \gamma n_p . \tag{3.18b}$$

In an ordinary laser $\gamma_{\perp}$ and $\gamma_{\parallel}$ constitute the transverse and longitudinal atomic decay rates. The rate w_{12} denotes the transition rate $|1\rangle \rightarrow |2\rangle$ due to the incoherent pumping and w_{21} stands for the rate $|2\rangle \rightarrow |1\rangle$ due to non-lasing transitions. The meaning of the above decay rates in the squeezed reservoir laser will become clear in Section 3.3, where we treat the semiclassical theory.

The Liouville operator denoted by L_{sq} (Eq.(3.17e)) represents the changes due to the squeezing in the reservoirs. Note the *qualitative difference* between squeezing the reservoir coupled to the atoms compared to squeezing the vacuum modes entering the cavity: a non-zero m_p affects the diffusion matrix *as well as* the drift vector of the FPE, whereas a non-zero m_c contributes only to the diffusion. It is thus obvious that squeezing the atomic bath not only introduces phase-dependent noise but at the same time changes the *deterministic* behaviour of the laser. For the other case, where one squeezes the vacuum cavity modes, a similar effect occurs and the anisotropy in the noise influences the steady state (cf. Section 3.3), although this is not apparent yet.

We emphasize that *all* second order derivative terms have been kept - in contrast to the usual procedure of a further truncation based on a scaling argument around the laser threshold (Haken, 1970). This is necessary because the steady state characteristics of a squeezed-pump laser differ from an ordinary laser (as will be discussed in the next section) and hence this kind of scaling no longer applies.

3.3 The Semiclassical Theory

In order to get an initial idea of the qualitative behaviour due to the squeezing in the reservoirs, we will study the semiclassical theory in this section. That is we ignore the intrinsic quantum fluctuations for the moment and treat all quantities as c-numbers. This corresponds to neglecting the second order derivatives or "diffusion" terms in the FPE and keeping only the first order derivatives or "drift" terms describing the deterministic behaviour. Thus one considers the so-called *optical Bloch equations:*

$$\begin{aligned}
\dot{\alpha}_x &= -\kappa\,\alpha_x + g\,v_x \\
\dot{\alpha}_y &= -\kappa\,\alpha_y + g\,v_y \\
\dot{v}_x &= -\gamma_\perp (1+M)\,v_x + g\,D\,\beta_x \\
\dot{v}_y &= -\gamma_\perp (1-M)\,v_y + g\,D\,\beta_y \\
\dot{D} &= -\gamma_{||}\,D + \gamma N - 4g\,(v_x\beta_x + v_y\beta_y)
\end{aligned} \tag{3.19}$$

for the field amplitude $\alpha = \alpha_x + i\,\alpha_y$ (with $\beta = \alpha + \varepsilon_p^*/g$). v_x and v_y are the components of the atomic polarization and D denotes the atomic inversion. Eq.(3.19) may also be derived directly from the master equation Eq.(3.13).

The parameter M is a re-scaled squeezing parameter:

$$M = \frac{\gamma\, m_p}{\gamma_\perp} = \frac{m_p}{n_p + \frac{1}{2}} \,. \tag{3.20}$$

It is easy to prove from Eq.(3.7) that $|M| \in (0,1)$. In Eq.(3.19) we have made the phase choice M *real and positive,* which will be assumed throughout the following analysis. Defining quadrature operators according to

$$X(t) = \frac{\Gamma_p^{\dagger}(t)\, e^{i\omega_o t} + \Gamma_p(t)\, e^{-i\omega_o t}}{2}$$

$$Y(t) = \frac{\Gamma_p^{\dagger}(t)\, e^{i\omega_o t} - \Gamma_p(t)\, e^{-i\omega_o t}}{2i} \quad , \qquad (3.22)$$

the above choice of the phase of M results in reducing the noise in the imaginary or Y– quadrature.

The limit that the bath approaches a quadrature operator eigenstate, i.e. $n_p \to \infty$ and $m_p = \sqrt{n_p(n_p + 1)}$ (Gardiner, 1986), then corresponds to the limit $|M| \to 1$. Note the *two different* decay rates for the real and imaginary part of the atomic polarization:

$$\gamma_x = \gamma_\perp (1 + M)$$
$$\gamma_y = \gamma_\perp (1 - M) \quad , \qquad (3.22)$$

just like in the one-atom-system considered by Gardiner (1986). It is easily verified by means of Eq.(3.18) that the two decay rates have the following asymptotic behaviour:

$$\left.\begin{array}{l} \gamma_x \to \infty \\ \gamma_y \to 0 \end{array}\right\} \qquad \begin{array}{l} \text{for} \quad n_p \to \infty \\ \text{and} \quad m_p = \sqrt{n_p(n_p + 1)} \; . \end{array}$$

Thus for large m_p one component of the atomic polarization decays very slowly while the decay rate of the other component and the decay rate of the atomic inversion grow beyond any finite limit.

Eliminating the atomic steady state solutions from Eq.(3.19), one easily derives the following equation determining the *steady state solutions* of the cavity mode alone:

$$\frac{d\alpha}{dt} \equiv F(\alpha,\alpha^*) = 0$$

$$F(\alpha,\alpha^*) = -\kappa\alpha + \kappa \frac{C(\beta - \beta^* M)}{R(\beta, \beta^*)} \quad . \tag{3.23}$$

Here n_o stands for the *saturation photon number*

$$n_0 = \frac{\gamma_{||}\gamma_{\perp}}{4g^2} \quad , \tag{3.24}$$

C denotes the *cavity-cooperativity parameter* (or "pump-parameter")

$$C = \frac{g^2 N\gamma}{\gamma_{\perp}\gamma_{||}\kappa} \quad , \tag{3.25}$$

and the function R is the *saturation denominator*, evaluated at $\beta = \alpha + \varepsilon^*/g$:

$$R(\beta, \beta^*) = \left(1 + \frac{|\beta|^2}{2n_0}\right)^2 - \left| M + \frac{\beta^2}{2n_0} \right|^2 . \tag{3.26}$$

We shall consider the following cases: First we will investigate the effects of squeezing the atomic reservoir without a coherent driving field. Then we will proceed to generalize these results by adding a coherent field. And finally, for comparison, we will analyze the consequences of squeezing the vacuum modes entering the laser cavity.

3.3.1 Squeezed Vacuum State in the Atomic Reservoir

The case $m_p \neq 0$ (chosen real and positive), $m_c = 0$ and $\varepsilon_p = 0$ (or equivalently $\alpha \equiv \beta$) will be referred to as *"squeezed vacuum pump"* .

The ordinary incoherently pumped laser has a steady state solution which is independent of phase. However, from Eq.(3.23) we derive that the following relation

$$\frac{\alpha}{\alpha^*} = \frac{M}{\left(1 - \frac{R}{C}\right)} \tag{3.27}$$

holds in the steady state. Since the pump-parameter C is real and the saturation denominator R is a real function (cf. Eq.(3.26)), it becomes evident that the phase symmetry is broken: the phase of $\frac{\alpha}{\alpha^*}$ is determined by the phase of the complex number M. Consequently, for the above reference phase choice $m_p \in R_+$ is only fields which are either purely imaginary or purely real may exist in the steady state. In fact in this case the steady state solutions are found to be:

$$\begin{aligned} &\alpha = 0 \\ &\alpha = \pm i \sqrt{n_0 [C - (1 - M)]} && \text{for } C > 1 - M \\ &\alpha = \pm \sqrt{n_0 [C - (1 + M)]} && \text{for } C > 1 + M \ . \end{aligned} \tag{3.28}$$

We interpret this in the following way: the *anisotropy* of the noise in the atomic reservoir breaks the phase symmetry of the laser. Hence stationary points with a well-defined phase exist. Note that a similar breaking of phase symmetry was reported in the micro-maser (Krause et al., 1987). In this case the phase of the coherent atoms which are injected into the cavity imprint some kind of reference phase onto the laser. That is, the phase of the atoms which are prepared in a coherent superposition state acts to lock the phase of the laser - similar to what the reference phase of the coherent external field does in a laser with injected signal. The above case is different inasmuch as no deterministic

input reference phase exists. Instead it is the anisotropy of the fluctuations in the bath that gives rise to the locking of the laser phase. This difference is reflected in the fact that some kind of "degeneracy" exists for the stationary points: if Ψ_0 is a stationary phase then $-\Psi_0$ is also a stationary phase; these statements will be illustrated below by means of a semiclassical potential function.

In order to investigate the *stability* of the solutions given in Eq.(3.28), we calculate the eigenvalues of the Jacobian of the function F in Eq.(3.23). For this purpose it is convenient to re-express the equation in terms of u and v, the real and imaginary part of the field amplitude:

$$\dot{u} = \kappa\left[\frac{C(1-M)}{R} - 1\right]u \equiv \mathrm{Re}\,F$$

$$\dot{v} = \kappa\left[\frac{C(1+M)}{R} - 1\right]v \equiv \mathrm{Re}\,F$$

with

$$R(u,v) = (1-M^2) + \frac{u^2}{n_0}(1-M) + \frac{v^2}{n_0}(1+M)\ . \qquad (3.29)$$

The Jacobian then reads

$$J = \begin{pmatrix} \frac{\partial \mathrm{Re}\,F}{\partial u} & \frac{\partial \mathrm{Re}\,F}{\partial v} \\ \frac{\partial \mathrm{Im}\,F}{\partial u} & \frac{\partial \mathrm{Im}\,F}{\partial v} \end{pmatrix}\ . \qquad (3.30)$$

Evaluating this matrix at the solutions Eq.(3.28), one finds

$$J = \begin{cases} \kappa \begin{pmatrix} \frac{1-M}{1+M} - 1 & 0 \\ 0 & -\frac{2}{C}[C-(1-M)] \end{pmatrix} & \text{for } u = 0,\ v = \pm\sqrt{n_0\,[C-(1-M)]} \\ \kappa \begin{pmatrix} \frac{C}{1+M} - 1 & 0 \\ 0 & \frac{C}{1-M} - 1 \end{pmatrix} & \text{for } u = v = 0 \\ \kappa \begin{pmatrix} -\frac{2}{C}[C-(1+M)] & 0 \\ 0 & \frac{1+M}{1-M} - 1 \end{pmatrix} & \text{for } v = 0,\ u = \pm\sqrt{n_0\,[C-(1+M)]}. \end{cases} \tag{3.31}$$

A solution is stable if and only if *both* eigenvalues of the Jacobian are locally negative. In the first and third matrix one eigenvalue depends on M only. With the above mentioned choice of phase this rules out the two real solutions since $\frac{1+M}{1-M} > 1$ for $M \in (0,1)$.

From Eq.(3.31) it is clear that a stability exchange between the trivial solution $\alpha = 0$ and the pair of imaginary solutions occurs at $C = 1 - M$: below $C = 1 - M$ the solution with $|\alpha|^2 = 0$ is stable, above this value of C, where the pair of imaginary solutions comes into being, one of these solutions with $|\alpha|^2 = n_0[C - (1-M)]$ will be realized in stable operation. This justifies calling

$$C_{thr} \equiv 1 - M \tag{3.32}$$

the *threshold* of the laser. Summarizing we have the following steady state values For $C > C_{thr}$:

$$\begin{aligned} \bar{\alpha} &= \pm i\,\sqrt{n_0\,[C-(1-M)]} \\ \bar{v} &= \frac{\kappa}{g}\,\bar{\alpha} \\ \bar{D} &= \frac{D_0\,(1-M)}{C}\ , \end{aligned} \tag{3.33}$$

where $D_o = \frac{\gamma_N}{\gamma_{||}}$ is the steady state value for the inversion below threshold. Viewing the expression of the atomic inversion above threshold one may choose to re-define the pump-parameter by introducing a new *"effective pump-parameter"*

$$\tilde{c}(M) = \frac{C}{1-M} > C \qquad (3.34)$$

and characterize the threshold by $\tilde{c}(M) = 1$.

There are two ways to look at this situation: one can either think of the threshold as being shifted compared to an ordinary laser, or of the cooperativity-parameter of the cavity as being changed due to the squeezing.

Had we chosen $m_p \in R_-$, thus quenching the noise in the *real* quadrature of the bath, m_p would be replaced by $-|m_p|$ throughout. Then the pair of real solutions would turn out to be the stable pair. In other words, the steady states which are *in phase with the low noise quadrature* in the bath are in general the stable ones.

Finally, we wish to illustrate the above results by calculating the *semiclassical potential function*, defined by

$$\frac{\partial \Phi}{\partial u} = -\,\mathrm{Re}\,F$$
$$\frac{\partial \Phi}{\partial v} = -\,\mathrm{Im}\,F\ . \qquad (3.35)$$

In general, if such a potential exists, then the stationary distribution function is proportional to $\exp(-\Phi)$. The semiclassical steady states given above correspond to local minima of the potential surface. It is easily

verified that the potential condition for the semiclassical Eq.(3.29), that is $\frac{\partial \mathrm{Re}\, F}{\partial v} = \frac{\partial \mathrm{Im}\, F}{\partial u}$, holds globally. Integration is straightforward and yields

$$\Phi(u, v) = \frac{\kappa}{2} [\, u^2 + v^2 - C\, n_0 \ln [\, R(u,v)] \,] \quad . \tag{3.36}$$

In Fig.7 the potential surface of the squeezed pump laser is compared with the result for the ordinary laser. It is clearly visible that the usual symmetry in phase is broken and that two local minima appear symmetrically due to the squeezing. Hence the semiclassical theory predicts *phase-locking*. In contrast to the case of a laser with injected signal or of a micro-maser, there exist *two* stable phases, corresponding to the two "directions" along which the noise is quenched in the bath. In Section 3.4 we will treat the laser dynamics in a van der Pol oscillator model and it will become clearer how such a steady state builds up above threshold.

Note also the difference to the laser model investigated by Yamamoto et al. (1986): these authors studied a semiconductor-laser which was incoherently pumped by a beam of electrons with sub-Poissonian statistics. However, the electron beam was assumed to be in a near number eigenstate, characterized by a well defined electron number - at the cost of a very noisy and therefore rather undefined phase. Hence the input does not possess a preferred phase, and the phase symmetry is *not* destroyed by such a pumping mechanism. Consequently, phase diffusion is present in such a laser.

Fig.7a

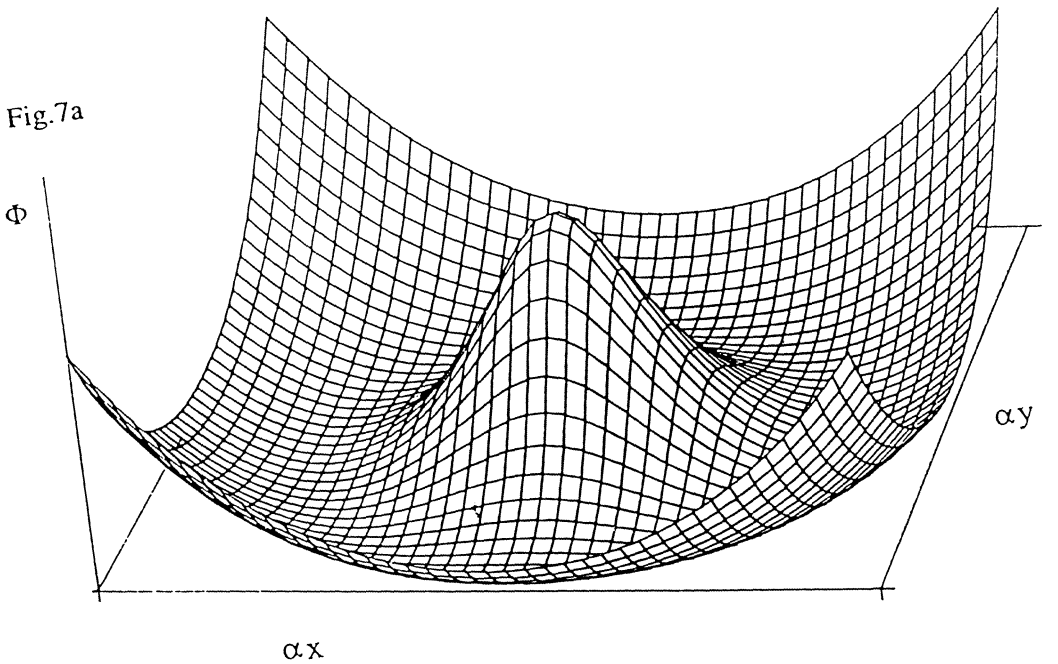

Fig.7b

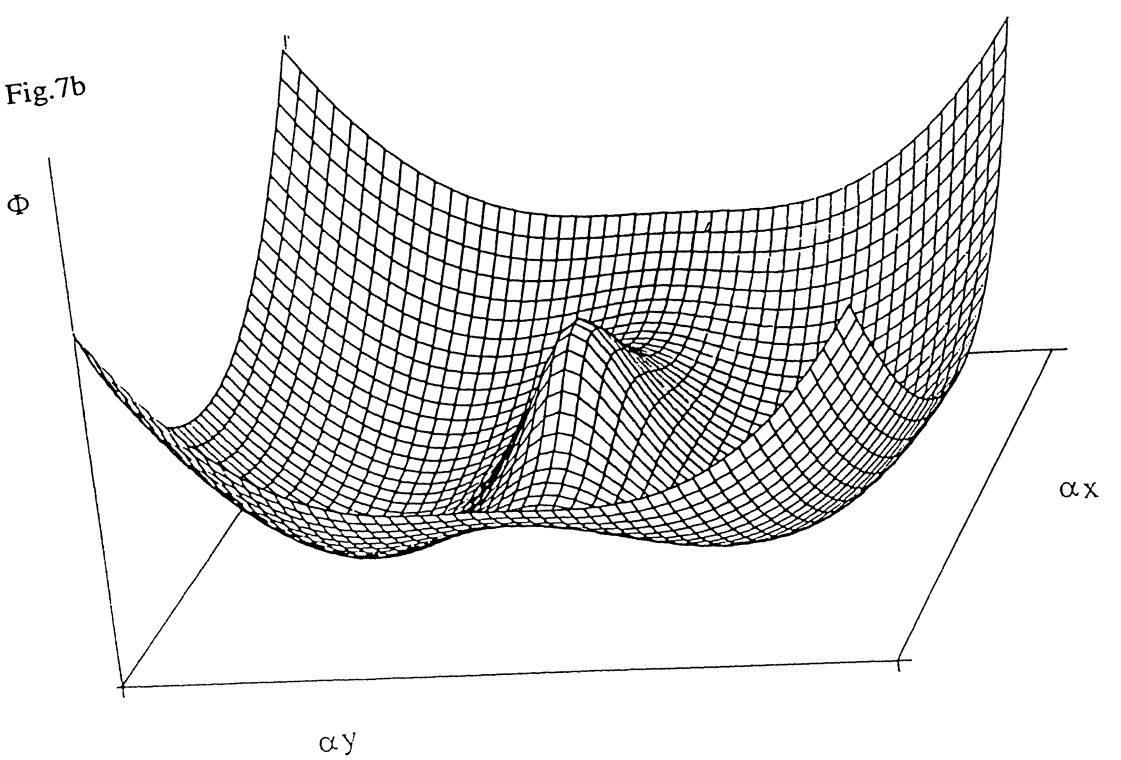

Fig. 7 The semiclassical potential surface of the laser field

(a) usual laser, C = 10

(b) squeezed vacuum pump, C = 10, M = 0.9

3.3.2 Squeezed-Pump in a General Squeezed State

We wish to generalize our previous results for the squeezed-pump laser to the case of a bath of inverted harmonic oscillators in a *general* squeezed state. The motivation for doing this is the fact that this allows us to study the influence of a bath which itself displays sub-Poissonian statistics (note that a squeezed vacuum state always has super-Poissonian statistics (Walls and Milburn (1983)). As mentioned at the beginning of this chapter it may be hoped that this leads to sub-Poissonian statistics in the laser output, similar to results found by Yamamoto et al. (1986) after suppression of the pump noise below the shot noise limit.

It is well known that such a generalization is easily achieved by adding a coherent classical field to the squeezed vacuum modes in the atom-bath coupling which has been considered so far. Such a classical field has already been included in the optical Bloch equations Eq.(3.19).

We will solve Eq.(3.19) for the two special cases of interest that ε_p is either purely real or purely imaginary. As we have chosen the squeezing parameter m_p to be real and positive, these two cases correspond to an input squeezed state with reduced phase or reduced amplitude fluctuations, respectively. Since the classical driving field is assumed to be strong the first case may be referred to as the *bunched* and the second one as the *antibunched* input (cf. Section 2.3.1). Fig.8 depicts a schematic error diagram for the two considered types of state-preparation of the reservoir.

The antibunched input, characterized by $m_p \in R_+$ and $\varepsilon_p = i\,|\varepsilon_p|$, models a squeezed input in the bath with enhanced noise in the real quadrature around a mean value ε_p which is imaginary. Therefore this

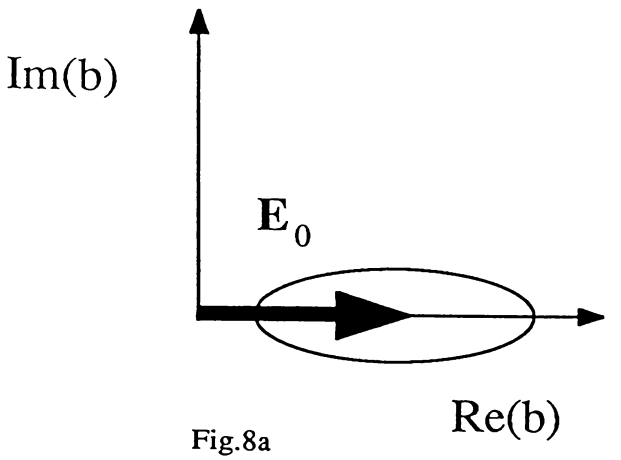

Fig.8a

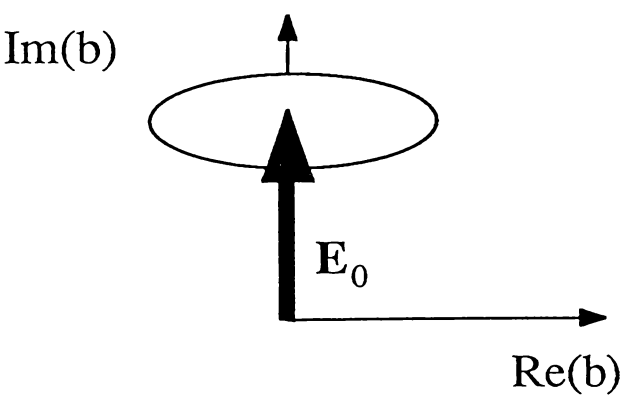

Fig.8b

Fig. 8 Schematic diagram of the relative phases between the classical driving field E_p and the squeezed noise in the bath damping the atoms (a) "bunched" input (b) "antibunched" input

case corresponds to a squeezed state with *reduced amplitude noise*. One easily derives the following two equations from Eq.(3.24):

$$\alpha_x R(\beta_x,\beta_y) = C\,\beta_x\,(1-M)$$
$$\alpha_y R(\beta_x,\beta_y) = C\,\beta_y\,(1+M) \qquad (3.37)$$

(where $\beta = \alpha + \varepsilon_p^*/g$ and the function R is given by Eq.(3.29)). Since $u \equiv \alpha_x = \beta_x$ for the antibunched input, the first line in Eq.(3.37) implies

$$\alpha_x = \beta_x = 0 \qquad \text{or} \qquad R(\beta_x,\beta_y) = C\,(1-M)\ .$$

In the first of these two cases, the remaining equation in Eq.(3.37) yields the following *cubic equation* for α_y:

$$\alpha_y\left[\,(1-M) + \frac{\beta_y^2}{n_0}\,\right] = C\,\beta_y \qquad \text{with} \qquad \beta_y = \alpha_y - i\,\left|\frac{\varepsilon_p}{g}\right| \ . \qquad (3.38)$$

In the second case it is straightforward to find the following two solutions:

$$\alpha_x^a = \pm\sqrt{n_0\,[C-(1+M)] - E^2\frac{1-M^2}{4M^2}} \qquad \alpha_y^a = E\,\frac{1+M}{2M}\ , \qquad (3.39)$$

existing for $C > C_a$, where

$$C_a = 1 + M + \frac{E^2}{n_0}\,\frac{1-M^2}{4M^2}\ , \qquad (3.40)$$

and $E=|\varepsilon_p/g|$. Therefore Eqs.(3.37) possess either three or five solutions, depending on whether the cubic has only one or three *real* solutions. It is easy to prove from Eq.(3.38) that the cubic possesses one negative and

two positive roots for α_x, provided that three solutions exist, i.e. provided that $C > 1 - M + \frac{E^2}{3n_0}$.

Note that corresponding results for the *bunched input* are conveniently found by replacing $m_p \rightarrow -m_p$, $E \rightarrow -E$ and interchanging $\alpha_x \leftrightarrow \alpha_y$ and $\beta_x \leftrightarrow \beta_y$ in all expressions derived for the antibunched input.

In order to determine the stability of the above semiclassical steady states we calculate the elements of the Jacobian (cf. Eq.(3.30)) as a function of the real and imaginary part of β:

$$J_{xx}(\beta_x,\beta_y) = -1 + \frac{C(1-M)}{R} - \frac{2C(1-M)^2 \frac{\beta_x^2}{n_0}}{R^2}$$

$$J_{xy}(\beta_x,\beta_y) = J_{yx}(\beta_x,\beta_y) = -\frac{2C(1-M^2) \frac{\beta_x\beta_y}{n_0}}{R^2}$$

$$J_{yy}(\beta_x,\beta_y) = -1 + \frac{C(1+M)}{R} - \frac{2C(1+M)^2 \frac{\beta_y^2}{n_0}}{R^2} \qquad (3.41)$$

with $R \equiv R(\beta_x,\beta_y)$.

Insertion into Eq.(3.41) shows that in the antibunched case the two square root solutions Eq.(3.39) are unstable in the region of parameter space where they exist, i.e. for $C > C_a$. Note that for $E \rightarrow 0$ these solutions turn into the pair of unstable solutions of the squeezed vacuum pump discussed in the previous section. Examining the stability of the roots of the cubic numerically, we found that the negative root and the larger positive one are stable for $C > C_a$, whereas for $C < C_a$ the negative one is always stable and the larger positive one can be stable depending on the values of both E and M.

For the bunched input on the other hand the result is that the two square root steady state solutions similar to Eq.(3.39) (which coincide with the stable pair of solutions of the squeezed vacuum pump for E=0) are always stable for $C > C_b = 1 - M + \frac{E^2}{n_0} \frac{1 - M^2}{4M^2}$. For $C < C_b$ one of the roots of the cubic equation corresponding to Eq.(3.38) is stable.

All the above results can again be illustrated by plotting the semiclassical potential which now reads

$$\Phi(\alpha_x,\alpha_y) = \frac{\kappa}{2} [\, \alpha_x^2 + \alpha_y^2 - C\, n_0 \ln [\, R(\beta_x,\beta_y)] \,] \quad . \tag{3.42}$$

Fig.9a depicts the potential surface for the antibunched input ($\beta_x = \alpha_x$, $\beta_y = \alpha_y - E$). There are two stable steady state solutions along the imaginary axis, a fact which is not surprising since the choice $\Psi = \frac{\pi}{2}$ for the phase of a classical driving field by itself tends to lock the laser phase to $\frac{\pi}{2}$, while a squeezed vacuum in the bath by itself leads to a locking of the phase to $\pm\frac{\pi}{2}$ as was demonstrated in the previous section. Consequently the *resulting* potential well in the direction $\frac{\pi}{2}$ is *deeper* than the one along $-\frac{\pi}{2}$.

For the bunched input ($\beta_x = \alpha_x + E$, $\beta_y = \alpha_y$), however, there is a *trade-off* between the tendency to lock to $\Psi = 0$ due to the driving field and a tendency to lock to $\Psi = \pm\frac{\pi}{2}$ due to the squeezed bath, so (for $C > C_b$) we get two stable steady states in the first and fourth quadrant which lie symmetrically about the real axis. This becomes visible as two equally deep valleys in the potential surface in Fig.9b. For increasingly large E and fixed (1 - M), these two solutions approach each other by wandering symmetrically towards the real axis.

The above results are summarized in Fig.10, a synopsis of the position of stable and unstable steady states for both cases considered.

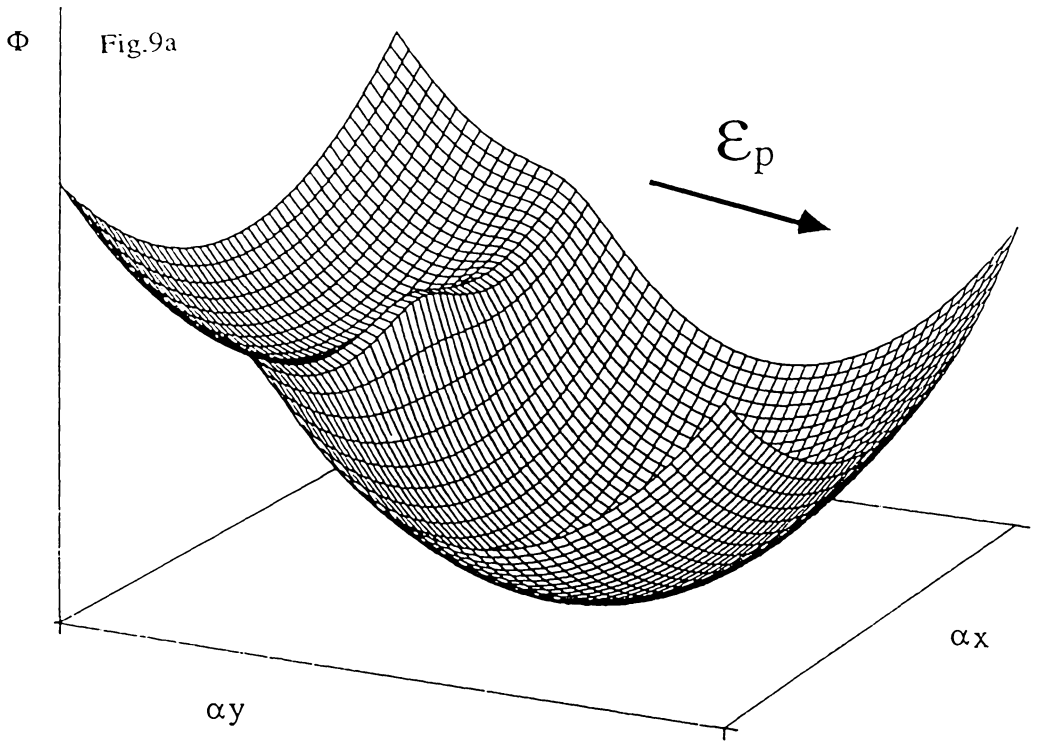

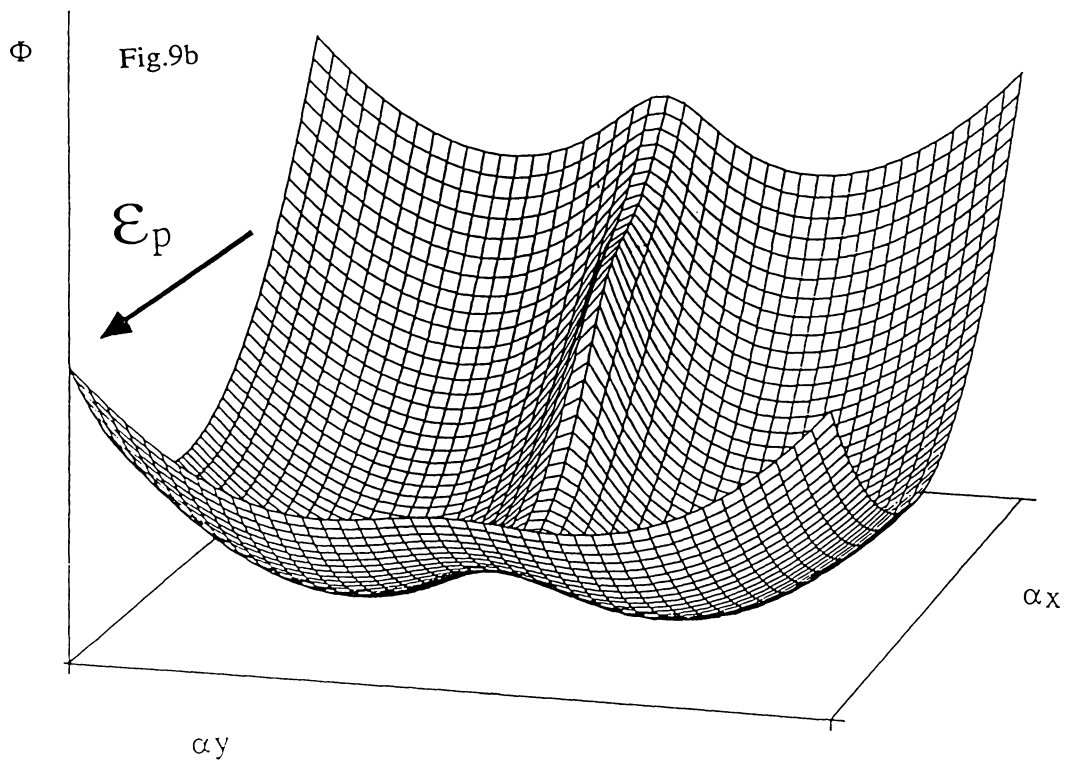

Fig. 9 Semiclassical potential of the laser for non-zero classical driving field E_p for the parameters M = 0.9, $|E_p|$ = 4, C = 10.

(a) antibunched input (b) bunched input

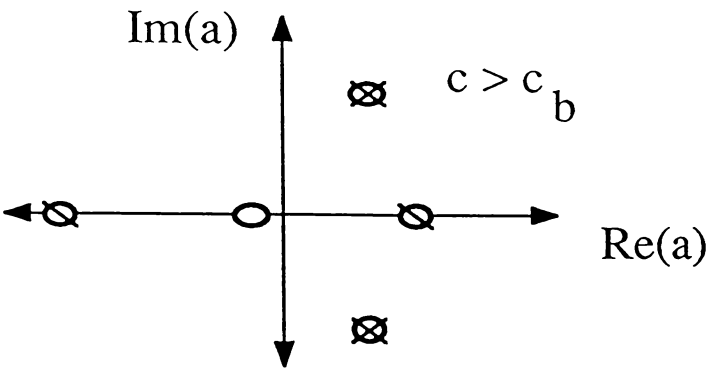

Fig.10a

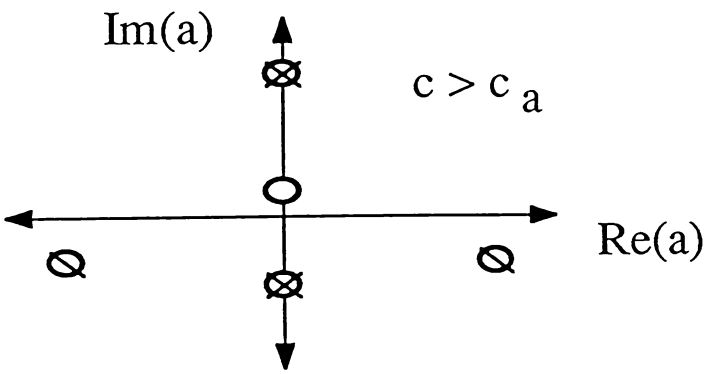

Fig.10b

Fig. 10 Schematic diagram of the position of semiclassical stationary points

○ unstable ⊘ saddlepoint ⊗ stable

(a) bunched input, $C > C_b$ (b) antibunched input, $C > C_a$

3.3.3 Squeezing the Cavity Modes

In this section we set $m_p = 0$ and $\varepsilon_p = 0$ and consider a non-zero $m_c \in R$, that is we will investigate the effects of squeezing the modes entering the laser cavity. Note that the optical Bloch equations Eq.(3.19), that is the semiclassical equations for α, α^*,v ,v* and D which followed from the FPE, do *not* contain the squeezing parameter m_c explicitly. Hence this set of equations does not differ from the semiclassical description of an ordinary laser. However, the noise in the reservoir modelling the vacuum modes entering the cavity is *phase-dependent* giving rise to new noise correlations in the FPE (cf. the terms proportional to m_c in the Liouville operator Eq.(3.17e)) or the corresponding stochastic differential (Ito) equation, which are absent in an ordinary laser.

From what we have seen in the last section dealing with the case of squeezing the atomic reservoir, one might suspect that the anisotropy of the noise similarly destroys the phase symmetry of the laser; in other words we expect a "locking" of the phase to occur due to the phase-dependent correlations in the laser fluctuations. This phase-locking, however, is hidden in the semiclassical equations in α, α^*,v ,v* and D and stems from an anisotropy in noise and not from a distortion in the corresponding semiclassical potential surface.

It may be hoped that one will gain more insight into the situation and in particular be able to decide whether the laser phase is locked or not by returning to the FPE and making a variable transformation to *intensity and phase variables* . To this end we adiabatically eliminate the atoms, which requires $\kappa \ll \gamma_\perp, \gamma_\parallel$ (satisfied in a typical laser cavity), and derive a FPE in the variables α and α^* only. The result reads

$$\frac{\partial \tilde{P}(\alpha,\alpha^*)}{\partial t} = \left[-\frac{\partial}{\partial x_i} A_i + \frac{\partial^2}{\partial x_i \partial x_j} D_{ij} \right] \tilde{P}(\alpha,\alpha^*) \qquad i,j \in \{1,2\}$$

$$\text{with} \qquad x_1 \equiv \alpha, \; x_2 \equiv \alpha^* \tag{3.43}$$

with the following drift vector and diffusion matrix:

$$A = \begin{pmatrix} -\kappa \left[1 - \dfrac{C}{1 + \dfrac{|\alpha|^2}{n_0}} \right] \alpha \\ -\kappa \left[1 - \dfrac{C}{1 + \dfrac{|\alpha|^2}{n_0}} \right] \alpha^* \end{pmatrix}$$

$$D = \begin{pmatrix} \left(\frac{g}{\gamma_\perp}\right)^2 g v \alpha + \kappa m_c & \left(\frac{g}{\gamma_\perp}\right)^2 \frac{w_{12} N}{2} + \kappa n_c \\ \left(\frac{g}{\gamma_\perp}\right)^2 \frac{w_{12} N}{2} + \kappa n_c & \left(\frac{g}{\gamma_\perp}\right)^2 g v^* \alpha^* + \kappa m_c \end{pmatrix}, \tag{3.44}$$

keeping only the dominant noise terms according to Haken's (1970) scaling around threshold which is appropriate for the squeezed-cavity laser (but not for the squeezed-pump laser). We transform this FPE to intensity and phase variables

$$I = \alpha^* \alpha \qquad \text{or} \qquad \alpha = \sqrt{I}\, e^{-i\Psi}$$

$$\Psi = \frac{1}{2i} \ln \frac{\alpha^*}{\alpha} \qquad \alpha^* = \sqrt{I}\, e^{i\Psi} \tag{3.45}$$

according to (Risken, 1984)

$$\bar{A}_i = \frac{\partial \bar{x}_i}{\partial x_k} A_k + \frac{\partial^2 \bar{x}_i}{\partial x_k \partial x_j} D_{kj}$$

$$\bar{D}_{ij} = \frac{\partial \bar{x}_i}{\partial x_k} \frac{\partial \bar{x}_j}{\partial x_m} D_{km} \qquad (3.46)$$

into a new FPE of the general form Eq.(3.43) with $\bar{x}_1 \equiv I$ and $\bar{x}_2 \equiv \Psi$. This yields

$$\bar{A} = \begin{pmatrix} e^{i\Psi}\sqrt{I}\, A_\alpha + e^{-i\Psi}\sqrt{I}\, A_{\alpha^*} + 2D_{\alpha^*\alpha} \\ \mathrm{Im}\left\{ \frac{e^{2i\Psi}}{I} D_{\alpha\alpha} \right\} \end{pmatrix}$$

$$\bar{D} = \begin{pmatrix} 2I\, D_{\alpha^*\alpha} + 2I\, \mathrm{Re}\{e^{2i\Psi} D_{\alpha\alpha}\} & \mathrm{Im}\{ e^{-2i\Psi} D_{\alpha^*\alpha^*}\} \\ \mathrm{Im}\{ e^{-2i\Psi} D_{\alpha^*\alpha^*} \} & \frac{1}{2I} D_{\alpha^*\alpha} + \mathrm{Re}\left\{ \frac{e^{2i\Psi}}{I} D_{\alpha\alpha} \right\} \end{pmatrix}, \qquad (3.47)$$

(where $D_{\alpha\alpha}$, A_α etc. are the components in Eq.(3.44) re-expressed in terms of I and Ψ).

Since the variable transformation Eq.(3.45) is nonlinear it need not lead to the same semiclassical steady states (Gardiner, 1983). From the transformed FPE we infer the following deterministic equations:

$$\dot{I} = -2\kappa I \left(1 - \frac{C}{1 + \frac{I}{n_0}} \right) + 2\kappa n_c + \left(\frac{g}{\gamma_\perp} \right)^2 w_{12} N \qquad (3.48a)$$

$$\dot{\Psi} = \frac{\kappa m_c}{I} \sin 2\Psi \qquad (3.48b)$$

from the new drift vector Eq.(3.47). Note that in Eq.(3.48b) we have neglected a term $\propto g^3 v\alpha$ in $D_{\alpha\alpha}$ which the standard laser theories also ignore around threshold. The last term in the equation of motion of the intensity Eq.(3.48a) stems from the spontaneous emission noise $\propto D_{\alpha^*\alpha}$

in the laser. The important thing to notice is that $\dot{\Psi} \neq 0$ for non-zero m_c - in contrast to an ordinary laser - thus revealing the steady state phases to be $\Psi = 0$ (or π) and $\Psi = \frac{\pi}{2}$ (or $-\frac{\pi}{2}$).

Viewing the equation of motion of the phase, it is obvious that $\Psi = \pm \frac{\pi}{2}$ correspond to stable stationary points, whereas $\Psi = 0,\pi$ are unstable if m_c is chosen real and positive. This is in agreement with recent results by Gea-Banacloche (1987).

Note the resemblance to the situation encountered in the stability analysis for the squeezed-pump laser: in both cases the phase is locked to a position where the amplitude fluctuations are smallest! Thus, when squeezing the noise in the Y-quadrature, the stable phases turn out to be $\Psi = \pm \frac{\pi}{2}$ for the squeezed-pump *and* the squeezed-cavity laser.

One might wish to derive a potential function for the semiclassical equations Eq.(3.48). However, from the fact that the right hand side of Eq.(3.48b) depends upon the laser intensity for $m_c \neq 0$, while Eq.(3.48a) is phase-*in*dependent, it is clear that the semiclassical potential conditions are *not* satisfied. This again reflects the fact that this "phase-locking" is not due to some minimum in the semiclassical potential surface, but is entirely an effect of unequally distributed noise.

Finally, we remark that the empty cavity limit is easily recovered from Eq.(3.48) by setting $g = 0$ and thus $C = 0$. The drift term in the phase equation will still be the same in this simplest possible case where we have a constant diffusion matrix, i.e. an Ornstein-Uhlenbeck process (Gardiner, 1983). This is so although $\alpha = 0$ holds in the steady state in an empty cavity and hence Ψ can no longer be interpreted as a proper physical phase.

3.4 Rotating Wave van der Pol Equation, Phase Diffusion and Laser Linewidth of the Squeezed Reservoir Laser

The fact that the laser, being a self-sustained oscillator in the optical frequency regime, can be quite adequately described as a so-called van der Pol oscillator is well known and has found its way into many textbooks (e.g. Risken(1984)). This oscillator satisfies the nonlinear differential equation

$$x'' - 2\beta\,(\kappa - x^2)\,x' + \omega^2 x = 0 \qquad \beta,\kappa > 0,$$

which was first used in 1927 by van der Pol in order to describe the typical self-excitation features of a vacuum-tube. The intensity-dependent amplification/damping "coefficient" of x' leads to the existence of a stable limit cycle, due to the self-excitation of amplitudes below this value and damping of.amplitudes beyond it. If ω is an optical frequency, as is the case for a laser, one can make the rotating wave approximation, that is neglect rapidly oscillating terms; this yields

$$\dot{b} - \beta\,(\kappa - b\,b^*)\,b = 0 \qquad \text{with} \qquad x = b\,e^{-i\omega t} + b^* e^{i\omega t}.$$

In the following we will derive a "noisy" rotating wave van der Pol equation for the amplitude of the squeezed reservoir laser with additional stochastic forces on the right-hand side, and use it as a starting point for calculating the laser linewidth.

To this end we consider the set of *Langevin equations* equivalent to the FPE Eq.(3.17), which read

$$\dot{\alpha} = -\kappa\alpha + g v + \Gamma_\alpha$$
$$\dot{v} = -\gamma_\perp v - \gamma m_p v^* + g D \beta + \Gamma_v$$
$$\dot{D} = -\gamma_{||} D + \gamma N - 2g(v^*\beta + \beta^* v) + \Gamma_D \qquad (3.49)$$

plus the corresponding equations for α^* and v^*. The stochastic "forces" Γ have non-zero correlations:

$$<\Gamma_\alpha(t)\,\Gamma_{\alpha^*}(t')> = <\Gamma_{\alpha^*}(t)\,\Gamma_\alpha(t')> = 2\kappa n_c\ \delta(t-t')$$
$$<\Gamma_\alpha(t)\,\Gamma_\alpha(t')> = <\Gamma_{\alpha^*}(t)\,\Gamma_{\alpha^*}(t')>^* = 2\kappa m_c\ \delta(t-t')$$
$$<\Gamma_v(t)\,\Gamma_{v^*}(t')> = <\Gamma_{v^*}(t)\,\Gamma_v(t')> = w_{12} N\ \delta(t-t')$$
$$<\Gamma_v(t)\,\Gamma_v(t')> = <\Gamma_{v^*}(t)\,\Gamma_{v^*}(t')>^* = [\gamma m_p(N+D) + 2gv\beta]\ \delta(t-t')$$
$$<\Gamma_v(t)\,\Gamma_D(t')> = <\Gamma_D(t)\,\Gamma_v(t')> = -2 w_{12} v\ \delta(t-t')$$
$$<\Gamma_D(t)\,\Gamma_D(t')> = [2(\gamma_{||}N - \gamma D) - 4g(\beta^* v + v^*\beta)]\ \delta(t-t')\ . \qquad (3.50)$$

For later reference we introduce the notation

$$<\Gamma_i(t)\,\Gamma_j(t')> = 2 D_{ij}\ \delta(t-t') \qquad (3.51)$$

for the elements of the diffusion matrix related with the correlations Eq.(3.50).

3.4.1 Squeezed Pump

For the moment we will not be concerned with the effects of the thermal photons in the cavity and thus we put m_c to zero and neglect the comparatively small terms proportional to n_c. Effects proportional to those terms will be brought up in Section 3.4.2.

In order to make a comparison of the squeezed-pump laser with the usual laser we will derive the FPE for the laser mode alone (similar to the derivation of Eq.(3.44) for the squeezed cavity), in the limit that the atoms can be *adiabatically eliminated* . This requires the cavity decay rate to be very much smaller than the atomic decay rates γ_x, γ_y and $\gamma_{||}$ and thus in particular

$$\kappa \ll \gamma_\perp(1 \pm M) \ . \tag{3.52}$$

The result of this procedure (cf. Haken's "noisy slave") is expressed in the following Langevin equation:

$$\dot{\alpha} = A_\alpha + F_\alpha^{tot}$$

with

$$A_\alpha(\alpha^*,\alpha) = [A_{\alpha^*}(\alpha^*,\alpha)]^* = -\kappa\alpha + \kappa\frac{C(\beta - \beta^* M)}{R(\beta,\beta^*)} \tag{3.53}$$

$$F_\alpha^{tot} = \frac{g}{\gamma_\perp R(\beta,\beta^*)}\left[\left(1+\frac{|\beta|^2}{2n_0}\right)\Gamma_v - \left(M+\frac{\beta^2}{2n_0}\right)\Gamma_{v^*} + \frac{g}{\gamma_\perp}\frac{\beta(1+M)}{2}\Gamma_D\right] .$$

The correlations of the resulting stochastic force can be worked out by means of Eq.(3.50), and using the notation established in Eq.(3.51) we get:

$$\begin{aligned} \langle F_\alpha^{tot}(t)\, F_\alpha^{tot}(t')\rangle = {} & \left(\frac{g}{\gamma_\perp R(\beta,\beta^*)}\right)^2 \times \\ & \{\,[(1+a)^2 + (a-M)^2]\, D_{vv} + 2(1+a)(a-M)\, D_{vv^*} \\ & + 2i\,\mathrm{Im}\{b\}(1+M)\, D_{vD} - |b|^2 D_{DD}\,\}\quad \delta(t-t') \end{aligned}$$

$$< F_{\alpha^*}^{tot}(t)\, F_{\alpha}^{tot}(t') > = \left(\frac{g}{\gamma_\perp R(\beta,\beta^*)}\right)^2 \times$$
$$\{\, [(1+a)^2 + (a-M)^2]\, D_{vv^*} + 2(1+a)(a-M)\, D_{vv}$$
$$- 2i\, \mathrm{Im}\{b\}\,(1+M)\, D_{vD} + |b|^2 D_{DD} \,\} \qquad \delta(t-t')$$

with

$$a \equiv \left(\frac{g|\beta|}{\gamma_\perp}\right)^2, \quad b \equiv \frac{g\beta}{\gamma_\perp}\,\frac{(1+M)}{2} \,. \tag{3.54}$$

For the sake of simplicity we shall take the coherent field to be ε_p zero in the following investigation of the laser fluctuations.

Expanding *around threshold* , that is assuming that $\frac{|\alpha|^2}{n_0} \ll 1$ or equivalently $C \approx 1 - M$, we obtain an equation possessing the above outlined general form of a *rotating wave van der Pol equation* (RWVPO):

$$\dot{\alpha} = G(\alpha,\alpha^*)\,\alpha + \alpha_{nl} + F_\alpha^{tot} \tag{3.55}$$

with a *phase-dependent gain*

$$G(\alpha,\alpha^*) = \kappa\left[-1 + \frac{C}{(1-M^2)}\left(1 - \frac{\alpha^*}{\alpha}M\right)\right] \tag{3.56}$$
$$= \kappa\left[-1 + \frac{C}{(1-M^2)}\left(1 - e^{2i\Psi}M\right)\right]$$

and a nonlinear saturation term

$$\alpha_{nl} = \kappa\,\frac{C}{(1-M^2)^2}\left(1 - \frac{\alpha^*}{\alpha}M\right)\left[\frac{|\alpha|^2}{n_0} - M\left(\frac{\alpha^2}{2n_0} + \frac{\alpha^{2^*}}{2n_0}\right)\right]\alpha \,. \tag{3.57}$$

Assuming small fluctuations around a well stabilized semiclassical steady state, we have treated α^* as the complex conjugate of α and identified $\alpha = \sqrt{I}e^{-i\Psi}$ and $\alpha^* = \sqrt{I}e^{i\Psi}$. Thus one notices that Eq.(3.55) has the same general form as Risken's equation for the ordinary laser (that is it contains a gain function which acts as a *self-excitation* term above threshold, balanced by a nonlinear saturation term preventing infinite growth). However, one difference is the dependence upon Ψ in the gain and in the saturation, which is a consequence of the anisotropy of the noise due to the squeezing in the atomic bath. From Eq.(3.56) it is clear that the gain is largest for $\Psi = \pm \frac{\pi}{2}$, hence a (stable) steady state on the imaginary axis is built up above threshold. Note that Eq.(3.55) reduces to the usual RWVPO model of the laser in the limit $m_p \to 0$.

For consistency we also expand the correlation functions around threshold and keep only the dominant noise terms. In particular we drop for the moment the noise in the atomic inversion and the second term $\propto g^3$ in the correlation $<\Gamma_v(t)\Gamma_v(t')>$, which is negligible compared to the spontaneous emission noise close to threshold. Thus the correlation functions "simplify" to

$$
\begin{aligned}
< F_{\alpha^*}^{tot}(t)\, F_{\alpha}^{tot}(t') > &= \left(\frac{g}{\gamma_\perp (1 - M^2)} \right)^2 \times \\
&\quad \{ (1 + M^2)\, w_{12} N \; - \; 2M\, \gamma m_p\, (N + D) \}\; \delta(t - t') \\
&\equiv D_{\alpha^* \alpha}\; \delta(t - t') \\
< F_{\alpha}^{tot}(t)\, F_{\alpha}^{tot}(t') > &= \left(\frac{g}{\gamma_\perp (1 - M^2)} \right)^2 \times \\
&\quad \{ (1 + M^2)\, \gamma m_p\, (N + D) \; - \; 2M\, w_{12} N \}\; \delta(t - t') \\
&\equiv D_{\alpha\alpha}\; \delta(t - t') \; . \qquad (3.58)
\end{aligned}
$$

Note that $\langle F^{tot}_{\alpha}(t)\, F^{tot}_{\alpha}(t')\rangle \rightarrow 0$ and $\langle F^{tot}_{\alpha^*}(t)\, F^{tot}_{\alpha}(t')\rangle$ reduces to the usual spontaneous emission term for $m_p \rightarrow 0$.

In Appendix B we prove that this two-dimensional FPE does not satisfy the potential condition in the presence of non-zero phase-dependent noise correlations $\langle F^{tot}_{\alpha}(t)\, F^{tot}_{\alpha}(t')\rangle$ and $\langle F^{tot}_{\alpha^*}(t)\, F^{tot}_{\alpha^*}(t')\rangle$. Thus the diagonal diffusion elements $\mathbf{D}_{\alpha\alpha}$ and $\mathbf{D}_{\alpha^*\alpha^*}$ related to the squeezing prevent the existence of a potential solution - in contrast to the situation encountered in the semiclassical theory.

Here we wish to remark that the semiclassical steady state solutions of the the approximate equation Eq.(3.55) differ from the exact solutions inasmuch as

$$|\alpha|^2_{RWVPO} = \frac{(1-M)}{C}\,|\alpha|^2\,, \tag{3.59}$$

but near threshold $C \approx 1 - M$ and hence the error is small and the qualitative behaviour unchanged, similar to the situation in the usual RWVPO model.

Using Eq.(3.47) the *phase diffusion rate* is given by

$$D_{\psi\psi}(I,\Psi) = \frac{1}{2I}\left[\,\mathbf{D}_{\alpha^*\alpha} - \mathbf{D}_{\alpha\alpha}\cos 2\Psi\,\right] \tag{3.60}$$

with $\mathbf{D}_{\alpha\alpha}$ and $\mathbf{D}_{\alpha^*\alpha}$ from Eq.(3.58). Evaluating this expression at the stable steady state solution with $\bar{I}$ given by Eq.(3.59) and phase $\bar{\Psi} = \pm\frac{\pi}{2}$, we find

$$D_{\psi\psi}(\bar{I},\bar{\Psi}) = \frac{1}{2\bar{I}}\,\frac{2\kappa C}{(1+M)^2}\left[1 + n_p + m_p\left(1 + \frac{1}{2n_p+1}\right)\right]. \tag{3.61}$$

For $m_p = 0$ this reduces to the usual phase diffusion rate due to spontaneous emission which may be written as (Haken, 1970, Risken, 1984, Sargent, Scully, and Lamb, 1974)

$$D_{\psi\psi} = \frac{1}{2\bar{I}} \frac{g^2 \bar{N}_2}{\gamma_\perp} , \tag{3.62}$$

with $\bar{N}_2$ being the number of excited atoms in the steady state.

Fig.11 compares the right hand side of Eq.(3.61) as a function of n_p (with m_p taken maximal, i.e. $m_p = \sqrt{n_p(n_p+1)}$, with the phase diffusion rate of an ordinary laser. The bath coupled to the ordinary laser is assumed to be in a vacuum state $n_p = 0$, and thus we get a straight reference line in the plots.

For the usual laser the threshold condition is $C = 1$, independent of n_p. However, in our laser model the threshold depends on m_p and thus on n_p :

$$C_{thr} = 1 - M = 1 - \frac{m_p}{n_p + \frac{1}{2}} . \tag{3.63}$$

Comparing the two models we have chosen $\frac{C - C_{thr}}{C_{thr}}$ to be the same number, that is the lasers are operating in corresponding regions with respect to threshold. We remark that the results of the comparison look very similar if one chooses to keep the output-intensity fixed.

Viewing Eq.(3.61) it is not obvious that $D_{\psi\psi}$ should decrease with increasing n_p. In fact, if one were to plot only the expression inside the outermost brackets in Eq.(3.61) one would find an *in*crease with n_p. Yet one has to bear in mind that the semiclassical steady state values of the

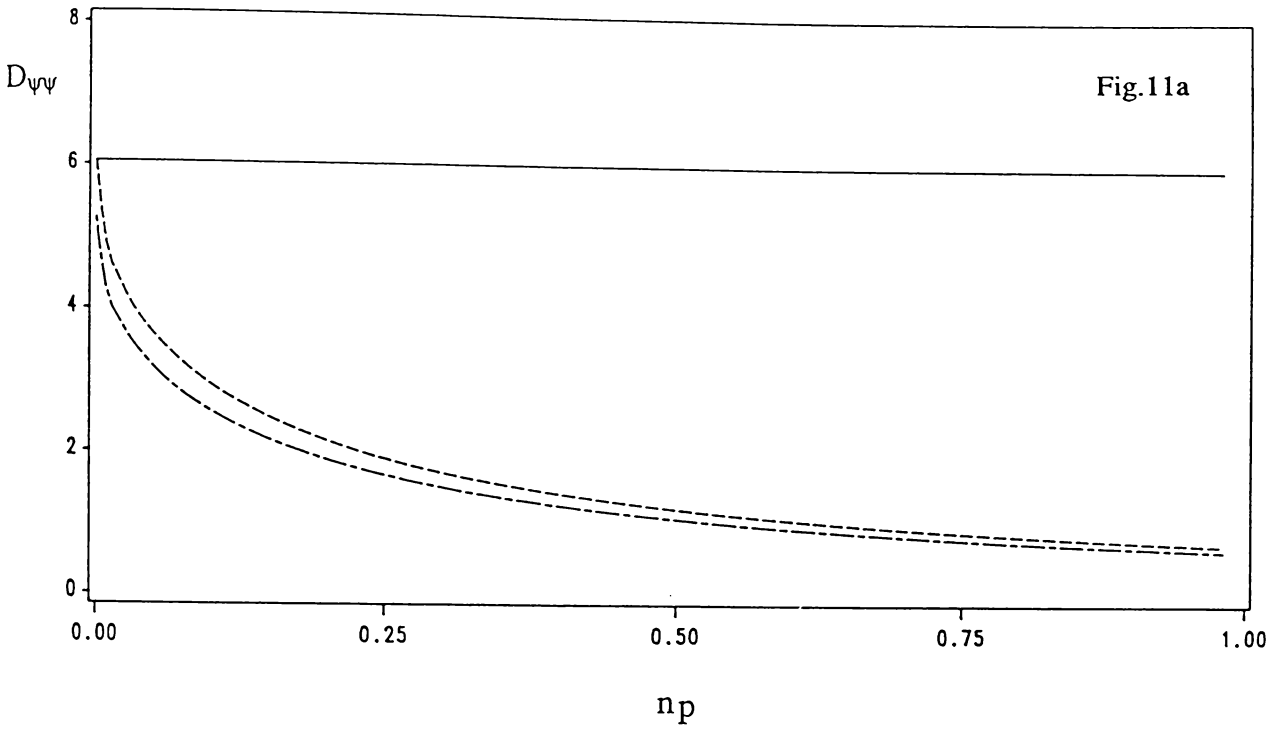

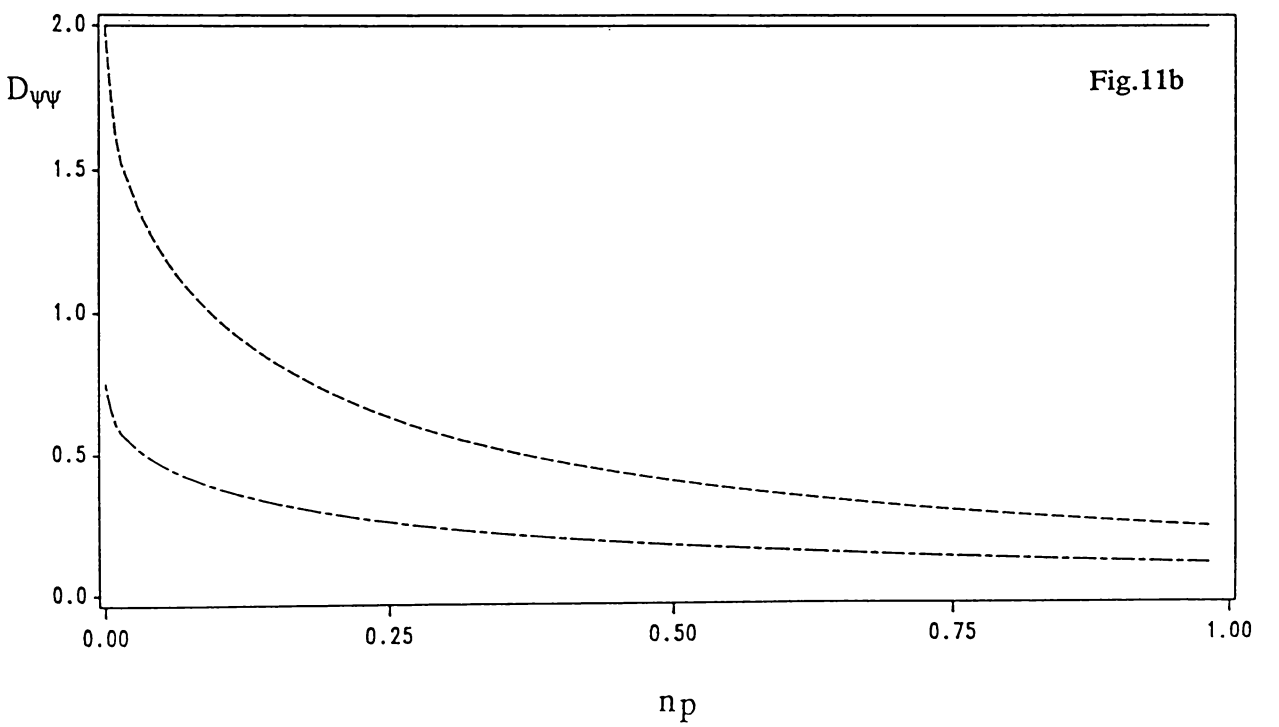

Fig. 11 The phase diffusion coefficient of the laser as a function of the photon-number n_p, assuming ideal squeezing in the bath:

$m_p = \sqrt{n_p(n_p + 1)}$

———— usual laser with bath in vacuum state ($n_p = 0$)

– – – – – rotating wave van der Pol approximation

—·—·— full expression Eq.(3.60)

(a) 10% above threshold (b) 100% above threshold

intensity and the atomic inversion also depend on n_p and m_p leading to an overall decrease in $D_{\Psi\Psi}$.

Obviously in the squeezed-pump laser $D_{\Psi\Psi}$ has to be given an interpretation which differs from the usual kicked rotator diffusion model, since the laser phase is locked for non-zero m_p. It can be shown analytically that the phase diffusion rate actually approaches zero in the limit $n_p \to \infty$, $m_p = \sqrt{n_p(n_p+1)}$ (equivalent to $M \to 1$), that is in the limit of a quadrature operator eigenstate in the bath. Of course this represents an unphysical limiting case for the present linearized theory since it involves *infinite* noise in one quadrature.

It appears that it is the vanishing of the threshold $C_{thr} = 1 - M$ as $M \to 1$ which causes the phase diffusion rate to approach zero. In order to illustrate this we note that the pump- or cooperativity-parameter

$$C = \frac{g^2 N \gamma}{\gamma_{\parallel}\gamma_{\perp}\kappa} = \frac{g^2 N}{2\gamma\left(n_p + \frac{1}{2}\right)^2 \kappa} \tag{3.64}$$

can become smaller and smaller for operation somewhat *above* threshold, i.e. where $C > C_{thr}$, if the threshold parameter C_{thr} itself approaces zero. In other words, it is possible to operate such a laser above threshold with a cooperativity-parameter less than unity!

On the other hand, the number of spontaneously emitted photons is given by

$$n_{sp} = \frac{w_{12}\, g^2 N}{2\kappa\, \gamma_{\perp}^2} = C\,(n_p + 1)\ , \tag{3.65}$$

as long as the thermal photon number n_c is negligible. Hence the spontaneous emission noise goes to zero for $n_p \to \infty$; this would also be the

case for the usual laser with $m_p = 0$. However, in that case (for any finite $\frac{g^2N}{\gamma\kappa}$) C would eventually drop below the usual threshold value $C_{thr} = 1$.

We conclude that it is the lowering of the threshold which allows a reduction of the spontaneous emission noise and thus diminishes the phase diffusion rate near threshold.

In Fig.11 we also compare the results obtained from the RWVPO model with results obtained from the full equations Eq.(3.49) and Eq.(3.50). Close to threshold the agreement is good, as expected. Further above threshold, where saturation becomes more important and where the neglected terms in the correlations become significant, the exact solution is seen to lie below the RWVPO result.

Assuming good stabilization of the laser intensity $r_0^2 = \bar{I}$ and small fluctuations we can now derive the *linewidth* of the squeezed-pump laser by linearizing Eq.(3.55) as follows:

$$\alpha(t) = r_0 e^{-i\left(\pm\frac{\pi}{2} + \delta\Psi(t)\right)} \tag{3.66}$$

around a stable semiclassical steady state with $\bar{\Psi} = \pm \frac{\pi}{2}$. This leads to the following equation of motion

$$\delta\dot{\Psi} = \left[-\frac{2\kappa M}{(1+M)} + \mathrm{Im}\left\{\frac{F_\alpha^{tot}}{r_0}\right\} \right] \delta\Psi + \mathrm{Re}\left\{\frac{F_\alpha^{tot}}{r_0}\right\} \tag{3.67}$$

for the phase fluctuations. (Setting the stochastic force $F_\alpha = 0$ in this equation again demonstrates the stability of $\bar{\Psi} = \pm \frac{\pi}{2}$; had we linearized around $\bar{\Psi} = 0, \pi$, we would have obtained an unstable equation for m_p real and positive.) Assuming a sufficiently large amplitude r_0 and small

noise we discard the term $\propto \mathrm{Im}\{F_\alpha^{tot}\}$ in Eq.(3.67) as negligible compared to the other term inside the brackets. Integration then yields

$$\delta\Psi(t) - \delta\Psi(0) = \int_0^t dt' \; \mathrm{Re}\left\{ \frac{F_\alpha^{tot}}{r_0} \right\} e^{\frac{2\kappa M}{1+M}(t'-t)} . \tag{3.68}$$

The laser linewidth is usually identified with the width of the stationary two-time correlation function

$$\begin{aligned} < a^\dagger(t)\, a(0) > &\approx r_0^2 < e^{i\left(\pm\frac{\pi}{2} + \delta\Psi(t)\right)} e^{-i\left(\pm\frac{\pi}{2} + \delta\Psi(0)\right)} > \\ &\approx r_0^2 e^{-\frac{1}{2} < [\delta\Psi(t) - \delta\Psi(0)]^2 >} . \end{aligned} \tag{3.69}$$

In our case we evaluate

$$\begin{aligned} & < [\delta\Psi(t) - \delta\Psi(0)]^2 > \\ &= e^{\frac{-4\kappa M}{1+M} t} \int_0^t dt' \int_0^t d\tau \, \frac{1}{4r_0^2} < [\, F_\alpha^{tot}(t') + F_\alpha^{tot*}(t')]\, [\, F_\alpha^{tot}(\tau) + F_\alpha^{tot*}(\tau)] > \\ &\qquad \times e^{\frac{2\kappa M}{1+M}(t'+\tau)} \\ &= \left[\frac{1 - e^{-\lambda t}}{\lambda} \right] D_{\Psi\Psi} \end{aligned} \tag{3.70}$$

with $\lambda = \frac{4\kappa M}{1+M}$ to lowest order in the stochastic terms. Hence we see that the two-time correlation function Eq.(3.69) does *not* decay to zero as in an ordinary laser; of course this is so, because the fluctuations are centered around a stable locked phase.

Nevertheless, our limit $m_p \to 0$ coincides with the usual result

$$< a^{\dagger}(t)\, a\,(0) > = r_0^2 e^{-\frac{1}{2} D_{\Psi\Psi} t}, \qquad (3.71)$$

obtained from the phase diffusion model, and moreover Eq.(3.70) also resembles the results derived for the laser with injected signal (Chow et al., 1975).

The absence of the random walk of the laser phase represents a reduction of the linewidth by itself, and it has already been demonstrated (cf. Fig.11) that $D_{\Psi\Psi}$ and thus the linewidth can be made as small as one pleases. However note that the theory used to derive Eq.(3.69) and Eq.(3.70) eventually breaks down when M approaches 1, as the noise in one quadrature becomes infinite.

The Fourier transform of Eq.(3.69) consists of a δ-function part stemming from the existence of a steady state phase around which we have linearized; plus the intensity fluctuation spectrum $S_{12}(\omega)$, the Fourier transform of $< a^{\dagger}(t), a(0) >$, which will be treated in Section 3.5.

3.4.2 Squeezed Cavity

Finally we will derive an analogous result for the case of a *squeezed cavity* . Since the semiclassical equations in α and α^* are unchanged, the RWVPO model formally coincides with the one for an ordinary laser (except for the noise correlation $< \Gamma_\alpha(t')\Gamma_\alpha(t) > = 2\kappa m_c\, \delta(t-t')$ due to the squeezing).

From the corresponding RWVPO equation in α and α^* it would thus not be apparent that the phase is locked. In order to derive the linewidth we therefore convert the original stochastic differential (Ito) equation (SDIE) in α and α^* into a SDIE in Ψ and I. This has already been treated in Section 3.3. Using those results we finally get

$$\delta\dot{\Psi} = -\frac{2\kappa m_c}{I}\delta\Psi + \Gamma_\Psi \tag{3.72}$$

with

$$\langle \Gamma_\Psi(t)\,\Gamma_\Psi(t')\rangle = D_{\Psi\Psi}\,\delta(t-t')$$

$$D_{\Psi\Psi} = \frac{1}{2I}\left(\frac{g^2 N w_{12}}{2\gamma_\perp} + \kappa(n_c + m_c)\right) \tag{3.73}$$

around a stable steady state $\bar{\Psi} = \pm\frac{\pi}{2}\,(m_c \in R_+)$. Thus a result similar to Eq.(3.70) for the squeezed-pump holds, but now we have $\lambda = \frac{2\kappa m_c}{I}$ and $D_{\Psi\Psi}$ given by Eq.(3.73). The reasoning following Eq.(3.70) still applies too.

Viewing Eq.(3.73) we note that $D_{\Psi\Psi}$ is increased at the stable semiclassical steady state. The expression for the unstable steady state is found by replacing $m_c \rightarrow -m_c$ and in this case one would obtain a reduction of roughly a factor $\frac{1}{2}$ near threshold in the limit $n_c \rightarrow \infty$. This is in agreement with a recent prediction by Gea-Banacloche (1987).

3.5 Variances and Squeezing Spectra

In this section we investigate the fluctuations of the laser field around a stable steady state in more general situations, such as in the low-Q cavity case where adiabatic elimination of the atomic variables is impossible. To this end we make use of a generalized (positive) P–function (Drummond and Gardiner, 1980) $P(\alpha,\alpha^\dagger,v,v^\dagger,D)$, that is we *double* the number of variables, treating $\alpha^\dagger$ and α and $v^\dagger$ and v as *independent* complex variables from now on.

We *linearize* the Langevin equations defined in Eq.(3.49) and Eq.(3.50) around a stable steady state according to

$$\delta \mathbf{x}^T = (\alpha - \alpha_0, \alpha^\dagger - \alpha_0^\dagger, v - v_0, v^\dagger - v_0^\dagger, D - D_0)^T, \tag{3.74}$$

this time keeping *all* terms. Note $\alpha_o{}^\dagger \equiv \alpha_o{}^*$ holds for the semiclassical steady state. This results in the following equation for the fluctuations:

$$\dot{\delta \mathbf{x}} = - A\, \delta \mathbf{x} + \Gamma$$

$$A = \begin{pmatrix} \kappa & 0 & -g & 0 & 0 \\ 0 & \kappa & 0 & -g & 0 \\ -gD_0 & 0 & \gamma_\perp & \gamma m_p & -g\beta_0 \\ 0 & -gD_0 & \gamma m_p & \gamma_\perp & -g\beta_0^* \\ 2gv_0^* & 2gv_0 & 2g\beta_0^* & 2g\beta_0 & \gamma_{||} \end{pmatrix}. \tag{3.75}$$

The correlations of the stochastic vector Γ are found by evaluating Eq.(3.50) at the steady state. In particular we find the following correlation for the atomic inversion:

$$\begin{aligned} <\Gamma_D(t)\ \Gamma_D(t)> &= \left[\ 2\gamma_{||}N - 2\gamma \frac{D_0}{C}(1-M) - 8\kappa n_0\,[C-1+M]\ \right]\delta(t-t') \\ &= \left\{ \left[\ 2\gamma_{||}N - 2\gamma \frac{D_0}{C} - 8\kappa n_0\,(C-1)\ \right] - M\frac{4w_{21}\,N}{C} \right\}\ \delta(t-t')\ , \end{aligned} \tag{3.76}$$

which is the usual expression *minus* a positive term proportional to $M = \frac{m_p}{\gamma}$. Hence it becomes clear why a laser with non-zero m_p should be called a *squeezed-pump* laser: the "pump" noise in the atomic inversion is decreased in (stable) steady state operation.

Setting

$$\Gamma(t) = B\, e(t)$$

$$\text{with} \quad \langle e(t)\, e^{T}(t') \rangle = \delta(t - t')\, Id(5) \tag{3.77}$$

(with Id(5) being the five-dimensional identity matrix), the constant matrix B satisfies $BB^{T}=D$, where D is the matrix defined in Eq.(3.51).

The standard expression of the *noise spectrum* according to the Wiener-Khinchine theorem reads (Gardiner, 1983):

$$S(\omega) = \frac{1}{\sqrt{2\pi}} \int_{-\infty}^{\infty} dt\; e^{-i\omega t} \langle \delta x(t)\, \delta x^{T}(0) \rangle \; . \tag{3.78}$$

Considering the Fourier transform of $\delta x(t)$:

$$\tilde{\delta x}(\omega) = \frac{1}{\sqrt{2\pi}} \int_{-\infty}^{\infty} dt\; e^{i\omega t}\; \delta x(t) \; , \tag{3.79}$$

satisfying the Fourier transform of Eq.(3.75), i.e.

$$(A - i\omega\, Id(5))\; \tilde{\delta x}(\omega) = \tilde{\Gamma}(\omega)$$

with

$$\tilde{\Gamma}(\omega) = \frac{1}{\sqrt{2\pi}} \int_{-\infty}^{\infty} dt\; e^{i\omega t}\; \Gamma(t) \; , \tag{3.80}$$

we derive

$$\langle \delta x(\omega)\, \delta x^{T}(\omega') \rangle = \delta(\omega + \omega')\, S(-\omega) \; . \tag{3.81}$$

Analogously setting

$$\tilde{\Gamma}(\omega) = B\,\tilde{e}(\omega)$$

$$\text{with} \quad \langle \tilde{e}(\omega)\,\tilde{e}^{T}(\omega') \rangle = \delta(\omega+\omega')\,Id(5) \tag{3.82}$$

with the *same* matrix B as before and using Eq.(3.79), Eq.(3.81) and Eq.(3.82) it is straightforward to obtain the well-known expression

$$S(\omega) = [A + i\omega\,Id(5)]^{-1}\,D\,[A^{T} - i\omega\,Id(5)]^{-1} \tag{3.83}$$

with the matrices A and D given by Eq.(3.75) and Eq.(3.51), respectively.

However, since we are mainly interested in the fluctuations of the laser mode we will use a *non-adiabatic elimination procedure* suggested by Reid (1988) in order to derive an analytical solution for the noise spectrum in $\alpha^{\dagger}$ and α alone.

Elimination of the variables $\delta\tilde{v}(\omega)$, $\delta\tilde{v}^{\dagger}(\omega)$, and $\delta\tilde{D}(\omega)$ from the linear set of Fourier transformed equations Eq.(3.79) yields

$$[A(\omega) - i\omega\,Id(2)] \begin{pmatrix} \delta\tilde{\alpha}(\omega) \\ \delta\tilde{\alpha}^{\dagger}(\omega) \end{pmatrix} = \tilde{F}(\omega) \tag{3.84}$$

for the remaining two equations. Note the explicit ω-dependence of the two-dimensional matrix A. In a straightforward calculation we have found

$$A(\omega) = \kappa \begin{pmatrix} 1 - U(\omega) & -V(\omega) \\ -V(\omega) & 1 - U(\omega) \end{pmatrix}$$

where

$$U(\omega) = \frac{(\Delta + a)(1 - M - a) + a(a - M)}{N}$$

$$V(\omega) = \frac{(a - M)(1 - M - a) + a(\Delta + a)}{N}$$

$$N(\omega) = (\Delta + a)^2 - (a - M)^2 \tag{3.85a}$$

with the following abbreviations

$$\Delta(\omega) = 1 - i\frac{\omega}{\gamma_\perp} \equiv \Delta^*(-\omega)$$

$$a(\omega) = 2\left(\frac{g|\beta_0|^2}{\gamma_\perp}\right)^2 \frac{1}{1+\Delta(\omega)} \quad . \tag{3.85b}$$

The stochastic term $\tilde{F}(\omega)$ was calculated to be

$$\tilde{F}(\omega) = \frac{g}{\gamma_\perp N}\begin{pmatrix}(\Delta+a)\,\Gamma_v(\omega) + (a-M)\,\Gamma_{v^\dagger}(\omega) + b\,\Gamma_D(\omega)\\ (\Delta+a)\,\tilde{\Gamma}_{v^\dagger}(\omega) + (a-M)\,\tilde{\Gamma}_v(\omega) - b\,\tilde{\Gamma}_D(\omega)\end{pmatrix}$$

with

$$b = \frac{g\beta_0}{\gamma_\perp}\left(\frac{\Delta+M}{\Delta+1}\right) \equiv -b^*(-\omega) \quad . \tag{3.86}$$

Setting

$$\tilde{F}(\omega) = B\ (\omega)\,\tilde{e}(\omega)$$

$$\text{with} \qquad \langle \tilde{e}(\omega)\,\tilde{e}^T(\omega')\rangle = \delta(\omega+\omega')\,\mathrm{Id}(2) \tag{3.87}$$

after the model of Eq.(3.82), we define a two-dimensional diffusion matrix $D(\omega) = B(\omega)B(-\omega)^T$. Making use of correlations of the form $\langle \tilde{F}(\omega)\,\tilde{F}^T(-\omega)\rangle$, we obtain the following matrix elements:

$$D_{\alpha\alpha}(\omega) = D_{\alpha^*\alpha^*}(\omega)^* = \left|\frac{g}{\gamma_\perp N}\right|^2 \times$$
$$\{\,[\,|\Delta+a|^2 + |a-M|^2]\,D_{vv} + 2\,\mathrm{Re}[(\Delta+a)(a-M)^*]\,D_{vv^\dagger}$$
$$+ 2i\ \mathrm{Im}[\,b(\Delta+M)^*]\,D_{vD} - |b|^2 D_{DD}\,\}$$

$$D_{\alpha^*\alpha}(\omega) = D_{\alpha^*\alpha}(\omega)^* = \left|\frac{g}{\gamma_\perp N}\right|^2 \times$$

$$\{ [\,|\Delta + a|^2 + |a - M|^2]\, D_{vv}\dagger + 2\,\mathrm{Re}[(\Delta + a)(a - M)^*]\, D_{vv}$$

$$- 2i\ \mathrm{Im}[\,b(\Delta + M)^*]\, D_{vD} + |b|^2 D_{DD} \} \qquad (3.88)$$

with D_{ij} from Eq.(3.51) (the thermal photon number n_c has been neglected in this analytical result). Note that this matrix is real and that $D(-\omega) = D^T(\omega) = D(\omega)$ holds for $\alpha = \beta$, i.e. for $\varepsilon_p = 0$. The spectra of interest are found along similar lines to the five-dimensional problem - with the difference that the matrices are no longer constant. We thus find

$$S(\omega) = [A(-\omega) + i\omega\,\mathrm{Id}(2)]^{-1}\, D(\omega)\, [A^T(\omega) - i\omega\,\mathrm{Id}(2)]^{-1}. \qquad (3.89)$$

Of course the "adiabatic elimination limit" Eq.(3.54) can be recovered by setting $\omega = 0$ which corresponds to looking at infinitely long time-scales in the Fourier transform.

Since we are interested in the amplitude and phase fluctuations of the laser let us introduce the quantity

$$S_{xx}(\omega) = \frac{1}{\sqrt{2\pi}} \int_{-\infty}^{\infty} dt\ e^{-i\omega t} < \tfrac{1}{2}[\delta\alpha + \delta\alpha^\dagger]\, \tfrac{1}{2}[\delta\alpha + \delta\alpha^\dagger] >$$

$$= \frac{1}{4}\,(\,S_{11}(\omega) + S_{22}(\omega) + S_{12}(\omega) + S_{21}(\omega)\,)\,. \qquad (3.90a)$$

As we have chosen a characteristic function involving a correspondence between c-numbers and normally ordered operators, this equals

$$S_{xx}(\omega) = \frac{1}{\sqrt{2\pi}} \int_{-\infty}^{\infty} dt\ e^{-i\omega t} < : \mathrm{Re}(a), \mathrm{Re}(a) : > \,, \qquad (3.90b)$$

where $<:A,B:> = <:AB:> - <:A:><:B:>$ for operator functions A and B of a and $a^\dagger$ (: : denotes normal ordering as usual). S_{xx} thus represents the normally ordered variance of the real part of the annihilation operator a of the laser mode. Visualizing *small* fluctuations around a stable steady state with imaginary amplitude (as is the case for the squeezed vacuum pump as well as the antibunched input), we conclude that S_{xx} relates to the spectrum of *phase* fluctuations of the laser. Analogously,

$$\begin{aligned} S_{yy}(\omega) &= \frac{1}{\sqrt{2\pi}} \int_{-\infty}^{\infty} dt\, e^{-i\omega t} < \frac{1}{2i}[\delta\alpha - \delta\alpha^\dagger] \frac{1}{2i}[\delta\alpha - \delta\alpha^\dagger] > \\ &= \frac{1}{4}(-S_{11}(\omega) - S_{22}(\omega) + S_{12}(\omega) + S_{21}(\omega)) \\ &= \frac{1}{\sqrt{2\pi}} \int_{-\infty}^{\infty} dt\, e^{-i\omega t} <: \mathrm{Im(a)}, \mathrm{Im(a)} :> \end{aligned} \tag{3.91}$$

approximately constitutes the spectrum of *amplitude* fluctuations.

The final quantity we want to calculate is the so-called *squeezing variance* (Collett and Gardiner, 1984, Collett and Walls, 1985), usually defined as

$$V_\Theta(\omega) = 1 + 2\kappa [\, S_{21}(\omega) + S_{12}(\omega) + e^{-2i\Theta} S_{11}(\omega) + e^{2i\Theta} S_{22}(\omega) \,] \,. \tag{3.92}$$

This variance is normalized in such a way that $V_\Theta(\omega) < 1$ indicates squeezing in the output quadrature X_Θ.

For the squeezed-pump laser we get the following analytical expressions for the peak value of the variances:

$$V_{xx}(\omega=0) \equiv V_{\Theta=0}(\omega=0)$$

$$= 1 + \frac{1}{M^2}\left[\, 1 - M^2 + C\left(\, 1+2\,(m_p+n_p)\,\right)\,\right] \qquad (3.93)$$

and

$$V_{yy}(\omega=0) \equiv V_{\Theta=\frac{\pi}{2}}(\omega=0)$$

$$= 1 + \frac{1}{\left(n_p+\frac{1}{2}\right)}\,\frac{f(\hat{C})}{\hat{C}^2}$$

with $$\hat{C} = C - 1 + M = C - 1 + \frac{m_p}{\left(n_p+\frac{1}{2}\right)}$$

$$f(\hat{C}) = \hat{C}^2\,[n_p^2+m_p^2] + \hat{C}\left[\frac{n_p-m_p+\frac{1}{2}}{\left(n_p+\frac{1}{2}\right)}\left(4m_p^2+\frac{1}{2}\right) - 1\right]$$

$$+ \frac{2(n_p+1)}{\left(n_p+\frac{1}{2}\right)}\left[n_p-m_p+\frac{1}{2}\right]^2 . \qquad (3.94)$$

They constitute symmetrical functions of ω (for simplicity this result was only derived for $\varepsilon_p = 0$). Obviously $V_{xx}(\omega=0)$ stays always greater than unity and hence we do *not* expect a noise reduction below the standard quantum limit in the *phase* noise.

On the other hand, we notice that the *amplitude* fluctuations corresponding to V_{yy} can drop below the coherent level, leading to sub-Poissonian statistics, similar to the effect predicted in the laser system examined by Yamamoto et al. (1986). For large M this happens for $C \approx C_{thr} = 1-M < 1$, corresponding to a cooperativity-parameter which would be *below* threshold in an ordinary laser.

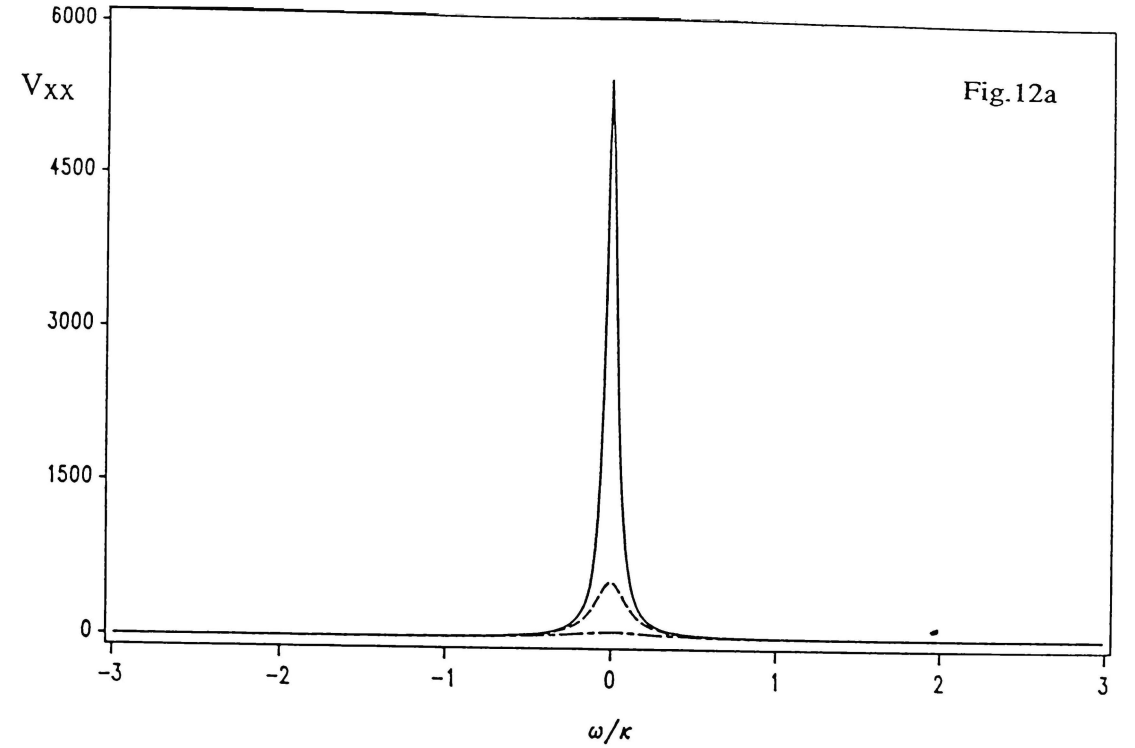

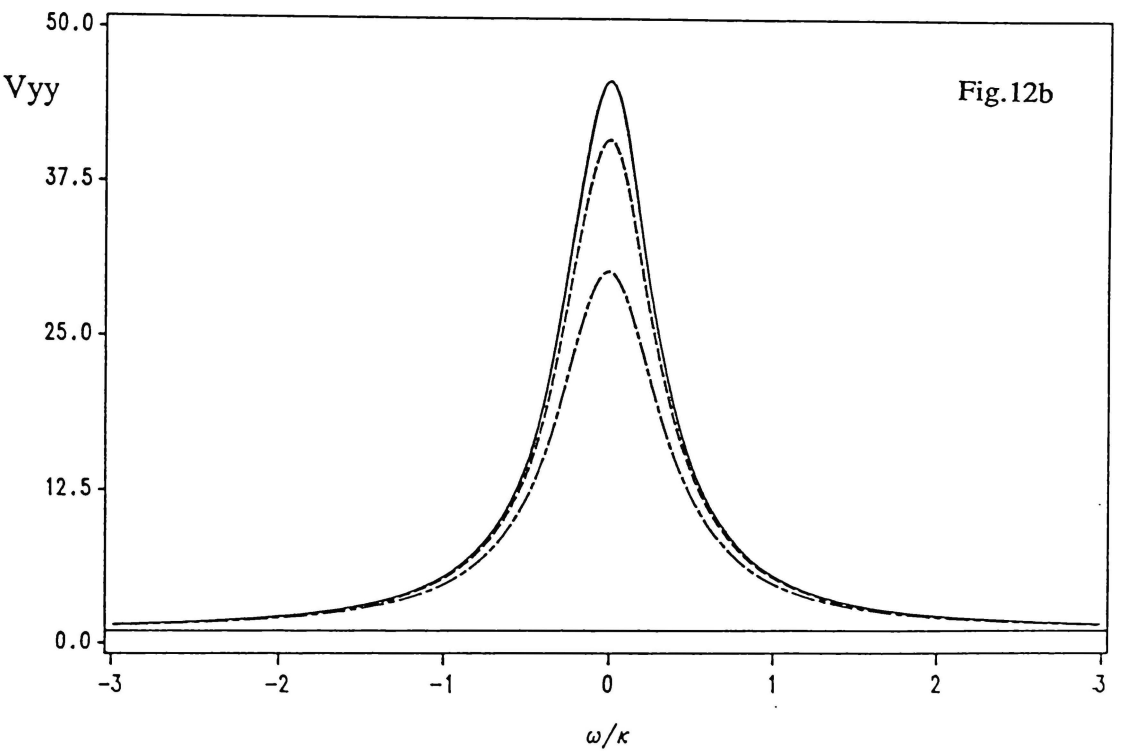

Fig. 12 Squeezing variances with fixed output intensity for three small M values, where the "phase" noise V_{xx} is dominant in the laser; parameters: $\gamma = 10^4\kappa$, $E_p = 0$, 20% above threshold

(a) V_{xx} (b) V_{yy}

_____ M = 0.02

_ . _ . _ . _ . _ M = 0.06

_ _ _ _ _ _ M = 0.20

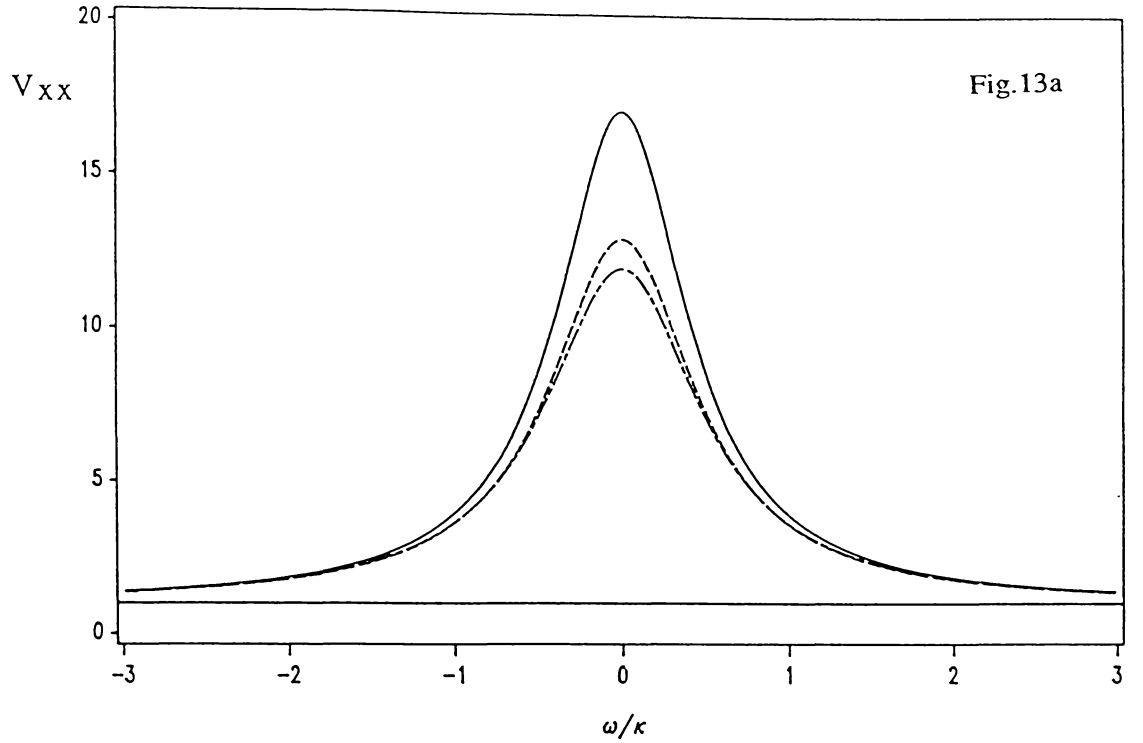

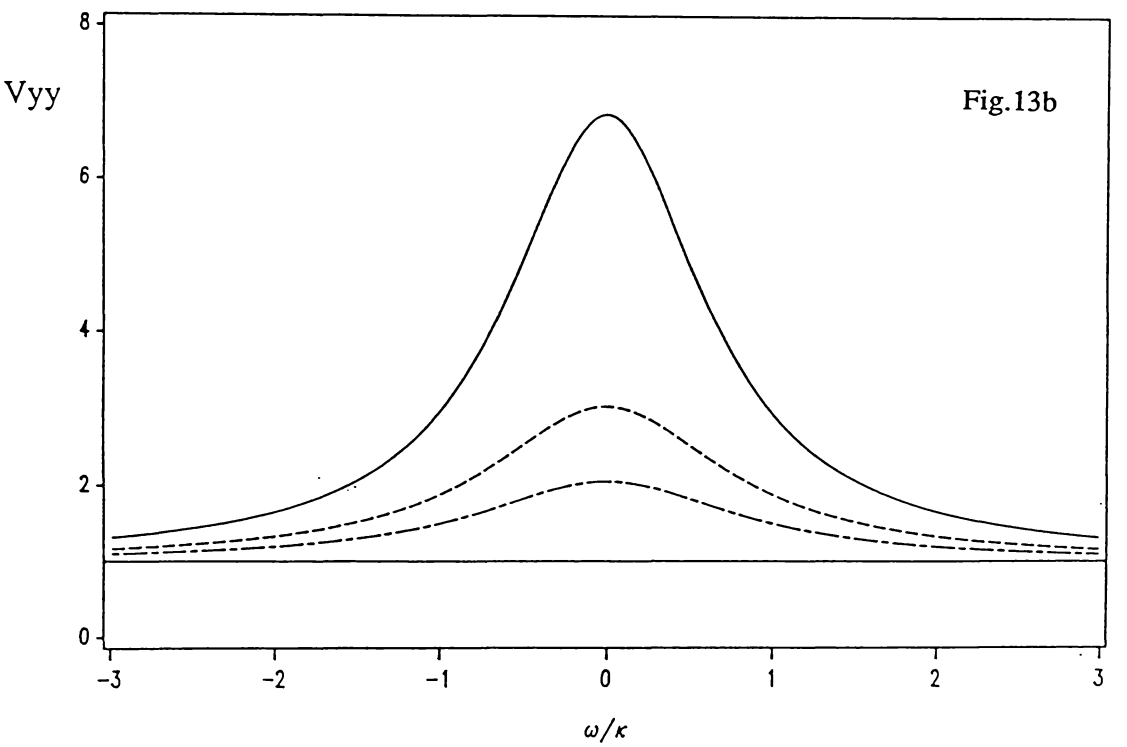

Fig. 13 Squeezing variances with fixed output intensity for three larger M values, where the "phase" and "amplitude" noise V_{xx} and V_{yy} become comparable; parameters: $\gamma = 10^4\kappa$, $E_p = 0$, 35% above threshold

(a) V_{xx} (b) V_{yy}

———— M = 0.55

_ · _ · _ · _ M = 0.78

_ _ _ _ _ _ M = 0.89

Finally we evaluate the full squeezing spectrum *numerically* starting from Eq.(3.83). In Fig.12 we show the squeezing variances V_{xx} and V_{yy} as a function of ω/κ, for increasing M values and fixed output intensity near threshold, for the case $\varepsilon_p = 0$. Note that the variance in X (the "phase noise") is for small M very much larger than the variance in Y (the "amplitude noise"), similar to the distribution of noise encountered in an ordinary laser where the phase undergoes a random walk. With increasing M both V_{xx} *and* V_{yy} decrease: V_{yy} due to the quenching of the noise and V_{xx} due to the M–dependent distortion of the semiclassical potential which leads to a localization of the laser phase.

Fig.13 depicts V_{xx} and V_{yy} for a set of larger M values. V_{xx} decreases more rapidly than V_{yy} ; it can even become less than V_{yy} , thus making the Y quadrature corresponding to the the direction of the coherent excitation the noisier one! Fig.14 displays the variance in Y further above threshold, where the fluctuations drop below the coherent level $V_{yy} = 1$, that is where we have sub-Poissonian statistics in the laser output. The squeezing can be *enhanced* by adding a coherent part $\varepsilon_p = i\,|\varepsilon_p|$ corresponding to sub-Poissonian statistics in the atomic reservoir. The results are shown in Fig.15 for various values of $|\varepsilon_p|$. For these curves we have linearized around the larger one of the two stable roots, which leads to better squeezing in comparison with the other stable root. The squeezing occurs for C around the "threshold" value C_a where two new (unstable) solutions come into being. This effect of squeezing arising around a *critical point* of the system has been observed before (see, e.g., Collett and Walls (1985)). For a bunched input, i.e. $\varepsilon_p = |\varepsilon_p|$, causing an increase of the variance in X with M for $C > C_b$, no substantial squeezing was found in either X or Y.

Finally Fig.16 displays some squeezing in a low-Q cavity with $\gamma \approx \kappa$ (which requires the non-adiabatic elimination procedure used above),

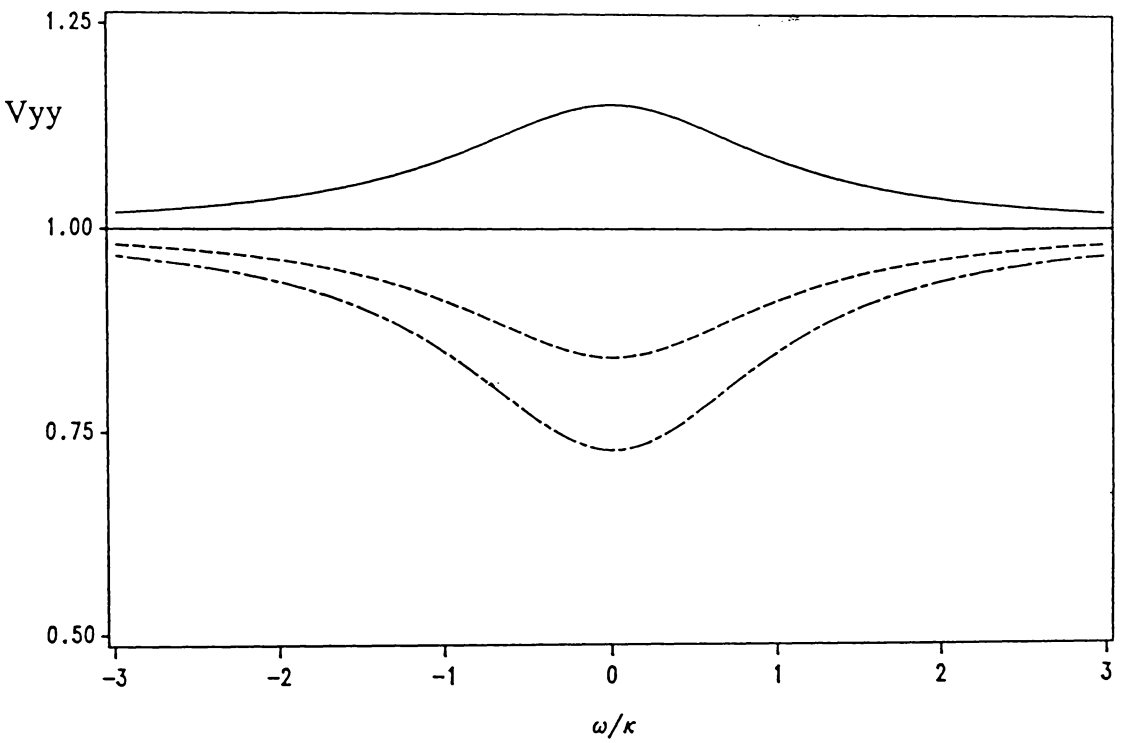

Fig. 14 V_{yy} dropping below the coherent level for $\gamma = 10^2\kappa$, 130% above the threshold $C_{thr} = 1 - M$

_____ M = 0.20, C = 1.04

_ . _ . _ . _ . _ M = 0.55, C = 0.59

_ _ _ _ _ _ M = 0.83, C = 0.22

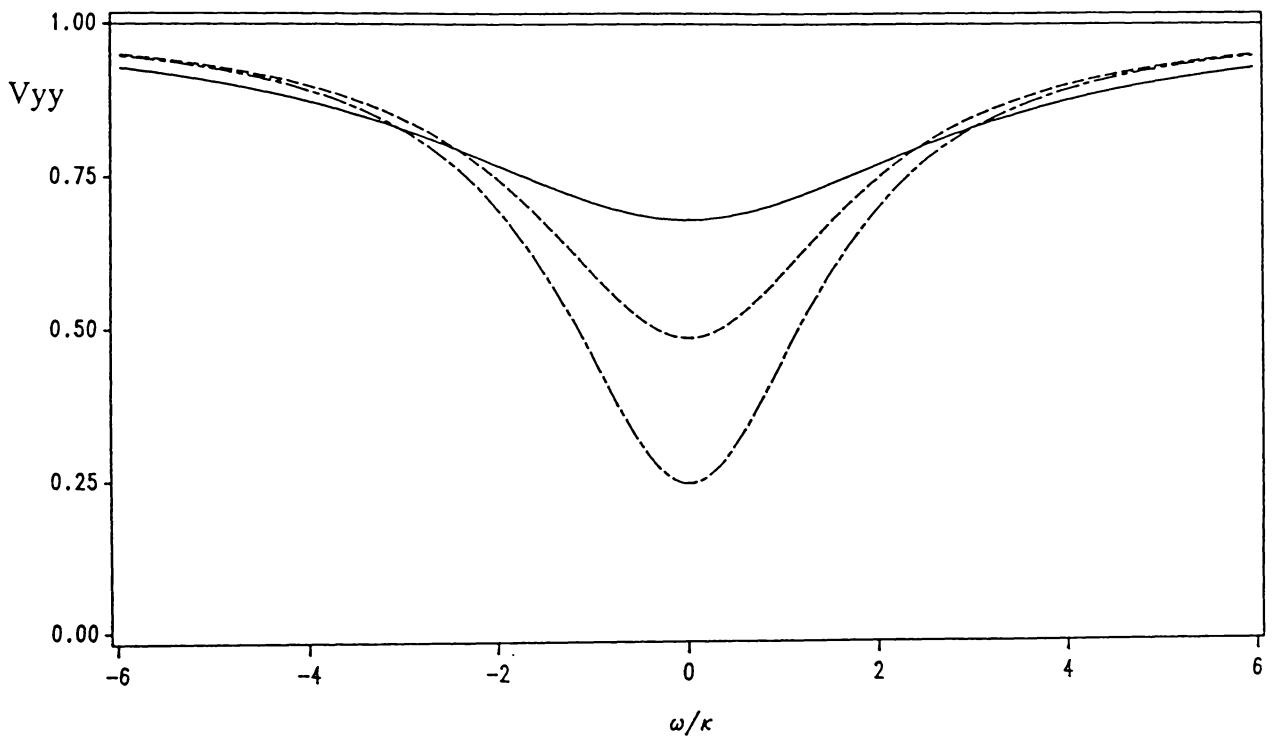

Fig. 15 V_{yy} for variable antibunched input E_p and constant M = 0.93, $\gamma = 2.8 \times 10^4 \kappa$, C = 0.66 C_b

———— $|E_p| = 0$

_ · _ · _ · _ · _ $|E_p| = 1.5 \times 10^4$

_ _ _ _ _ _ $|E_p| = 2.5 \times 10^4$

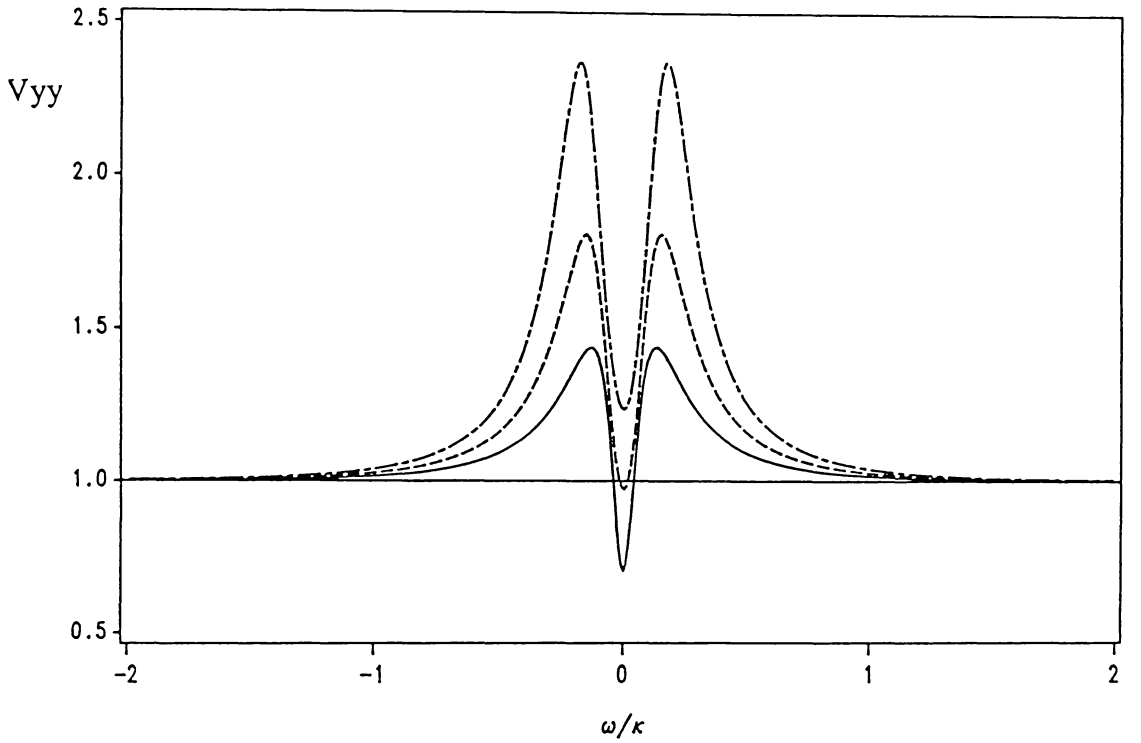

Fig. 16 Squeezing variance V_{yy} with Rabi sidepeaks in a low-Q cavity with $\gamma_{||} = 0.3\ \kappa$, $E_p = 0$, $M = 0.88$

_____ 160% above threshold

_ . _ . _ . _ 260% above threshold

_ _ _ _ _ _ 400% above threshold

where the Rabi sidebands become visible in the "intensity fluctuation spectrum", as $S_{21}(\omega)$ is sometimes referred to. (Note, however, that this is misleading as $S_{21}(\omega)$ is in general *not* identical with the spectrum of the fluctuations in the intensity or photon number which is the Fourier transform of the stationary correlation function $< : N(t)\, N(0) : >$ with $N=a^{\dagger}a$.)

We repeat the above analysis for the case of additionally squeezing the cavity , that is keeping the thermal photons in the cavity reservoir. This amounts to adding the terms

$$\delta S_{xx}(\omega = 0) = \frac{1}{2\kappa}\left(\frac{1+M}{M}\right)^2 (n_c + m_c)$$

$$\delta S_{yy}(\omega = 0) = \frac{1}{2\kappa}\left(\frac{C}{C-(1-M)}\right)^2 (n_c - m_c) \qquad (3.95)$$

to the matrix-elements of the fluctuation spectrum (m_c assumed real and positive). The present linearized theory is only expected to be valid in the small noise limit $n_c \ll |\alpha|^2$.

The calculation of the *output* variance differs from the case of the squeezed-pump laser: it has recently been shown that the normally ordered output variance contains antinormally ordered contributions from the field inside the cavity, if the modes entering the cavity are squeezed (Gardiner et al., 1987, Collett, 1987). However, on the grounds of very qualitative physical arguments, it can be expected that the effect of the additional terms due to squeezing the cavity will be to further reduce the fluctuations in Y in the output, thus leading to improved squeezing compared to the squeezed pump alone.

3.6 Conclusions and Outlook

The major results will be summarized briefly in this section. For the squeezed-vacuum pump we have seen that the anisotropy of noise in the reservoir coupled to the atoms of the laser breaks the symmetry in phase encountered in an ordinary laser. This leads to a phase-locking phenomenon (cf. Fig.7), and the solution settles down where the amplitude fluctuations are smallest. Alternatively, by treating the squeezed-pump laser as a rotating wave van der Pol oscillator, this effect can be interpreted as a stabilization of the laser phase above threshold to the directions where the phase-dependent gain is largest.

However, in contrast to the phase-locking occurring in the laser with injected signal, there exist two stable phases corresponding to the two "directions" in phase, along which the noise is quenched in the squeezed vacuum state in the bath. This might give rise to quantum coherence phenomena between the two macroscopically distinct phases.

The steady state values of the cavity field and the atomic polarization and inversion have been seen to differ from an ordinary laser. Another important feature is the lowering of the threshold compared to a conventional laser, brought about by squeezing the reservoir damping the atoms. This allows one to operate the laser *above* threshold, in regions where the cavity cooperativity-parameter is less than unity, which is favourable for reducing the spontaneous emission noise.

By means of the rotating wave van der Pol oscillator model one can calculate a formal expression for the phase diffusion rate. This quantity decreases with the spontaneous emission noise, if one gradually increases the "strength" of the squeezing in the bath - while staying at a *constant* percentage above threshold. However, the phase is locked, so

this quantity cannot be given the usual interpretation. The expression derived for the linewidth of the squeezed-pump laser resembles the result of the laser with injected signal.

Analyzing the laser output fluctuations, two effects were observed. For moderate squeezing parameters the noise in the quadrature phase operator Y, that relates to the amplitude, is quenched due to the squeezing of this quadrature in the bath. *Simultaneously* the phase noise, too, is reduced (compared to the usual situation with phase diffusion) due to the localization of the phase. This is, of course, possible, since the system is not in a number-phase minimum uncertainty state. However, for increasing squeezing parameters one eventually reaches a point where a further reduction of squeezing in the amplitude leads to increased noise in the phase.

Reduction of the amplitude noise below the standard quantum limit, that is squeezing in the quadrature phase operator corresponding to the laser amplitude, is possible; however, the squeezing is typically found for small cavity cooperativity-parameters which are never considered in a conventional laser theory. It can be shown analytically that the quadrature phase which relates to the laser phase, never displays fluctuations reduced below the vacuum level.

Noticing that the squeezed vacuum in the bath corresponds to super-Poissonian statistics in the bath provides the motivation to add a coherent part to the squeezed vacuum pump. The squeezing in the laser output can be improved by adding an appropriate coherent field driving the atoms, which models a pump-bath with sub-Poissonian statistics to start with.

Depending on the relative phase between the squeezing parameter M and the additional coherent driving field ε, the photon statistics in the bath may display sub- or super-Poissonian statistics. Two special cases

of interest were dealt with: since the coherent amplitude ε is assumed strong, the case that corresponds to enhanced amplitude fluctuations (both M and ε are real) can be referrred to as the "bunched input", whereas the complementary case (M real and ε imaginary), characterized by reduced amplitude fluctuations, is called the "antibunched input", as they display bunching or antibunching, respectively.

Fig.9 illustrates the existence and positioning of the stable points of oscillation that result from the combination of phase-locking due to squeezing and driving field for both types of inputs. By adding an imaginary or antibunched field to the squeezed vacuum pump, one makes one of the two previously degenerate local minima in Fig.7b, more precisely the one in direction of the coherent field, deeper than the other. If one chooses a real or bunched input, then a trade-off between a tendency to lock the phase to the imaginary axis due to the squeezing and a tendency to lock to the real driving field takes place. The outcome of this, two equally deep local minima which lie symmetrically about the real axis, is depicted in Fig.7a. Finally, it should be remarked that an antibunched input does indeed give rise to enhanced squeezing in the laser output.

Finally, the case of squeezing the vacuum modes entering the the cavity, which was also considered on the way, was seen to differ drastically from the previous case of squeezing the pump - at least as far as the technical methods required are concerned. The difference lies in the fact that squeezing the cavity does not alter the semiclassical equations for the complex amplitude of the laser field. The change brought about by the squeezing consists entirely of new phase-dependent noise correlations, so the effect is of lower order than the "deterministic" changes in the squeezed-pump laser.

Thus a variable transformation to phase and intensity variables is required in order to reveal the phase-locking that takes place due to the anisotropic fluctuations. In close analogy to the result derived for the formally very different, but physically related situation of the squeezed-pump laser, the laser phase is locked such as to minimize the amplitude fluctuations. However, for the squeezed cavity a semiclassical potential cannot be derived, as the semiclassical potential condition is not satisfied in the new set of variables. This again reflects the difference between the two situations.

Finally it is worth mentioning that the above theory may be used to treat optical bistability in the presence of a squeezed reservoir, upon the well-known formal replacement $N \rightarrow -N$, where N denotes the number of atoms. Qualitative discussions show that by changing the phase of the squeezing parameter, one might be able to "switch" between the two solutions of optical bistability, turning the deeper local minimum into the shallower one and vice versa.

Appendix A: Two-Frequency Photodetection

The following is a generalization of Mollow's (1968) quantum mechanical model of photodetection to the situation in which the spectrum of the light incident on the photodetector has (narrow) peaks around *two* frequencies.

If the frequencies are well separated the total number of photon counts should amount to the sum of the independent photon counts for either of the two frequencies. However, if the two peak frequencies approach each other and if there is an appreciable overlap in the Glauber sensitivity function of the detector for the two frequencies in the incident light (Glauber, 1963a, 1965), one would expect some sort of interference effect to occur. In this section this behaviour will be explicitly demonstrated in a particular quantum model of the detector.

Again, we model the photodetector as a reservoir of harmonic oscillators, initially in their ground state. There are two distinct modes $a(\mathbf{k}_1, \lambda_1)$ and $a(\mathbf{k}_2, \lambda_2)$ coupled to this reservoir. We assume dipole coupling and optical frequencies, so that the rotating wave approximation can be made. An appropriate Hamiltonian is thus given by

$$H = \hbar\omega_1 a^\dagger_{\mathbf{k}_1,\lambda_1} a_{\mathbf{k}_1,\lambda_1} + \hbar\omega_2 a^\dagger_{\mathbf{k}_2,\lambda_2} a_{\mathbf{k}_2,\lambda_2} + \hbar\sum_{j=0}^{\infty}\omega_j b_j^\dagger b_j - i\hbar\left[a^\dagger_{\mathbf{k}_1,\lambda_1}\sum_{j=0}^{\infty} g_j^{(1)} b_j + a^\dagger_{\mathbf{k}_2,\lambda_2}\sum_{j=0}^{\infty} g_j^{(2)} b_j + \text{h.c.}\right] . \tag{A.1}$$

The creation and annihilation operators satisfy the usual commutation relations:

$$[\, a^\dagger_{\mathbf{k}_1,\lambda_1}\,,\, a^\dagger_{\mathbf{k}_2,\lambda_2}\,] = \delta_{\lambda_1\lambda_2}\,\delta^3(\mathbf{k}_1-\mathbf{k}_2) \ . \tag{A.2}$$

Let us assume $\lambda_1 \neq \lambda_2$. Hence even in the limit $\omega_1 = \omega_2$ we have two distinguishable and thus *commuting* modes $a_1 \equiv a(\mathbf{k}_1, \lambda_1)$ and $a_2 \equiv a(\mathbf{k}_2, \lambda_2)$, described by the two-mode Hamiltonian Eq.(A.1). From this Hamiltonian one may derive the following Heisenberg equations of motion:

$$\begin{aligned}
\dot{a}_1 &= -i\,\omega_1\, a_1 - \sum_{j=0}^{\infty} g_j^{(1)}\, b_j \\
\dot{a}_2 &= -i\,\omega_2\, a_2 - \sum_{j=0}^{\infty} g_j^{(2)}\, b_j \\
\dot{b}_j &= -i\,\omega_j\, b_j + g_j^{(1)^*} a_1 + g_j^{(2)^*} a_2 \; .
\end{aligned} \tag{A.3}$$

Since this a *linear* set of equations, we make a linear ansatz:

$$\begin{aligned}
a_1(t) &= \mu_{11}(t)\, a_1(0) + \mu_{12}(t)\, a_2(0) + \sum_{j=0}^{\infty} \zeta_j^{(1)}(t)\, b_j(0) \\
a_2(t) &= \mu_{21}(t)\, a_1(0) + \mu_{22}(t)\, a_2(0) + \sum_{j=0}^{\infty} \zeta_j^{(2)}(t)\, b_j(0) \\
b_j(t) &= \lambda_j^{(1)}(t)\, a_1(0) + \lambda_j^{(2)}(t)\, a_2(0) + \sum_{k=0}^{\infty} \nu_{jk}(t)\, b_k(0)
\end{aligned} \tag{A.4}$$

with initial conditions

$$\begin{aligned}
&\mu_{ik}(0) = \delta_{ik} && i,k \in \{1,2\} \\
&\nu_{ik}(0) = \delta_{ik} && \\
&\lambda_j^{(i)}(0) = \zeta_j^{(i)}(0) = 0 && \forall\, i \in \{1,2\},\, \forall\, j \in \mathbb{N}_0
\end{aligned} \tag{A.5}$$

The solution satisfying these initial conditions is easily found by using the Laplace transform, defined by

$$\tilde{f}(s) = \int_0^\infty dt\, e^{-st} f(t) \ . \tag{A.6}$$

We thus find

$$\begin{aligned} \tilde{\mu}_{11}(s) &= \frac{[\, s + i\omega_2 + F_{22}(s)\,]}{[\, s + i\omega_1 + F_{11}(s)\,][\, s + i\omega_2 + F_{22}(s)\,] - F_{12}(s)\, F_{21}(s)} \\ \tilde{\mu}_{21}(s) &= \frac{-F_{12}(s)}{[\, s + i\omega_2 + F_{22}(s)\,]}\, \tilde{\mu}_{11}(s) \end{aligned} \tag{A.7}$$

and corresponding equations for $\mu_{22}(s)$ and $\mu_{12}(s)$ using the definition

$$F_{ij}(s) = \sum_{j=0}^{\infty} \frac{g_j^{(i)}\, g_j^{(k)^*}}{s + i\omega_j} \ . \tag{A.8}$$

Assuming optical frequencies and weak dipole coupling constants $g_j^{(i)}$, one may neglect quadratic terms in F_{ij} and make the *pole approximation* at the same time, that is treat the functions $F_{ij}(s)$ as small regularizations around a pole s_{pole} and evaluate them at $s = s_{pole}$. This procedure leads to the following approximate version of Eq.(A.7):

$$\begin{aligned} \tilde{\mu}_{11}(s) &\approx \frac{1}{[\, s + i\omega_1 + F_{11}(-i\omega_1)\,]} \\ \tilde{\mu}_{21}(s) &\approx \frac{-F_{21}(-i\varpi)}{[\, s + i\varpi + F_+(-i\varpi)\,] + f^2(\Delta)} \end{aligned} \tag{A.8}$$

with the definitions

$$\begin{aligned} f^2(\Delta) &= \Delta^2 + i\Delta\, \{\, F_{22}(-i\varpi) - F_{11}(-i\varpi)\,\} \\ F_+(s) &= \frac{1}{2}\, [\, F_{11}(s) + F_{22}(s)\,] \end{aligned} \tag{A.9}$$

and

$$\Delta \equiv \frac{\omega_1 - \omega_2}{2} \qquad \varpi \equiv \frac{\omega_1 + \omega_2}{2} \quad . \tag{A.10}$$

Note that the cross-terms μ_{21} and μ_{12} are smaller by a factor of F_{ij} than the diagonal terms μ_{11} and μ_{22}.

Taking the inverse Laplace transform, we get

$$\mu_{11}(t) = e^{-\{\, i\omega_1 + F_{11}(-i\omega_1)\,\}t}$$

$$\mu_{21}(t) = -F_{12}(-i\varpi)\,\frac{\sin(f(\Delta)t)}{f(\Delta)}\; e^{-\{\, i\varpi + F_{+}(-i\varpi)\,\}t}\,, \tag{A.11}$$

satisfying the initial conditions Eq.(A.5). Since the Hamiltonian Eq.(A.1) conserves the *total* number of quanta, that is the sum of quanta in the two modes and in the bath, the following useful relations for the unknown functions $\lambda_j^{(i)}$ may be derived:

$$\sum_{j=0}^{\infty} |\lambda_j^{(i)}(t)|^2 = 1 - |\mu_{ii}(t)|^2 - |\mu_{ik}(t)|^2 \qquad i \neq k \in \{1,2\} \tag{A.12}$$

$$\sum_{j=0}^{\infty} \lambda_j^{(i)}(t)^* \lambda_j^{(k)}(t) = -\mu_{ii}(t)^* \mu_{ik}(t) - \mu_{ki}(t)^* \mu_{kk}(t) \qquad i \neq k \in \{1,2\}\ . \tag{A.13}$$

Following Mollow (1968) we proceed to calculate the photon counting probability, assuming that initially the sytem is in a state

$$|\,\psi(0)\rangle = |\,\alpha_1^0\rangle\ |\,\alpha_2^0\rangle \otimes \prod_{j=0}^{\infty} |\,0\rangle_j\ , \tag{A.14}$$

a multiple tensor product of coherent states (the bath being in the ground-state). In general, the probability of finding m photons (of arbitrary frequency and polarization) in the detector is given by the trace (over bath and field variables) of the total density matrix multiplied by P_m, the projector onto the subspace with exactly m photons in the bath:

$$\begin{aligned} p_m(t) &= Tr_{F,B} \{ W(t) P_m \} \\ &= Tr_F \{ \rho_F(0) \; Tr_B \{ P_{|0>_B} e^{iHt/\hbar} P_m e^{-iHt/\hbar} \} \} , \end{aligned} \tag{A.15}$$

where

$$W(t) = e^{-iHt/\hbar} (\rho_F(0) \otimes P_{|0>_B}) \, e^{-iHt/\hbar} \tag{A.16}$$

denotes the density matrix for the bath and the field with $P_{|0>_B}$ being the projector onto the groundstate of the bath.

For a linear interaction as given by Eq.(A.1) the system *stays* in a coherent state and the coherent amplitudes $\alpha_1(t)$, $\alpha_2(t)$, and $\beta_j(t)$ satisfy the *same* equations of motion Eq.(A.3) as the Heisenberg operators:

$$\begin{aligned} \dot{\alpha}_1 &= -i \dot{\omega}_1 \alpha_1 - \sum_{j=0}^{\infty} g_j^{(1)} \beta_j \\ \dot{\alpha}_2 &= -i \omega_2 \alpha_2 - \sum_{j=0}^{\infty} g_j^{(2)} \beta_j \\ \dot{\beta}_j &= -i \omega_j \beta_j + g_j^{(1)^*} \alpha_1 + g_j^{(2)^*} \alpha_2 \; . \end{aligned} \tag{A.17}$$

Hence it follows that the state of the bath at time t is given by

$$|\psi(t)\rangle_B = \prod_{j=0}^{\infty} |\lambda_j^{(1)}(t)\ \alpha_1^0 + \lambda_j^{(2)}(t)\ \alpha_2^0\rangle \ . \tag{A.18}$$

The probability introduced in Eq.(A.15) in our case of a linear interaction of coherent states is found to be a Poissonian distribution

$$p_m(t) = \frac{[\bar{m}(t)]^m}{m!}\, e^{-\bar{m}(t)} \tag{A.19}$$

around the mean number of photons absorbed by the bath

$$\bar{m} = {}_B\langle\psi(t)| \sum_{j=0}^{\infty} b_j^{\dagger}(0)\, b_j(0)\ |\psi(t)\rangle_B \ . \tag{A.20}$$

Here the mean photon number reduces to

$$\begin{aligned}\bar{m} &= \sum_{j=0}^{\infty} \left(|\alpha_1^0|^2\, |\lambda_j^{(1)}|^2 + |\alpha_2^0|^2\, |\lambda_j^{(2)}|^2 + 2\,\mathrm{Re}[\ \alpha_1^0\, \alpha_2^{0*}\, \lambda_j^{(1)}\, \lambda_j^{(2)*}\ ] \right) \\ &= |\alpha_1^0|^2 \left(1 - |\mu_{11}(t)|^2 - |\mu_{12}(t)|^2\right) + |\alpha_2^0|^2 \left(1 - |\mu_{22}(t)|^2 - |\mu_{21}(t)|^2\right) \\ &\quad - 2\,\mathrm{Re}[\ \alpha_1^0\, \alpha_2^{0*}\, \{\mu_{11}(t)\, \mu_{12}(t)^* + \mu_{22}(t)^*\, \mu_{21}(t)\}\ ] \ ,\end{aligned} \tag{A.21}$$

where Eq.(A.12) and Eq.(A.13) have been used to express the mean photon number in terms of the known functions μ_{ik}.

If we are interested in observing *interference* effects at the detector when the two peak frequencies approach each other, the *sensitivity function* of the detector, a term introduced by Glauber (1965), must not be flat or a finite sum of delta functions. Instead we choose a detector with a sensitivity function which is the sum two Lorentzians of width b, centered around the two frequencies of the incident light. With such a detector one is not able to distinguish

which mode a particular absorbed photon came from if the separation Δ of the two incident frequencies (cf. Eq.(A.10)) is comparable to the bandwidth b of the detector. Hence one expects quantum mechanical interference.

Taking the *continuum limit*, as is usually done (assuming a very large number of oscillators and a weak coupling):

$$\sum_{j=0}^{\infty} g_j^{(i)}\, g_j^{(k)*} \longrightarrow \int_0^{\infty} d\omega\, N(\omega)\, g^{(i)}(\omega)\, g^{(k)}(\omega)^*, \tag{A.22}$$

we thus specify

$$\sqrt{N(\omega)}\, g^{(j)}(\omega) = \frac{\kappa}{\sqrt{\pi}} \frac{\sqrt{b}}{(\omega - \omega_j) + ib} \ . \tag{A.23}$$

With this choice, $N(\omega)\, |g^{(j)}(\omega)|^2$ is a Lorentzian of width b, centered around ω_j.

A few remarks on the *time-scales* involved in the problem. For the above approximations to hold and the Hamiltonian Eq.(A.1) to be appropriate, we require that the interaction time t is very much larger than one optical cycle and is also larger than the resolution time of the detector, which is roughly given by the inverse bandwidth b^{-1}. Furthermore we assume the frequencies ω_i to be larger than the bandwidth of the detector and - in order to justify the above pole approximation - also to be very much larger than F_{ik}, evaluated at ω_j.

Evaluating the functions F_{ik} for the choice Eq.(A.23), we find

$$F_{ik}(-i\omega) = -i \int_0^{\infty} d\omega' \frac{\kappa^2}{\pi} \frac{b}{[(\omega' - \omega_i) + ib]\,[(\omega' - \omega_k) - ib]} \frac{1}{\omega' - \omega} \ . \tag{A.24}$$

If ω_i and ω_k are optical frequencies then the lower limit of this integral may be extended to - ∞ without changing the value of the integral appreciably. Then Eq.(A.24) can be evaluated by means of integration in the complex ω' plane. This yields

$$F_{kk}(-i\omega_k) = \frac{\kappa^2}{b} \equiv \gamma \qquad k \in \{1,2\}$$

$$F_{12}(-i\varpi) = F_{21}(-i\varpi)^* = \frac{-\kappa^2 b\,[\,\Delta + ib\,]^2}{[\,\Delta^2 + b^2\,]^2}$$

$$F_+(-i\varpi) = \frac{\kappa^2\, b}{\Delta^2 + b^2} \equiv \bar{\gamma}\ . \tag{A.25}$$

Straightforward insertion leads to the final expression

$$\begin{aligned} \bar{m}(t) &= |\alpha_1^0|^2\,(\,1 - e^{-2\gamma t}\,) + |\alpha_2^0|^2\,(\,1 - e^{-2\gamma t}\,) \\ &\quad + C_1(\Delta)\; e^{-2\bar{\gamma}t}\,(\sin\Delta t)^2 + C_2(\Delta)\; e^{-(\gamma+\bar{\gamma})\,t}\,\sin\Delta t\,\cos\Delta t \\ &\quad + C_3(\Delta)\, e^{-(\gamma+\bar{\gamma})\,t}\,(\sin\Delta t)^2 \end{aligned}$$

$$\begin{aligned} &= |\alpha_1^0|^2\,(\,1 - e^{-2\gamma t}\,) + |\alpha_2^0|^2\,(\,1 - e^{-2\gamma t}\,) \\ &\quad + \left[\frac{C_1(\Delta)\, e^{-2\bar{\gamma}t} + C_2(\Delta)\, e^{-(\gamma+\bar{\gamma})\,t}}{2}\right](\,1 - \cos\Delta\omega t\,) \\ &\quad + \frac{C_3(\Delta)}{2}\, e^{-(\gamma+\bar{\gamma})\,t}\,\sin\Delta\omega t \end{aligned} \tag{A.26}$$

for the mean photon number with $\Delta\omega = \omega_1 - \omega_2 = 2\Delta$ and the coefficients being

$$C_1(\Delta) = -\left(|\alpha_1^0|^2 + |\alpha_2^0|^2 \right) \left| \frac{\kappa^2 b}{[\Delta^2 + b^2]^2} \frac{[\Delta - ib]^2}{\Delta} \right|^2$$

$$C_2(\Delta) = -4\, \alpha_1^0\, \alpha_2^0 \frac{\kappa^2 b}{[\Delta^2 + b^2]^2 \Delta} \mathrm{Re}([\Delta + ib]^2)$$

$$C_3(\Delta) = -4\, \alpha_1^0\, \alpha_2^0 \frac{\kappa^2 b}{[\Delta^2 + b^2]^2 \Delta} \mathrm{Im}([\Delta + ib]^2) \qquad \text{for } \alpha_j^0 \in R \quad .(A.27)$$

The first two terms in Eq.(A.26) correspond to the result found when the photons from the two modes are counted *independently*, that is simply the sum of the two single-mode results. For large frequency separation Δ the full expression approaches this limit. However, for $\Delta \approx b$ there are interference terms oscillating (about the level corresponding to independent photon counts) at a rate $2\Delta = \omega_1 - \omega_2$. Depending on the relative phases of the initial amplitudes $\alpha_i{}^o$ of the field, one observes destructive or constructive interference. A generalization of this method to more modes is straightforward in principle, but soon becomes tedious.

Appendix B: Potential Condition for the Fokker-Planck Equation Around Threshold of the Squeezed-Pump Laser

In this section we will briefly discuss how the phase-dependent noise correlations which are characteristic for squeezing violate the potential conditions for a FPE describing the laser around threshold.

Recalling the approximate FPE derived in Section 3.4 by adiabatically eliminating the atoms, the P-function for the real and imaginary part of the laser field α satisfies

$$\frac{\partial P}{\partial t} = \left[-\frac{\partial}{\partial x_i} A_i + \frac{\partial^2}{\partial x_i \partial x_j} D_{ij} \right] P$$

with $\qquad x_1 = u \equiv \mathrm{Re}\,\alpha, \qquad x_2 = v \equiv \mathrm{Im}\,\alpha\ ,$ (B.1)

(summation over repeated indices is implied throughout). For small M the above expressions are given by

$$A = -\kappa \begin{pmatrix} u\left[1 - C\left(1 - M - \dfrac{u^2+v^2}{n_0}\right)\right] \\ v\left[1 - C\left(1 + M - \dfrac{u^2+v^2}{n_0}\right)\right] \end{pmatrix}$$

$$D = \left(\frac{g}{2\gamma_\perp}\right)^2 \begin{pmatrix} \mathbf{D}_{\alpha^*\alpha} - \mathbf{D}_{\alpha\alpha} & 0 \\ 0 & \mathbf{D}_{\alpha^*\alpha} + \mathbf{D}_{\alpha\alpha} \end{pmatrix} \qquad \text{(B.2)}$$

in the regime where saturation is not important. The (constant) diffusion matrix elements $\mathbf{D}_{ij}$ are given in Eq.(3.58). The condition for a potential solution

$$P(u,v) = N_0\, e^{-\Phi(u,v)}$$

with

$$\Phi(u,v) = \int_{(u_0,v_0)}^{(u,v)} dx_i\, D_{ij}^{-1} \left[-A_j + \frac{\partial D_{jk}}{\partial x_k} \right] \qquad \text{(B.3)}$$

(where N_0 stands for a normalization constant) the so-called *potential condition* for a system with two degrees of freedom, reads

$$\frac{\partial G_1}{\partial x_2} = \frac{\partial G_2}{\partial x_1}\ , \qquad \text{(B.4)}$$

when the "generalized forces" G_i are defined as

$$G_i \equiv D_{ij}^{-1}\left[-A_j + \frac{\partial D_{jk}}{\partial x_k}\right]. \qquad \text{(B.5)}$$

Insertion easily leads to the answer that the potential condition is satisfied if and only if $D_{\alpha\alpha}$ is zero. Viewing Eq.(3.58) one realizes that this would require a vanishing squeezing parameter m_p. Thus we conclude that the diagonal or "phase-dependent" correlations which are typical for squeezing prevent the existence of a potential solution.

References

Braginsky, V.B., Y.I. Vorontsov, and K.S. Thorne, 1980, Science **209**, 547

Carmichael, H.J., A.S. Lane and D.F. Walls, 1987, J. of Mod. Opt. **34**, 821

Carruthers, P., and M.M. Nieto, 1968, Rev. Mod. Phys. **40**,411

Caves, C.M. , 1981, Phys. Rev. D **23**, 1693

Caves, C.M. , 1987, Optics Letters **12**, 971

Caves, C.M. and B.L. Schumaker, 1985, Phys. Rev. A **31**, 3093

Caves, C.M., K.S. Thorne, R.W.P. Drever, V.D. Sandberg, and M. Zimmermann, 1980, Rev. Mod. Phys. **52**, 341

Chow, W.W., M.O. Scully, and E.W. van Stryland, 1975, Opt. Commun. **15**, 6

Collett, M.J, 1987, *Environmental Correlations in the Theory of Open Quantum Systems,* D. Phil. Thesis, University of Essex

Collett, M.J. and C.W. Gardiner, 1984, Phys. Rev. A **30**, 1386

Collett, M.J. and D.F. Walls, 1985, Phys. Rev. A **32**, 2887

Cohen-Tannoudji, C., B. Diu, and F. Laloë, 1977, *Quantum Mechanics*, Vol.1, p.286 (Hermann, Paris)

Cresser, J.D., W.H. Louisell, P. Meystre, W. Schleich, and M.O. Scully, 1982, Phys. Rev. A **25**, 2214

Cresser, J.D., D. Hammonds, W.H. Louisell, P. Meystre, and H. Risken, 1982, Phys. Rev. A **25**, 2226

Dorschner, T.A., H.A. Haus, M. Holz, I.W. Smith, and H. Statz, 1980, IEEE J. Quantum. Electron. **QE-16**, 1376

Drummond, P.D. and C.W. Gardiner, 1980, J. Phys. A: Math. Gen. **13**, 2353

Ezekiel, S. and H.J. Arditty, 1982, in *Proceedings of the International Conference on Fiber-Optic Rotation Sensors* (Springer, Berlin)

Filipowicz, P., J. Javanainen, and P. Meystre, 1986, Phys. Rev. A **34**, 3077

Gardiner, C.W., 1983, *Handbook of Stochastic Methods* (Springer, Berlin)

Gardiner, C.W., 1986, Phys. Rev. Lett. **56**, 1917

Gardiner, C.W. and M.J. Collett, 1985, Phys. Rev. A **31**, 3761

Gardiner, C.W., A.S. Parkins, and M.J. Collett, 1987, J. Opt. Soc. Am. B **4**, 1683

Gilmore, R., 1974, *Lie Groups, Lie Algebras, and Some of Their Applications* (Wiley, New York)

Gea-Banacloche, J., 1987, Phys. Rev. Lett. **59**, 543

Glauber, R.J., 1963, Phys. Rev. **130**, 2529

Glauber, R.J., 1963, Phys. Rev. **131**, 2766

Glauber, R.J., 1965, in *Quantum Optics and Electronics,* Editors C. DeWitt et al., p.78 (Gordon and Breach, New York)

Glauber, R.J., 1986, in *Frontiers in Quantum Optics,* edited by E.R. Pike and S. Sarkar (Adam Hilger, Boston)

Grangier, P., R.E. Slusher, B. Yurke, and A. LaPorta, 1987, Phys. Rev. Lett. **59**, 2153

Grübl, G., 1985, private communication

Haake, F., 1973, in *Quantum Statistics in Optics and Solid State Physics,* Springer Tracts in Modern Physics Vol. 66 (Springer, Berlin)

Haken, H., 1970, *Licht und Materie Ic* , Vol.XXV/2c, (Springer, Berlin)

Haken, H., 1981, *Light,* Vol.2 (North-Holland Publishing Company, Amsterdam)

Heidmann, A., R.J. Horowicsz, S. Reynaud, E. Giacobino, C. Fabre, and G. Camy,1987, Phys. Rev. Lett. **59**, 2555

Hollenhorst, J.N., 1979, Phys. Rev. D **19**, 1669

Kaplan, A.E. and P. Meystre, 1981, Opt. Lett. **6**, 590

Kelly, P.L. and W.H. Kleiner, 1964, Phys. Rev. **136**, 316

Krause, J., M.O. Scully, and H. Walther, 1986, Phys. Rev. A **34**, 2032

Lax, M. and M. Zwanziger, 1973, Phys. Rev. A **7**, 750

Loudon, R., 1973, *The Quantum Theory of Light*, p.120
(Oxford University Press, Oxford)

Loudon, R. and P.L. Knight, 1987, J. Mod. Opt. **34**, 709

Louisell, W. H., 1973, *Quantum Statistical Properties of Radiation*
(Wiley, New York)

Lu, E.Y.C., 1971, Nuovo Cimento **2**, 1241

Lu, E.Y.C., 1972, Nuovo Cimento **4**, 585

Machida, S. and Y. Yamamoto, 1988, Phys. Rev. Lett. **60**, 792

Machida, S., Y. Yamamoto, and Y. Itaya, 1987, Phys. Rev. Lett. **58**, 1000

Maeda W., P. Kumar, and J.H. Shapiro, 1987, Opt. Lett. **12**, 161

Mandel, L., 1979, Opt. Lett. **4**, 205

Mandel, L., 1982, Phys. Rev. Lett. **49**, 136

Marte, M.A.M. and D.F. Walls, 1987, J. Opt. Soc. Am. B **4**, 1849

Marte, M.A.M. and D.F. Walls, 1988, Phys. Rev. A **37**, 1235

Marte, M.A.M., H. Ritsch, and D.F. Walls, submitted to Phys. Rev. A

Milburn, G.J., 1982, *Squeezed States and Quantum Non-Demolition Measurements* , D.Phil. Thesis, University of Waikato

Milburn, G.J., 1984, J. Phys. A **17**, 737

Milburn, G.J., M.D. Levenson, R.M. Shelby, and D.F. Walls, 1987,
Opt. Soc. Am. B **4**, 1476

Mollow, B.R., 1968, Phys. Rev. **168**, 1896

Post, E.J., 1967, Rev. Mod. Phys. **39**, 475

Raizen, M.G., L.A. Orozco, M. Xiao, T.L. Boyd, and H.J. Kimble, 1987
Phys. Rev. Lett. **59**, 198

Reid, M.D., 1987, private communication

Reid, M.D., 1988, to be published in Phys. Rev. A

Risken, H., 1984, *The Fokker-Planck Equation* (Springer, Berlin)

Ritsch, H. and P. Zoller, 1987, Opt. Commun. **64**, 523

Sanders, B.C., S.M. Barnett, and P.L. Knight, 1986, Opt. Commun. **58**,290

Sargent, M., M.O. Scully, and W.E. Lamb, 1974, *Laser Physics* , p.172 (Addison-Wesley, Reading)

Schumaker, B.L. and C.M. Caves, 1985, Phys. Rev. A **31**, 3068

Schumaker, B.L., 1986, Phys. Rept. **135**, 317

Schumaker, B.L., 1984, Opt. Lett. **9**, 189

Scully, M.O. and W.E. Lamb, 1969, Phys. Rev. **179**, 368

Shapiro, J.H. and S.S. Wagner, 1984, IEEE J. Quantum. Electron. **QE-20**, 803

Shelby, R.M., M.D. Levenson, S.H. Perlmutter, R.G. DeVoe, and D.F. Walls, 1986, Phys. Rev. Lett. **57**, 691

Slusher, R.E., L.W. Hollberg, B. Yurke, J.C. Mertz, and J.F. Valley, 1985, Phys. Rev. Lett. **55**, 2409

*) Steel, W.H., 1983, *Interferometry,* second edition (Cambridge University Press, Cambridge)

Stoler, D., 1970, Phys. Rev. D **1**, 3217

Stoler, D., 1971, Phys. Rev. D **4**, 1925

Susskind, L. and J. Glogower, 1964, Physics **1**, 49

Yamamoto, Y., S. Machida, and O. Nilsson, 1986, Phys. Rev. A **34**, 4025

Yuen, H.P., 1976, Phys. Rev. A **13**, 2226

Yuen, H.P. and V.W.S. Chan, 1983, Opt. Lett. **8**, 177

Yuen, H.P. and J.H. Shapiro, 1978, IEEE Trans. Inf. Theory **IT-24**, 657

Yuen, H.P. and J.H. Shapiro, 1980, IEEE Trans. Inf. Theory **IT-26**, 78

Yurke, B., 1985, Phys. Rev. A **32**, 300

Yurke, B., 1985, Phys. Rev. A **32**, 311

Yurke, B., S.L. McCall, and J.R. Klauder, 1986, Phys. Rev. A **33**, 4033

Walls, D.F., 1983, Nature **306**, 141

Walls, D.F. and G.J. Milburn, 1983, in *Quantum Optics, Experimental Gravitation, Measurement Theory,* Edited by P. Meystre and

* Slusher, R.E., P. Grangier, A. La Porta, B. Yurke, and M.J. Potasek, 1987, Phys. Rev. Lett. **59**, 2566

M.O. Scully (Plenum, New York)

Walls, D.F., G.J. Milburn, and H.J. Carmichael, 1982, Optica Acta **29**,1179

Wright, E.M., P. Meystre, W.J. Firth, and A.E. Kaplan, 1985,
Phys. Rev. A **32**, 2857

Wódkiewicz, K. and J.H. Eberly, 1985, J. Opt. Soc. Am. B **2**, 458

Wu, L., H.J. Kimble, J.L. Hall, and H. Wu, 1986, Phys. Rev. Lett. **57**, 2520

Wybourne, B.G., 1974, *Classical Groups for Physicists* (Wiley, New York)